NDOT Research Report

Report No: RDT97-011

SENSITIVITY ANALYSIS of FATIGUE EVALUATION of STEEL BRIDGES

July 2001

Prepared by Research Division
Nevada Department of Transportation
1263 South Stewart Street
Carson City, Nevada 89712

NEVADA DOT

TECHNICAL REPORT DOCUMENTATION PAGE

Report No. RDT97-011	2. Government Accession No.	3. Recipient's Catalog No.
4. Title and Subtitle **Sensitivity Analysis of Fatigue Evaluation of Steel Bridges**	5. Report Date **September 1997** 6. Performing Organization Code	
7. Author(s) **Prem P. Rimal; Ahmad M.**	8. Performing Organization Report No.	
9. Performing Organization Name and Address **Center for Civil Engineering Earthquake Research** **University of Nevada, Reno** **Reno, Nevada 89557**	10. Work Unit No. 11. Contract or Grant No. P520-95	
12. Sponsoring Agency Name and Address **Nevada Department of Transportation** **1263 South Stewart** **Carson City, Nevada 89712**	13. Type or Report and Period Covered October 1, 1995 thru December 31, 1996 14. Sponsoring Agency Code **NDOT**	

15. Supplementary Notes

16. Abstract

This report presents the sensitivity analysis of fatigue evaluation for Nevada steel bridges. Parameters affecting applied stress ranges were studied and varied in a three-span four steel plate girder bridge to determine their effect on fatigue evaluation. The allowable stress range parameters were examined to determine their effect on the overall fatigue behavior. The current research and practice of other major state DOT's in dealing with fatigue cracks, evaluation procedures and repair methods were studied and examined.

From the study, it was found that for closely spaced and widely spaced bridges, the 3-D structural analysis gave approximately 50% and 25% higher stress range values than the 2-D analysis respectively. For normally spaced bridges, the 2-D structural analysis gave 50% higher values. For the case of skewed bridges, the 2-D structural analysis gave approximately 50%, 75%, and 170% higher values of stress ranges than 3-D analysis for 0^0, 30^0 , and 60^0 skewed bridges, respectively. It was also found that increasing the skew angle, girder spacing and depth would decrease the stress ranges. The applied ranges did not vary with the configuration and cross-sectional area of cross frame and lateral bracing. However, as skew angle increases, cross frame and lateral bracing members attracted more axial forces having these locations prone to out-of-plane fatigue cracking. The single HS20 Truck was found to be the most damaging load in terms of fatigue life due to its high frequency of occurrence during the life span of a bridge. Over thirty states responded to the questionnaire about fatigue evaluation and repair methods. Many of these responses could be applicable to Nevada steel bridges.

17. Key Words	18. Distribution Statement
Steel Bridges, Fatigue Evaluation, Structure Analysis	**Unrestricted. This document is available through the National Technical Information Service, Springfield, VA 21161**

19. Security Classif. (of this report)	20. Security Classif. (of this page)	21. No. Of Pages	22. Price
Unclassified	**Unclassified**	181	

Acknowledgments

This study was conducted under grant number P520-95-803 from the Nevada Department of Transportation. The opinions expressed in this paper belong only to the authors, and do not represent the official position of either the University of Nevada, Reno, nor the Nevada Department of Transportation.

The authors would like to express their appreciation to Mr. Floyd I. Marcucci, NDOT chief bridge engineer and Mr. William Crawford, assistant chief bridge engineer for their assistance during this project. Special thanks are due to the state bridge engineers who responded to our questionnaire.

This report is based on a Master of Science thesis written by Prem P. Rimal, under the direction of Prof. A. Itani.

Abstract

This report presents the sensitivity analysis of fatigue evaluation for Nevada steel bridges. Parameters affecting applied stress ranges were studied and varied in a three-span four steel plate girder bridge to determine their effect on fatigue evaluation. The allowable stress range parameters were examined to determine their effect on the overall fatigue behavior. The current research and practice of other major state DOTs in dealing with fatigue cracks, evaluation procedures and repair methods were studied and examined.

From the study, it was found that for closely spaced ($S \leq 5.83$ ft.) and widely spaced ($S \geq 17.5$ ft.) bridges, the 3-D structural analysis gave approximately 50% and 25% higher stress range values than the 2-D analysis respectively. For normally spaced ($10 \leq S \leq 14$ ft.) bridges, the 2-D structural analysis gave 50% higher values. For the case of skewed bridges, the 2-D structural analysis gave approximately 50%, 75%, and 170% higher values of stress ranges than 3-D analysis for 0°, 30°, and 60° skewed bridges, respectively. It was also found that increasing the skew angle, girder spacing and depth will decrease the stress ranges. The applied stress ranges did not vary with the configuration and cross-sectional area of cross frame and lateral bracing. However, as skew angle increases, cross frame and lateral bracing members attracted more axial forces having these location prone to out-of-plane fatigue cracking. The single HS20 Truck was found to be the most damaging load in terms of fatigue life due to its high frequency of occurrence during the life span of a bridge. Over thirty states responded to the questionnaire about fatigue evaluation and repair methods. Many of these responses could be applicable to Nevada steel bridges.

Contents

List of Tables

List of Figures

Chapter 1

Introduction

1.1 Background

More than fifteen steel plate and box girder bridges in the Nevada State Highway System have experienced fatigue cracks. These cracks will pose a threat if not detected and adequately retrofitted because they might propagate and fracture flanges of steel girder which will significantly reduce the strength of the bridge. Current bridge design specifications, such as the Standard Specifications for Highway Bridges, AASHTO 15th Edition [1], and AASHTO LRFD Bridge Design Specifications [2], do not offer guidelines for fatigue evaluation of steel bridges since they only deal with the design of new bridges.

Recognizing this fact and the importance of fatigue evaluation of steel bridges, the Nevada Department of Transportation, NDOT, with the collaboration of the Civil Engineering Department at the University of Nevada, Reno initiated a study to identify the significant parameters, understand and quantify their influence, survey and study fatigue evaluation and repair methods by other major states, and recommend appropriate strategies for fatigue evaluation for Nevada steel bridges.

The basic definition of fatigue in steel is the initiation and/or propagation of cracks due to repeated variation of normal stresses with tensile components. This statement identifies the significant parameters of basic metal fatigue or in-plane fatigue such as applied stress ranges, number of stress cycles, and the fatigue resistance of the

material. However, in steel bridges fatigue might be the cause of distortion induced fatigue in addition to the in-plane fatigue. The distortion induced fatigue is due to secondary stresses not normally quantified in the typical analysis and design of steel bridges. This type of fatigue can be minimized by the removal of the source of distortion.

1.2 Objective and Scope of the Study

The objective of this study is to identify and recommend appropriate fatigue evaluation and repair methods for Nevada steel bridges. To achieve this objective a steel bridge in Nevada that experienced fatigue cracking was selected to study the influence of significant fatigue parameters. The current research and practice of other major state DOTs in dealing with fatigue cracks, and their evaluation procedures and repair methods were surveyed and examined to determine whether they are applicable to bridges in Nevada.

Fatigue evaluation of steel bridges can be established based on the fundamental equation:

$$\text{Fatigue Demand} < \text{Fatigue Capacity} \qquad (1)$$

The demand side of the above equation represents applied stress ranges which are affected by the following parameters:

- Mathematical Model: 2-D or 3-D
- Bridge geometry: Skew angle, girder spacing, and girder depth
- Configurations and area of cross frame and lateral bracing
- Types of live loads: Single HS20, Multi HS20 Lane & Truck Load, and P13

These parameters were varied to determine the applied stress ranges and examine their effect on the overall fatigue evaluation process.

On the other hand, the capacity side of equation (1) represents allowable stress ranges which is affected by:

- Redundancy
- Number of cycles due to legal and permit loads
- Detail categories

A survey questionnaire on "Fatigue Evaluation Procedures and Repair Methods for Steel Bridges" was sent to the 50 states, the Commonwealth of Puerto Rico, and the U.S. Department of Transportation to determine their current practices in dealing with fatigue evaluation procedures and repair methods. Thirty two states responded to the questionnaire. The evaluation procedures and repair methods obtained from those responses were studied extensively to determine their applicability to Nevada steel bridges.

Chapter 2 describes fatigue problems and identifies the significant fatigue evaluation parameters. Chapter 3 focuses on allowable fatigue stresses and the parameters that affect them. Number of stress cycles due to various loading are investigated and damage assessment due to legal and permit loads are presented. The proposed fatigue evaluation procedure is presented in Chapter 3. Chapter 4 discusses the fatigue survey of other major states and their responses. Chapter 5 presents the summary and recommendations of the study.

Chapter 2

Fatigue Evaluation-Applied Stress Ranges

2.1 Introduction

This chapter identifies the significant parameters that influence fatigue evaluation of steel bridges. These parameters were studied and varied in order to determine their sensitivity on the overall fatigue behavior. This chapter also describes the selection process that was used to choose a bridge on which the parametric analysis will be carried on. The mathematical modeling and structural analysis procedures that were utilized in this study to determine the bridge internal forces due to moving live load are also presented in this chapter.

2.2 Types of Fatigue Problems

Sometimes cracks develop in steel bridges as a result of repeated loading in which they are subjected to. The primary factors leading to the development of such cracks are the frequency of truck traffic loading, the age of the bridge, the magnitude of the stress range, the type of details, the quality of the fabricated details, and the material toughness.

Fatigue in highway steel bridges can be mainly categorized as load-induced or distortion-induced stresses. Load induced fatigue problems are due to in-plane stresses which can be quantified during the design of steel bridges. The in-plane fatigue cracks are very sudden and can cause brittle fracture. Examples of these types of problems are

in-plane web cracks at welded connections, in-plane tension flange cracks, and cracks at stringer-to-floor beam connections.

Distortion-induced fatigue problems, on the other hand, are the result of secondary stresses, caused by the interaction between transverse and longitudinal members, which were not considered during the design process. Transverse and longitudinal members, such as cross frames, diaphragms and lateral bracing are the main cause of secondary stresses in steel bridges. Cross frames and diaphragms between girders can also cause out-of-plane movements in the girder webs when there is considerable relative deflection between the girders. Previous studies [10] have showed that the out-of-plane movements caused by bracing are usually much greater in skewed and curved bridges than in right bridges.

2.3 Fatigue Terminology

The following are fatigue terminology that will be used in this study:

- Fatigue Stress Range: Is the algebraic difference between maximum and minimum stresses resulting from the passage of a load across the structure at a particular detail. If a part of the stress cycle is not in tension, there is no fatigue concerns.
- Fatigue Design Life: Is number of years that a detail is supposed to resist the assumed traffic loads without fatigue cracking. According to the current specifications this life ranges between 50 to 75 years.
- Fatigue Life: Is the number of repeated stress cycles that results in fatigue failure of a detail.

- Constant Amplitude Fatigue Threshold (CAFL): Is the nominal stress range below which a particular detail can withstand an infinite number of repetitions without fatigue failure.
- Finite Fatigue Life: Is the number of cycles to failure of a detail when the maximum probable stress range exceeds the CAFL.
- Required Fatigue Life: Is defined as a product of the Single-lane average daily truck traffic, the number of cycles per truck passage and the design life in days.
- Fatigue Resistance: Is the maximum stress range that can be sustained without failure of the detail for a specified number of cycles.

2.4 Fatigue Design and Evaluation

The fatigue design of new bridges is generally governed by bridge specifications [1, 2]; however, limited guidelines are available for fatigue evaluation of steel bridges. The following fundamental equation can be used to establish fatigue evaluation of steel bridges:

$$\text{Fatigue Demand} < \text{Fatigue Capacity}$$

or

$$\text{Applied Stress Range} < \text{Allowable Stress Range}$$

The left hand side of the equation represents the applied fatigue stress ranges which depends on the following factors:

- Mathematical Model: 2-D and 3-D

- Geometry: Skew angle and girder spacing/depth
- Configuration and area of cross frame and lateral bracing
- Type of Loading: Legal and permit loads

This chapter will discuss the applied stress range and its main parameters while the effect of allowable stress range will be discussed in Chapter 3.

2.5 Bridge Selection

Three steel bridges were selected by NDOT as representative steel bridges in the State of Nevada that suffered fatigue cracking. Rose Creek Overpass, NDOT bridge No. IR80-HU3.4, was chosen to carry the sensitivity analysis of fatigue parameters on. The location map of this bridge is shown in Figure 2.1. This bridge had experienced fatigue cracks at two critical locations: i) interior supports at maximum negative moment and ii) middle of the second span at maximum positive moment. The main types of fatigue cracks in this bridge were web cracks above the welded connection of the bottom flange and web, and cracks at the toe of the stiffener. Both types of cracks were located around the transverse stiffener where cross frames were connected. These cracks and their locations are shown in Figure 2.2 as mapped by NDOT engineers.

This bridge consists of three spans, 95 ft, 130 ft, 95 ft, and has four steel plate girders. The girders have a constant depth equal to 4 ft and are spaced at 11 ft and 8 inches. The steel girders support an 8 1/2 inch thick reinforced concrete deck. The overall width of bridge including the two overhangs is 44 ft. The bridge is supported on roller supports at the abutments and is pinned at the intermediate piers. The bridge has a significant skew angle equal to 60°. The variation of the longitudinal plate girder cross

section is presented in Table 2.1. The bridge has lateral bracing between the two interior girders of the second span. The elevation of the bridge with abutments and bents is shown in Figure 2.3. Figure 2.4 shows the view of the pier, steel plate girders and bridge deck. Figures 2.5 and 2.6 show the cross frames and lateral bracings with their connection details. The cross sectional area of the horizontal members of the lateral bracing, cross frames, and diaphragms are presented in Table 2.2.

2.6 Parametric Studies

The primary objective of the parametric studies is to identify and study the sensitivity of significant parameters on fatigue evaluation. The main parameters varied in this study are:

- Mathematical models and structural analyses
- Bridge geometry: Skew angle and girder spacing/depth
- Configuration and area of cross frame and lateral bracing
- Type of loading: Legal and permit loads

2.6.1 Bridge Mathematical Models and Bridge Structural Analyses

Two types of mathematical models: 2-D and 3-D were used to evaluate the applied fatigue stress ranges. In the 2-D model, all steel girders were lumped together with the concrete slab and were modeled as a beam element with an equivalent moment of inertia. The AASHTO distribution factors are normally utilized to evaluate individual girder moments and shears. The 3-D mathematical model, on the other hand, explicitly models the deck, plate girders, and cross frames. Influence surfaces are normally

generated along the longitudinal and transverse direction of the bridge to determine the maximum moments and shears on individual girders.

2.6.1.1 Two Dimensional Structural Analysis (SIMON Program)

This study utilized the SIMON program [6] for the 2-D structural analysis. The structural analysis subroutine that is used in this program was originally written by the Wisconsin Department of Transportation while the whole program was developed by U.S. Steel, Inc. more than twenty five years ago. Recently, it was made available on PC by AISC Inc. The analysis routines of the program divide each span into twenty segments of equal length and compute the cross-sectional properties of each segment. From the moment of inertia of each segment, the stiffness characteristics of each span are calculated and used to set up a stiffness matrix. Influence values are based on twenty ordinates per span and are generated at the tenth points of each span. Using these influence values, dead-load and maximum and minimum live-load moments and shears are computed at the tenths points of each span. The 2-D mathematical models utilize one dimensional moving load and use AASHTO live load distribution factors to calculate the maximum values of the internal forces and reactions in a single girder.

2.6.1.2 Three Dimensional Structural Analysis (CBridge Program)

The 3-D structural analyses were performed using the CBridge program [7] which is normally used for the 3-D analysis of right or horizontally curved girder bridges. This program has been developed by Syracuse University for the purpose of 3-D structural analysis of steel plate girder bridges. The program explicitly models the deck, diaphragms, lateral bracing, and girders. In this program, the nodes are selected where

displacements, rotations, and forces in the members meeting at the joint will be computed. The nodes are usually located at structural joints, where the cross-section changes and intersections of girders and diaphragms. The program utilizes six equilibrium equations for each joint and accounts for cross frames and lateral bracing configurations.

The 3-D models generate influence surfaces on the entire bridge and place as much Truck Load as needed to calculate the internal forces and support reactions. This method does not need AASHTO's live load distribution factors since each girder shares its load according to its stiffness and distance from the applied load.

2.6.2 Bridge Geometry

Bridge geometrical parameters that have direct effect on the applied stress range are:

- Skew angle
- Girder spacing
- Girder depth.

2.6.2.1 Skew Angle

The use of skew superstructures in highway bridges is becoming quite common to adapt to the roadway geometry and withstand the ever-increasing speed and traffic. To understand the effect of this geometrical parameter on the overall fatigue stress ranges, the skew angle, a, was investigated at 0°, 30° and 60°.

2.6.2.2 Girder Spacing

Bridges could be classified as closely spaced or widely spaced according to their girder spacing. The current AASHTO specifications use the S/D factor or lever rule to determine the live load distribution factors for closely and widely spaced bridges respectively. To investigate the influence of girder spacing on applied stress ranges the girder spacing, S, of the original bridge (11'-8") was varied to one-half (5'-10") and to one-and-half (17'-6") times the original girder spacing. The longitudinal girders and the concrete deck for each case were re-designed according to the NDOT "Bridge Design and Procedures Manual" [5]. The weight of the girder section, the concrete deck thickness, and the maximum live load deflections on the mid span in each case are given in Table 2.3.

2.6.2.3 Girder Depth

To determine the influence of girder depth, D, on the applied stress fatigue ranges, the bridge girders were re-designed for three cases: 1/2 the original depth (24"), the original depth (48"), and 1.5 times the original depth (72"). The weight of the girder section and the maximum live load deflections on the mid span for each case are given in Table 2.3.

2.6.3 Cross Frame and Lateral Bracing Configurations

Cross frames in steel highway bridges are usually of K or X type. Cross frames are primarily used in steel bridges to reduce the buckling length of compression flanges and to provide lateral stability to the girders against lateral torsional buckling. To

investigate their effect on applied fatigue stress ranges and internal forces, K type and X type cross frames with various areas were studied. Figures 2.7-a shows cross frame configurations at supports with different girder spacings for both K and X types of cross frames whereas Figure 2.7-b shows the intermediate cross frame configurations for K and X types cross frames. The cross sectional area of the cross frames was doubled ($A=1.93\ in^2$ to $A=3.86\ in^2$) for both the K Type and X Type.

Similar to cross frames, lateral bracings are used to prevent buckling of main structural members and to resist lateral loads such as wind effect. Lateral bracings were used between two girders to investigate their effect on applied stress ranges, deflections, and the value of forces that they are subjected to. Figures 2.8-a, b and c show the location of lateral bracings, supports, diaphragms, intermediate cross frames for three different skewed bridges.

2.6.4 Type of Loading

The type of live loads considered in this study are AASHTO's legal loads: HS20 Truck Load and HS20 Lane Load, which are composed of a distributed live load with a single or double concentrated live load. This study also utilized California Permit Truck P Loads [4] since it represents NDOT's overload [5]. Similar to the "Bridge Design Specifications" of Caltrans, NDOT "Bridge Design and Procedures Manual" [5] uses a P13 Load in checking the serviceability under fatigue in steel bridges. The P Loads are composed of modular truck and trailer combinations with the maximum P13 as shown in Figure 2.9. The following symbols are used to abbreviate the four different live loads.

- HS20 MLTL = HS20 Multi-lane Truck Load.

- HS20 MLLL = HS20 Multi-lane Lane Load.
- S HS20 TL = Single HS20 Truck Load
- S P13 TL = Single P13 Truck Load

2.7 Results of Parametric Studies

The applied stress ranges were plotted at the tenth points of each span in order to study their variations with the several different parameters. These plots are presented in Figures 2.10 to 2.67. On the horizontal axis of the these figures, the points 0 and 30 represent the location of two abutments while the points 10 and 20 represent the locations of the two interior supports. The vertical axis of the plot is the applied stress range in ksi.

2.7.1 Mathematical Models and Structural Analyses

The effect of the mathematical models on the applied fatigue stress ranges was studied by performing both 2-D and 3-D structural analyses. Figures 2.10-a and b represent the variation of the applied stress ranges of the 2-D and 3-D structural analyses along the longitudinal direction of the original right bridge. Since the 2-D structural analysis program performs analysis for right bridges only, the comparison between the 2-D and 3-D structural analysis will be made for a right bridge. The 3-D program gave analytical results for all of the girders whereas the 2-D program gave the analytical results for only one girder. Girder G2 was selected to compare the results between two structural analyses.

Figure 2.10-a illustrates the applied stress ranges at the top flange due to a Single HS20 Truck Load while Figure 2.10-b represents the stress ranges at bottom flange of the original bridge. The original bridge is a right bridge having a girder spacing of 11.67 ft

and a girder depth of 4 ft. From the figure, it can be seen that the 2-D structural analysis gave 50% higher stress ranges than the 3-D structural analysis. This could be attributed to the difference in the live load distribution factors between the two analyses. Figures 2.11-a and b represent the stress ranges at the top and bottom flanges due to a Single HS20 Truck Load for a girder depth equals to one-half times the original depth. In this case, the 2-D analysis gave 25% higher stresses than the 3-D analysis. Figures 2.12-a and b represent the stress ranges at the top and bottom flanges for a girder depth equal to one and one-half-times the original depth. The same trends between the 2-D and 3-D were observed from both cases.

Figures 2.13 and 2.14 show the variation of stress ranges at the top and bottom flanges due to a Single HS20 Truck Load for two different girder spacings in both 2-D and 3-D. In the first case, a girder spacing of 5.83 ft was used. The 3-D analysis gave 50% higher values of stress ranges than the 2-D analysis. For the second case, the girder spacing was equal to 17.5 ft. The 3-D analysis gave only 25% higher values of stress ranges than the 2-D analysis. As the girder spacing increases, the difference in the stress ranges between the two programs decreases by approximately 25%. The difference in stress ranges between the 2-D and 3-D results, in each of the cases, can be attributed to the difference in live load distributions of both programs.

Figures 2.15 to 2.19 represent the same five cases as mentioned earlier. The only difference between them is the type of truck loading. The truck loading in these cases is a Single P13 Truck. These figures show that the stress range values are higher than the stresses due to a Single HS20 Truck Load. However, the difference in stress ranges from

the 2-D and 3-D analyses due to a Single P13 Truck Load follow the same trend as for the Single HS20 Truck Load. In conclusion, it was found that for closely spaced ($S \leq 5.83$ ft) and widely spaced ($S \geq 17.5$ ft) bridges, the 3-D structural analysis gave approximately 50% and 25% higher stress range values than the 2-D analysis. However, for normally spaced ($10 \leq S \leq 14$ ft) bridges, the 2-D structural analysis gave 50% higher values.

2.7.2 Skew Angle

Though the analytical capability of the 2-D analysis program was limited to right bridges only, it is appropriate to compare these results with those obtained from 3-D analysis for skewed bridges. Figures 2.20-a and b show the variation of the applied stress ranges at the top and bottom flanges of girder G2 due to a Single HS20 Truck Load with respect to the different skew angles. From these figures, it can be observed that 2-D analysis for a right bridge gave approximately 50%, 75%, and 170% higher values than 3-D analysis for a bridge having skew angles of 0°, 30°, and 60° respectively.

The magnitude of the applied stress ranges from the 3-D analysis for the three different skew angles (0°, 30°, 60°) were plotted in Figures 2.21 to 2.22. Figures 2.21-a and b represent the variation of the applied stress ranges at the top and bottom flanges of girder G2 due to a Single HS20 Truck Load with respect to the different skew angles. These plots show that an increase in the skew angle causes a decrease in the values of applied stress ranges. This is due to the three-dimensional coupling interaction between the longitudinal girders and diaphragms in skewed bridges. Figures 2.22-a and b represent the variation of the applied stress ranges at the top and bottom flanges of girder G2 on a bridge having a girder depth of one-half times the original depth (D = 24 in.) due

to a Single HS20 Truck Load with the different skew angles. Similarly, Figures 2.23 to 2.25 represent the variation of stress ranges in the other cases: 1 1/2 times the original girder depth, 1/2 times of the original girder spacing, and 1 1/2 times of the original girder spacing. From all of these figures, it can be summarized that increasing the skew angle from 0° to 30° causes a 15% decrease in the stress ranges while increasing the skew angle from 0° to 60° causes a 40% decrease in the stress ranges.

2.7.3 Girder Spacing

The results of applied stress ranges of the 2-D structural analysis of the bridges with different girder spacings were plotted along the longitudinal direction of bridge. Figures 2.26-a and b represent the variation of the stress ranges at the top and bottom flanges of a girder on a right bridge due to a Single HS20 Truck Load for the different girder spacings. For the girder spacing of S = 5.83' & 11.67', AASHTO S/D factor was used, while for S = 17.5', lever rule was used to determine the live load distribution factors.

Figures 2.27-a and b represent the variation of the stress ranges from the 3-D analysis at the top and bottom flanges of girder G2 on a right bridge due to a Single HS20 Truck Load at the different girder spacings. From these figures, it is observed that the increase in the girder spacing would decrease the stress ranges. Similarly, Figures 2.28 to 2.30 show the stress range variations due to the other three live loads.

2.7.4 Girder Depth

The original bridge was re-designed for a girder depth equal to 1/2 and 1 1/2 times the original girder depth of 4 ft. Figures 2.31-a and b show the stress range variations at

the top and bottom flanges in girder G2 of the right bridge due to a Single HS20 Truck Load and different girder depths. From these figures, it can be seen that by increasing the girder depth, the stress ranges, except for the original bridge, would decrease. Similarly, Figures 2.32 to 2.34 show the variation of the applied stress ranges due to the other three loads with the different girder depths. These figures show a similar trend as before. This is due to variation in girder section weight from the original bridge girder section weight as shown in table 2.3. The cross section of the original bridge does not follow the pattern of the other two cases, i.e., the deeper the section, the lighter the weight. From Table 2.3, it can also be observed that the section modulus in the original bridge (D = 48 in.) is less than the section modulii in the two cases with varying girder depths (D = 24 in. and D = 72 in.). From these two cases, it can be proven that an increase in the section modulus results in a decrease in the applied stress ranges.

2.7.5 Cross Frame Configurations

Cross frame configurations were varied between X and K shapes to study their influence on applied stress ranges. Figures 2.35-a and b show the stress ranges due to a Single HS20 Truck Load at the top and bottom flanges of girder G2 on a right bridge for the two types of cross frames. From these figures, it can be seen that the stress ranges did not vary due to X and K configurations. Similarly, Figures 2.36 and 2.37 represent the stress ranges with a 30° and 60° skewed bridges, respectively. These figures also show that the applied stress ranges do not vary with the two types of cross frames.

Though cross frame configurations do not play a significant role in the variation of applied stress ranges, their role in attracting axial forces is important. During

analytical simulation of the skewed bridges, diaphragms were provided parallel to the support whereas intermediate cross frames were normal to the girders, according to AASHTO requirements for the supports skewed more than 20°. From the analytical simulation, total axial forces due to composite and non-composite dead loads and multi-lane HS20 Truck and Lane Loads in the different cases of diaphragms (as shown in Figure 2.7-a) were obtained and are presented in Tables 2.4 to 2.21. In the case of right bridges, the axial forces in those members are almost zero. This might be attributed to the zero differential vertical deflection between girders at the support locations. Tables 2.4 and 2.6 present the axial force in different members of X Type diaphragms of 30° and 60° skewed bridges. From these tables, it can be seen that the exterior diaphragms are subjected to more axial forces than the interior diaphragms. This might be attributed to either the differential displacement between girders at roller supports in the longitudinal direction, the differential vertical deflection of the adjacent girders, or the combination of the two reasons. As skew angle increases from 0° to 30°, there is substantial increase in the axial forces of the diaphragm member. However, increase in skew angle from 30° to 60° resulted in little decrease of axial forces. This might be attributed to the difference in support positions and additional cross frames in the case of the 60° skewed bridge.

Axial forces of K Type diaphragm members in the 30° and 60° skewed bridges are tabulated in Tables 2.8 and 2.10. Similar patterns of increase in axial forces from 0° to 30° skews and little decrease from 30° to 60° skews can be observed in K Type diaphragm members as in X type. However, due to the stiffer geometry and clear load path of X Type diaphragm members, these members attracted almost 100% more axial forces than

K Type members. Tables 2.12 through 2.15 present the axial forces in the K Type diaphragm members of 30° to 60° skewed bridges with different girder depths. Axial forces in diaphragm members are not influenced by different girder depths. In these cases, diaphragm members are subjected to relatively small forces than the other previous cases. Similarly, Tables 2.16 through 2.19 present the axial forces in the K Type diaphragm members of 30° and 60° skewed bridges with different girder spacings. In the case of widely spaced girders with same cross-sectional area, diaphragm members attracted lower axial forces because they had lower stiffness due to longer length. In the closely spaced case, these members, being very stiff, attracted the highest axial forces.

The axial forces in the intermediate cross frames of the second span of the representative bridge for the three different skew angles were tabulated in Table 2.20. This table indicates that intermediate cross frames are subjected to relatively smaller axial forces than the diaphragms at the supports. As skew angle increases, the axial force in the intermediate cross frames increases. The axial forces in the lower chord member between the two interior girders substantiate this statement.

2.7.6 Cross Sectional Area of Cross Frames

Figures 2.38-a and b show the variation of the stress ranges at the top and bottom flanges of girder G2 on a right bridge of K type cross frame due to a Single HS20 Truck Load and varying cross sectional area. From these figures, it can be seen that the cross sectional area does not have any effect on the stress ranges in the girder. Similarly, Figures 2.39 and 2.40 show the stress range variations for skew angles of 30° and 60°,

respectively. These figures also show that the applied stress ranges do not vary with the cross sectional area of the K Type cross frame.

Similar to the K Type cross frame analysis, the applied stress ranges were plotted for varying cross sectional area of the X Type cross frame. Figures 2.41 through 2.43 show the variation of the applied stress ranges at the top and bottom flanges of girder G2 on a right bridge and two skewed bridges due to a Single HS20 Truck Load and varying cross sectional area. From these figures, it can be concluded that varying the cross sectional area of X Type cross frames did not influence stress range values.

Cross frame cross-sectional area plays a significant role in attracting more axial forces. Analytical simulation of the representative bridge with different cross frame cross-sectional areas was carried out with both X and K Types, and results are tabulated in Tables 2.4 through 2.13. Tables 2.5 and 2.7 present the axial forces in X Type diaphragm members with double cross-sectional areas for 30° and 60° skewed bridges. As cross-sectional area doubles, the axial forces also double in those members. A similar pattern can be observed in Tables 2.8 through 2.11 for K Type cross frames. From these tables, it can be concluded that the axial forces of cross frames increase with an increase in cross-sectional area. This might be attributed to the proportionality of axial force to cross-sectional area of axial member.

2.7.7 Lateral Bracing Configuration

To find the effect of the lateral bracing on the applied stress ranges, the original bridge in right form, with and without lateral bracing, was simulated by using the 3-D structural analysis. Figures 2.44-a and b show the variation of stress ranges at the top and

bottom flanges of girder G2 of a right bridge with and without lateral bracing subjected to a Single HS20 Truck Load. From these figures, it can be observed that the presence and absence of lateral bracing did not cause any variation in the stress ranges.

The effect of skew angle on axial forces in lateral bracing was studied in three skewed bridges. The location and numbering of lateral bracings are given in Figure 2.8, and corresponding axial forces for the three skewed bridges are presented in Table 2.21. Lateral bracings connected to support locations are subjected to higher axial forces. It can be concluded that as the skew angle increases, the axial force in lateral bracing members also increases.

2.7.8 Effect of Cross Frame and Lateral Bracing on Overall Bridge Deflection

Figures 2.45 and 2.46 represent the variation in the deflection of each girder along the longitudinal direction of a bridge with the varying cross sectional area of X type cross frame and due to HS20 multi-lane Truck Load. From these figures, it was observed that the vertical deflection of the girder does not show any variation with the different cross sectional areas of the cross frames. Similarly, Figures 2.47 and 2.48 show the variation of the vertical deflection of the girder with the varying cross sectional area of K type cross frame. These figures showed the same trend as in X type cross frames. Figures 2.49 and 2.50 show the variation of the vertical deflection for different bridge skew angles. These figures gave the same results for the variation of vertical deflection with support skewness.

2.7.9 Types of Live Loads

Figures 2.51-a and b represent the variation of applied stress ranges in girder G1 of the right bridge due to four different live loads. From these figures, it can be observed that HS20 multi-lane Truck Load and HS20 multi-lane Lane Load caused 75% higher stress ranges and a Single P13 Truck Load caused 200% higher stress ranges than a Single HS20 Truck Load. Similarly, Figures 2.52 and 2.53 represent the variation of the stress ranges of girder G1 for 30° and 60° skewed bridges, respectively. From the figures, it can be seen that the Single HS20 Truck Load applied the smallest magnitude of stress ranges while a Single P13 Truck Load applied the highest magnitude. The stress ranges produced by multi-lane Truck and Lane Loads were almost equal.

Similar to girder G1, the stress ranges were compared with the four different live loads for the other three girders (G2, G3, and G4). Figure 2.54 represents the variation of the applied stress range of girder G2 on a right bridge due to the four different live loads. Figure 2.55 represents the stress range variation for a 30° skewed bridge, and Figure 2.56 represents the stress range variation for a 60° skewed bridge. In the case of girder G2, the multi-lane Truck Load, Lane Load and a Single P13 Truck Load produced approximately the same value of stress ranges whereas in girder G1, only the multi-lane Truck Load and the Lane Load produced approximately the same value of stress ranges. The main difference between the results in girders G1 and G2 is that the tributary area for the multi-lane Truck Load and the Lane Load for girder G2 is larger than that for girder G1. Figures 2.57 to 2.59 illustrate the variation of the applied stress ranges for girder G3 due to the four different live loads at the three skewed angles. These figures show that girders

G2 and G3 are subjected to equal and similar patterns of stress ranges due to the symmetry of the interior girders. Similarly, Figures 2.60 through 2.62 show the variation of the applied stress ranges for girder G4 for three skewed cases. In conclusion, it was observed that a Single P13 Truck Load gave approximately 200% higher stress range values than a Single HS20 Truck Load for all of the girders at different values of skew angle.

Chapter 3

Fatigue Evaluation-Allowable Fatigue Stress Ranges

3.1 Introduction

As outlined in Chapter 2, fatigue evaluation of steel bridges depends mainly on applied and allowable stress ranges. Fatigue cracking and/or propagation will occur if the applied stress range at a particular detail exceeds the allowable fatigue stress range. The allowable fatigue stress ranges that are in the 15th Edition of AASHTO are based on the experimental tests that were originally conducted in the 1970's at Lehigh University [14, 15]. These values are dependent on the number of cycles, type of details and redundancy.

In early fatigue design specifications, the allowable stresses were expressed in terms of maximum and minimum stresses. These provisions were based on the available data at that time and on some small-scale specimens. Two million cycles was generally assumed to be the infinite fatigue life. Current bridge design specifications express the allowable stresses in terms of stress ranges from the minimum to maximum value. Most of these current provisions are based on the constant amplitude fatigue test data while the actual bridge structures experience variable and random amplitude fatigue cycles. Fatigue damage due to a given number of cycles of different stress ranges of variable and random amplitude fatigue can be related by the equal number of effective stress ranges. This concept of effective stress range will be presented in this chapter.

3.2 Allowable Fatigue Stresses in AASHTO

According to 15th Edition of AASHTO, the allowable fatigue stresses depends mainly on the following factors:

- Number of stress cycles
- Types of connection details

3.2.1 Number of Load Cycles

The 15th edition of AASHTO bridge design specifications combines an artificially high stress range with an artificially low number of applied fatigue stress cycles. The number of load cycles in the present AASHTO design procedures is based on approximations of actual conditions of steel bridges. These values were established before rational information were available on the variable-amplitude fatigue behavior of bridge members and actual stresses were recorded in bridges. The AASHTO fatigue values do not accurately represent the loading conditions that occur over the life span of the bridge. This can be shown by calculating the number of loading cycles on a bridge due to numerous truck passages. For example, by taking the design life of a simple span girder bridge to be 50 years, the number of cycles per truck passage is equal to 1.5 (will be discussed later), and the Average Daily Truck Traffic (ADTT) is equal to 2000; therefore, the life of this bridge would be approximately 54,750,000 cycles. The allowable fatigue stresses in a Category C detail of a redundant structure for this number of cycles can be calculated by taking the detail constant value to be 44×10^8 (Table 3.1) and using it in equation 2, which will be given later. This gives a value of allowable stress as 4.3 ksi, which is 43 percent of the allowable stress value allowed by the 15th

edition of AASHTO. It has also been shown by field measurements that the actual stress ranges in steel bridges are generally substantially less than those calculated for the HS20 Truck Load by current AASHTO procedures [9].

3.2.2 Allowable Stresses

The bridge details that are susceptible to load induced fatigue cracking are classified into eight categories by fatigue resistance, called detail categories. These categories, i.e. A, B, B', C, D, E, E', and F, are associated with severity and allowable stresses corresponding to various design lives. These categories were defined by the 95 percent confidence limits for 95 percent survival based on the regression analysis of the test data [15]. In the AASHTO LRFD Specifications, Category F for the allowable shear stress range on the throat of a fillet weld has been eliminated and replaced by Category E because shear stresses in the weld are usually low enough so that cracks do not occur in the weld itself [2, 10].

Since the stress range is the important stress parameter in determining fatigue life, a stress range (S)-cycle life (N) relationship of each detail category can be developed. This relationship for fatigue behavior in each category is conservatively represented by corresponding S-N curves. An S-N curve is defined as a plot in which the horizontal axis represents the number of cycles, N, until the failure of a particular detail, and the vertical axis represents the stress range (S). Regression analysis showed that the relationship between S and N was log-log in nature with a constant slope [15]. These S-N curves can be defined in log form by:

$$\log N = \log A - B \times \log S_r \quad (2)$$

and in exponential form by:

$$N = A \times S_r^{-B} \quad (3)$$

where log A is the log-N-axis intercept of the S-N curve, S_r is the nominal stress range, and B is the slope of the curve. The linear regression analysis for each category yielded a unique value for the slope, B, of -3. AASHTO LRFD Specifications [2] replaces S_r of equation 3 by $(\Delta F)_n$ and establishes the new equation for plotting S-N curves as:

$$(\Delta F)_n = (A/N)^{(1/3)} \geq 1/2(\Delta F)_{TH} \quad (4)$$

for which :

$$N = (365)(75)\, n\, (ADTT)_{SL} \quad (5)$$

where:

A = constant LRFD Table 6.6.1.2.5-1

n = number of stress range cycles per truck passages

$(ADTT)_{SL}$ = single lane ADTT (the average daily truck traffic)

$(\Delta F)_{TH}$ = CAFL taken from Table 3 (ksi) [2]

$(\Delta F)_n$ = nominal fatigue resistance of the details.

From the values n and $(ADTT)_{SL}$, the value of N can be calculated by using equation 5. Then by taking the value of detail constant, A, for each detail category and the calculated value of N, the nominal fatigue resistance of each category can be determined using equation 4.

3.3 Number of Cycles Due to Truck Passage

The number of stress range cycles per truck passage, n, is dependent upon several factors, such as span length, bridge type, member type and member location. Each complex cycle produced by a truck passage consists of a primary cycle with superimposed secondary cycles. The secondary cycles can be the result of dynamic effects, roadway surface conditions, axle spacing, or multiple truck loadings and all are effected by the span length of bridge. As a single HS20 truck moves across a bridge, the theoretical moment variation at any point is similar to actual variation of stress in a bridge subjected to traffic loading, although the curve is more rounded and may have small vibration stresses superimposed as a result of dynamic effects [13, 14].

These vibration stresses in a bridge form different shapes of complex cycles which can be obtained by plotting the moment variation of particular point of interest along the length of bridge. These complex cycles can be decomposed into many individual simple cycles (primary, secondary, and tertiary) of different sizes. These simple cycles of different sizes can be represented by an equivalent number of cycles of the same size. The decomposition of a complex cycle into simple cycles can be done by keeping in mind that the reversals involved in any complex cycle can cause the same extent of fatigue damage as individual simple cycles of the same size. Thus, the equivalent number of simple cycles for complex cycles can be calculated.

The formula that can be used for this procedure is given by [3]:

$$(N_{ec,p}) = 1 + (S_2 / S_1)^3 + . (S_i / S_1)^3 ...+... (S_n / S_1)^3 \qquad (6)$$

where $N_{ec,p}$ is the equivalent number of cycles (primary cycles) for a complex cycle and S is the mean stress range the member can sustain for a given number of applied stress cycles, N. Table 3.2 presents an example that outlines sample calculations. The number of equivalent stress cycles per HS20 and P13 Truck passages was equal to 1.5 and 1.1 respectively. The first value obtained for a single HS20 Truck Load is the same as the value in the new LRFD Specification [2]. By substituting these values of n in equation 5 to obtain N and taking the corresponding value of A from Table 3.1, S-N plots due to Single HS20 and P13 Truck Loads for each detail category were obtained and are given in Figures 3.1 and 3.2 . These plots represent the variation of allowable stress ranges with the number of applied stress cycles due to a Single HS20 Truck and a Single P13 truck.

Since LRFD Table 3.1 specifies the same value of detail constant, A, for Categories E and E', variation of allowable stress ranges of both these details is represented by one line of Category E in Figures 3.1 and 3.2. From these figures, it can be seen that detail categories E and E' are very susceptible to fatigue cracking since they have very low allowable stress ranges.

3.4 Fatigue Damage due to Legal and Permit Loads

Most structures that are loaded cyclically are subjected to random variable loading during their lifetime. The magnitude and frequency of occurrences of such a loading are functions of time. Miner's Rule is widely used to relate this variable-amplitude fatigue behavior to constant-amplitude behavior.

According to Miner's assumptions, variable stress cycle damage is accumulated in proportion to the relative frequency of occurrence of each level of stress range. This can

be summarized in the form of cycle ratio, $\frac{m}{N}$,or damage fraction, where m is the number of cycles applied at a certain stress level S, and N is the number of stress cycles to failure at stress level S. When the accumulation of these "increments of damage" at several stress levels becomes unity, failure could occur. The damage fraction, $\frac{m}{N}$, due to one cycle of loading is given by $\frac{1}{N}$. It can be noted that $\frac{1}{N}$ of the fatigue life of any loading is consumed by the application of one cycle of that loading. The cumulative damage concept states that failure occurs when $\Sigma\left(\frac{m}{N}\right) = 1$ [8].

A stress-range histogram obtained from field measurements on a bridge under normal traffic can be used to calculate the nominal stress range. The effective stress range [10] is given by:

$$S_r = (\Sigma\, \alpha_i\, S^3_{ri})^{1/3} \quad \text{.....(7)}$$

where α_i = fraction of stress ranges within an interval i,

S_{ri} = mid width of stress interval i,

S_r = effective stress range.

Equation 7 can be used to evaluate the fatigue capacity of steel bridges by calculating the effective stress range as shown in Table 3.3.

Miner's cumulative damage rule was applied to determine the most damaging live load. The ADTT were approximated based on the current NDOT loading for fatigue design. Currently, NDOT uses the following number of cycles in fatigue design:

- Over 2 million cycles for a Single HS20 Truck
- 2 million cycles for Multi HS20 Truck
- 500,000 cycles for Multi HS20 Lane
- 100,000 cycles for a Single California P13 Truck

By using equation (5) and substituting the value of n as 1.1 for a single P13 Truck, 1.5 for a single HS20 Truck, and 1 for both Multi Lane HS20 Truck and Lane loading, the values of ADTT were obtained. To accommodate all the factors that affect ADTT, such as location of the bridge, time of the day, day of the week and season, the ADTT values obtained from above equation were varied between the lower and upper ranges of the actual ADTT obtained from equation 5. The ADTT that were assumed in this study are:

- Single P13 Truck: 3, 4 and 5
- Single HS20 Truck: 2000, 3000, and 4000
- Multi-HS20 Lane Loading: 15, 18, and 20
- Multi-HS20 Truck: 60, 70, and 80

With these ADTT and n values, the total number of cycles for each interval were obtained and the frequency of occurrences of each interval was calculated. The maximum stress range values obtained from analytical simulation for different bridges cases were selected, and stress histograms were plotted and presented in Figures 3.3 through 3.6. In these figures, the X-axis represents the frequency of occurrences of stress

ranges, and the Y-axis represents the stress ranges. As it can be seen from column 5 of Table 3.3, the first three intervals of frequency of occurrences (0.008, 0.016, 0.032) are for stress ranges caused by a P13 Truck. Similarly, values for the other three intervals of frequency of occurrences for stress ranges due to Multi HS20 Lane Loading, Multi HS20 Truck Loading, and Single HS20 Truck Loading are given in column 5 of Table 3.3. These histograms represent the frequency of occurrence of stress ranges caused by legal and permit loads with different magnitudes for each case of simulation and with variation of each parameter.

From these histograms, it can be seen that a Single HS20 Truck Load has the highest percentage of frequency of occurrence. The percentage of damage for the original bridge was calculated by using equations 5 and 7 and is presented in Table 3.3. It is clear that a Single HS20 Truck produces higher percentages of damage than the other loadings. This also indicates that the fatigue damage results from the average or typical condition rather than the extreme condition of loading. High frequencies of occurrence of low stress ranges are more damaging than the small frequencies of occurrence of high stress ranges. This is because more repetitions are required to cause a failure of the member under consideration. Though a Single P13 Truck, Multi HS20 Truck, and Multi-Lane Load gave the higher stress ranges, the lower values of frequencies of occurrence of their higher stress ranges caused less damage than the higher values of frequencies of occurrence of low stress ranges due to a Single HS20 Truck. In conclusion, a Single HS20 Truck causes the most fatigue damage because of its higher frequencies of occurrence.

Chapter 4

Survey of Fatigue Evaluation Procedures, and Repair Methods for Steel Bridges

4.1 Introduction

The fatigue design of steel highway bridges varies from state to state because of different approaches to bridge rehabilitation and fatigue retrofit. The variation is due to different climates, intensity and volume of traffic flow, present age of bridges, bridge geometry, past experience, etc. Since the Nevada State Highway System has experienced fatigue problems with some steel bridges, it started a research project to identify appropriate parameters for fatigue evaluation and strategies for fatigue crack repair. To avoid duplication and to learn from the collective experience of various states, it was felt relevant to collect and compile different fatigue repair methods currently used by the fifty states. To obtain information on how different states are approaching the fatigue evaluation procedures and repair methods for steel bridges, a survey questionnaire was prepared with the coordination of NDOT bridge engineers.

4.2 Survey Questionnaire

Concentrating on fatigue crack problems and repair strategies, a fatigue evaluation procedures, and repair methods for steel bridges questionnaire was compiled. The states were asked to provide brief information on fatigue problems that they have experienced, their evaluation procedures to resolve in-plane load induced and out-of-plane distortion

induced fatigue problems and their fatigue analysis procedures. Questions were also asked also on repair methods, relation of applied stress range to repair methods, and exclusion of welding from fatigue. Evaluation of remaining life for fatigue cracks and its effect on choice of repair methods, and their view on welding on tension flange and the termination of welding on tension zones were also included in the questionnaire. Every aspect associated with fatigue evaluation procedures and repair methods was tried to address in the questionnaire.

4.3 Survey Process

A letter with the survey questionnaire was sent to the bridge division of the transportation (highway) departments of all 50 states, the Commonwealth of Puerto Rico, and the U.S. Department of Transportation in June of 1996. The model of survey questionnaire that was used is presented in Appendix 1. Each state was asked to provide information mainly concentrating on the questionnaire sent to them and any special measures or strategies that they have followed for fatigue evaluation and repair that were included in the questionnaire.

4.4. Responses

Information was received from the 32 states, representing all geographic regions of the country, which are presented in Figure 4.1. The information obtained from each question was compiled and compared to the ideas of other states on particular question. The following are the verbatim responses of states who responded to the survey.

1. **Please categorize any fatigue problems that you have experienced in steel bridges in the last 15 years.**

AK

- Floor beam girder connections

AR

- Box and plate girder web cracks at end of transverse connection plate due to out-of-plane bending.
- Flange cracks at end of coverplates on simple spans due to improper length of coverplate.
- Cracks in other members (trusses, arches) due to out-of-plane bending.

CA

- **Out-of-plane bending**: on girder webs at the bottoms of tight fit transverse stiffeners usually where cross frames (mostly staggered) are connected, primarily on the stiffener/web weld, web plate, web to bottom flange weld; on transverse deck floorbeams at the tops/bottoms of welded transverse stiffeners where deck stringers are attached to the stringer, same areas as above.
- **High cycles low amplitude vibrations/distortions**: on secondary bracing elements and their connection gusset plates.
- **In-plane load induced**: deck system stringers at the stringer-to-floorbeam connection, in the stringer web at or very near the connection detail, usually initiating at a cope cut into the stringer web.

CT

- Coverplated rolled beams
- Floorbeam Connections
- Distortion Induced web cracking
- Cracking in diaphragm
- Wind bracing gusset plate weld
- Fracture of flange at notch from impact damage.

DE

- Cracking.

FL

- Fatigue cracks initiation in tack welds
- Out-of-plane bending at diaphragms of steel box girders
- In machinery supports-movable bridges
- Fatigue cracks in connection plates between bascule girder and counterweight.

GA

- Out-of-plane bending from floor beam connections in a deck truss.

IN

- Tapered cover plates
- Jacking frames details
- Intermediate diaphragm details.

IA

- Out-of-plane web cracks at transverse member connections

- In-plane web cracks at welded connections in tension areas
- In-plane tension flange cracks
- We have experienced about every conceivable type of fatigue crack.

KS

- Cracks at top of stiffeners- out-of-plane bending; cracks through girder flange and web due to weld problems.
- Horizontal cracks in web due to weld and fatigue problems.

KY

- Cracking in plate girders due to longitudinal stiffeners.
- Cracking in clip angles at stringer to floor beam connection.

LA

- Out-of-plane bending with plate girder cross-frames, cover plates, cracking at plate termination.

MD

- 90% cracks in the weld that rapped around the bottom, positive moment region, and top, negative moment region, of an intermediate diaphragm connection plate that is not welded to the girder flange.

MI

- Category B, C, for plate girder; and Category E or rolled beam

MN

- Floor beam to stiffener connections
- Stiffener/Gusset weld intersection
- Material Flaw
- Cover Plate ends

NE

- In-plane bending, out-of-plane bending, corrosion induced cracking, cracking from copes at tops of floorbeam ends, fractured bridge pins in pin and hanger expansion devices, cracking in floorbeam to girder connection angles.

NJ

- Cracks in welds at the end of cover plates (Category E & E')
- Cracks in welds at the termination of longitudinal web stiffener sections (Category E)
- Cracks in coped flanges at the re-entrant corners
- Cracks in girder webs at the end of diaphragm connection plates.

NC

- Floor beam to main member connection in movable bridges.

ND

- We haven't experienced any fatigue problems.

OK

- Cracks in diaphragm copes, some stringer copes
- Cracks at ends of welded cover plates
- Cracks to welds of transverse stiffeners. (often at diaphragm connections)

- Cracks to girder webs above or below welded diaphragm connections. (due to out-of-plane forces).

OR

- Approximately 60% of the fatigue problems are web cracks that are caused by out-of-plane bending. Another 25% is found in clip angles connecting stringers to floor beams and copes ends of stringers. The remaining 15% are cracked tack welds on riveted members and welded attachments. These numbers do not include the fatigue problems we have with expansion joints or machinery in movable bridges.

PA

- Load induced fatigue
- Displacement induced fatigue.

SD

- Majority has been out-of-plane bending due to web gaps.

TN

- Termination of stiffener welds at crossframes connections
- Termination of coped flanges in crossframes members
- Gusset plate to web plate welds in the plane of lateral bracing
- Cracks in butt welds and base material of tension flanges.

TX

- Out-of-plane bending. This is our primary problem in Texas.
- Live load induced in-plane bending This has been rare in Texas and when it has occurred, it has usually been induced by some type of impact damage.

UT

- Cover plate cracks at the toe of the fillet welds, especially where the intermediate fillet welds are used
- Coped flange of the floor beam in a riveted structure
- Short stiffener below stringer framed into the floor beam
- End of stiffeners on web-gap region.

VT

- We have experienced very few fatigue problems in Vermont. The only problems that we have experienced are the following:
- Cracks in a longitudinal stiffener butt weld, perhaps due to a poor weld
- We also have some cracking occurring in the coped area of some **cantilevered ears or pork chops** on a two girder interstate bridges.

VA

- Cracks

WA

- See attached list of bridges with fatigue cracking for location and repair method
- Ragged web copes in floor beams and stringers
- Riveted truss tension chord
- Out-of-plane web plate

- Top plate weld in pin bearings
- Gusset plate of laterals(long spans)
- Rivet heads
- Large modular expansion joints
- Skewed bridges
- Clip angles stringer or chord to floor beam
- Open steel grid decks and their connections.

WV

- Web cracks in steel girders caused by out-of-plane bending
- Cracks welds in riveted girders where welds were placed, without being documented on shop drawings.

WI

- Out-of-plane bending-floorbeams to main girder.

WY

- Cracks in welded plate girder webs caused by out-of-plane bending at cross-frame locations. Approximately 15 bridges.
- Cracks propagating from coped areas of steel floor beams at connection points with girders.

2. **What are the evaluation procedures that you use to resolve in-plane load induced and out-of-plane distortion induced fatigue problems?**

AK

- No formalized policy.

AR

- Check stress and allowable fatigue stress range for in-plane loads.
- Visual inspection and judgment to resolve difference.

CA

- Inspection; penetrant NDE; strain gauging where appropriate; traffic data; structural analysis/modeling where appropriate; empirical data/past experience.

CT

- We most often try to eliminate the distortion by bolting or welding. Evaluation is almost impossible, even with finite element.

DE

- Nondestructive testing.

FL

- Analysis, review by structural engineer.

GA

- Periodic inspection: Investigation of fatigue cracks using magnetic particle analysis and dye penetrant analysis.

IN

- Not answered

IA

- Do not understand the question.

KS

- Calculation of stresses and deflections caused by live loads
- Field data to check stress range.

KY

- Visual inspection of all bridges of two year intervals. We do not have a special evaluation procedure for fatigue problems other than locate poor fatigue details.

LA

- Not answered

MD

- We have had consultants perform finite analysis and non-destructive field load tests to determine the stresses resulting from in-plane load induced and out-of-plane distortions for at least three bridges. From this analysis, we have made retrofit repairs to locations that exceed the allowable fatigue stress levels.

MI

- Bolt plate to resolve the out-of-plane distortion.

MN

- Review fatigue detail repair procedures in AASHTO and other relevant publications and we rely on repairs that have worked well for us in the past.

NE

- We try to limit the stress by using more rigid connections or splice plates or eliminate the member driving the out-of-plane bending.

NJ

- Hands on inspection of fatigue prone details as a part of fracture critical member inspections and close visual as a part of routine inspection.

NC

- No set procedure.

ND

- None.

OK

- Usually GTSTRUDL -3D.

OR

- In-plane loading problems are generally solved with linear elastic stress analyses. If no fatigue cracks are known to exist in the structural member of concern we will compare the calculated stress range to the variable amplitude fatigue limit (VAFL) for the particular detail. If the calculated stress range is significantly lower than the VAFL, the analysis is terminated and we conclude that fatigue problems will most likely not occur in this situation.

- If fatigue cracks are present and/or the calculated stress range is above the VAFL we will specify the initial and final crack geometry and perform a

fatigue life evaluation using linear elastic fracture mechanics (LEFM). If cracks exist we also calculate the fatigue life after retrofitting using the same principles.

If loading is difficult to calculate we typically will use strain gauges or other testing instruments to quantify the loading. We are heavy users of nondestructive testing (NDT) including UT, MT and AE testing. The field data will then be used for a fatigue life estimate.

There are a few occasions when an elastic-plastic fracture mechanics approach is used but this is not typical .

Most out-of-plane problems have come from transportation loading. In this situation we will calculate the size of a threshold crack and compare it to the existing cracks. Those that came from actual love load or thermal loading are typically subject to a field test to quantify the load spectrum. Sometimes it is not practical to perform a field test. In these cases we will use rough estimates and good engineering judgment.

PA

- Ref. attached procedures which are an excerpt of Pennsylvania Design Manual Part 4

SD

- Calculate theoretical live load stress range.
- In some cases, verify by the use of strain gages.
- Research history of problem
- Based on above data, select a repair detail

TN

- Visual based on in-service performance.

TX

- Not answered

UT

- Drill hole usually one inch in diameter.
- Increase web-gap.

VA

- None

WA

- Determine if repair should provide flexibility or load path and detail repair accordingly. Repairs are only made if cracks are found.

WV

- Visual inspection

WI

- On site observation

WY

- Not answered

3. **Please explain how do you account for the following in fatigue analysis.**
   ⇒ Structural Analysis Level (2D or 3D)

AK

- No familiar

AR

- 2D

CA

- 2D analysis is not widely used, except for gross stress range; 3D analysis is rarely used. We have found that the distressed areas are very difficult to accurately model, the loads are difficult to predict; strain gauge calibrations to model forces may cloud the actual driving mechanisms(s)

CT

- 2D

DE

- 2D

FL

- Generally 2D

GA

- 2D Analysis, Avoidance of fatigue prone details, Limit Stress Range

IN

- Not answered

IA

- 2D only

KS

- 2D analysis, also applied to floor beams where they exist.

KY

- Division of Bridge Design has not performed a fatigue analysis for repair purposes.

LA

- Normally 2D, although we have 3D capabilities.

MD

- 3D Finite element analysis.

MI

- No.

MN

- We frequently do not perform a detailed analysis. For situations where the solution requires modifications more extensive than drilling holes we will use 2D analysis and have used 3D rarely.

NE

- Not answered

NJ

- 2D

NC

- 2D

ND

- 2D

OK

- Only AASHTO fatigue truck

OR

- Almost every fatigue problem is given some form of analysis. If the problem lends itself we use 2D, if not we use 3D. For non linearity's such as composite action of steel and concrete we will typically bracket the analysis and find the bounds of the solution. If the conservative assumptions do not provide desirable solutions we go and field test the structure and use that data for analysis. We also have non-linear FEA code that is used for some problems.

PA

- Refined Methods of analysis
- Please reference P A5-6 of the attached
- Note that α in eq 5-2 is equal to 0.5 for AASHTO simplified and is equal to 0.8 for refined methods.

SD

- Straightforward bending analysis is used.
- We do not use finite element

TN

- Analysis done is 2D.

TX

- 2D

UT

- Not answered

VT

- Our fatigue analysis is calculated using 2D analysis.

VA

- Not answered

WA

- WSDOT does not distinguish between analysis levels for fatigue evaluation.

WV

- 2D

WY

- Calculate stress range from live load moment from BRASS analysis for 2D.

⇒ **Type and configuration of truck that you use in fatigue evaluation. Do you include the permit truck in your fatigue evaluation?**

AK

- Permit truck have not been considered except for industrial use highways.

AR

- AASHTO truck; permit truck not included

CA

- HS20 truck family or utilize test vehicles of known axle configuration and weight (similar to Type 3); we have not included permit vehicles in the analysis.

CT

- We use actual truck history data.

DE

- AASHTO HS-25 Loads including Delaware legal truck.

FL

- Generally AASHTO design truck, may investigate FL legal trucks

GA

- HS20. No, we do not use the permit truck.

IN

- Not answered

IA

- AASHTO HS design truck only

KS

- H, HS, T-3, T352, T3-3 are rated using fatigue criteria.
- Permit truck are not rated for fatigue.

KY

- Not answered

LA

- HS20 Truck

MD

- Legal size vehicles-usually both the HS20 and T-3 dump Truck

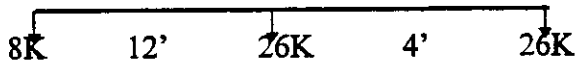

The permit truck is included in the fatigue evaluation.

MI

- No.

MN

- We use AASHTO fatigue vehicle to evaluate existing bridges unless weigh in Motion information is available.

NE

- HS25

NJ

- AASHTO HS
  Type 3
  Type 3-3
  Type 3S2(Modified to 80 tons)

NC

- Legal load vehicles and HS vehicles. No permit trucks.

ND

- HS25

OK

- Only AASHTO fatigue truck.

OR

- For analysis we use the AASHTO fatigue truck. On some long span structures, we include permit trucks. Typically axle loads control the fatigue life for most of our inventory. For field testing we typically use our Snoopier truck as a load source because it resembles the AASHTO fatigue truck. For the best assessment we will leave strain gages in select locations and collect rain flow data for a period of time-- typically one day to two weeks. We also collect burst time histories to validate the larger loads in the rain flow collection. From this data we calculate an effective stress range based on Miner's damage law. This effective stress range is used either for comparison to the VAFL or used in the LEFM analysis.

PA

- Ref. P.A.5-20 of attachment.

SD

- We use typical design load trucks.

TN

- We do not perform re-analysis of structures exhibiting fatigue problems, We simply correct the problems in the field.

TX

- HS15 truck in accordance with 1990 AASHTO "Fatigue Evaluation of Existing Steel Bridges". Permit loads are not considered in our fatigue analysis.

UT

- AASHTO HS20 Truck
- No

VT

- We use AASHTO HS25 truck in fatigue evaluation and do not use the permit truck.

VA

- Not answered

WA
- WSDOT does not include any permit trucks in our fatigue evaluation. All analysis is based on the AASHTO Standard Specification loads.

WV
- HS-25, Military
- Do not include the permit truck.

WI
- No analysis

WY
- Just HS20

⇒ **The number of truck passages. Do you use AASHTO or do you utilize weight station data?**

AK
- Generally AASHTO

AR
- AASHTO

CA
- When used, traffic counts/ADTT are used.

CT
- Weigh station data is used most often.

DE
- AASHTO

FL
- Use AASHTO

GA
- >2,000,000 cycles. We use AASHTO criteria

IN
- Not answered

IA
- AASHTO Only

KS
- AASHTO criteria.

KY
- Not answered

LA
- Use AASHTO specs.

MD
- AASHTO is used.

MI
- AASHTO 10.3.3.5 is used.

MN
- Use Weigh in Motion Data when available. Otherwise we use ADTT's.

NE

- In design, we use ADTT and use the 15th edition of AASHTO. We are switching over to LRFD.

NJ

- AASHTO

NC

- AASHTO

ND

- AASHTO - 100,000 cycles
- 500,000 cycles for some urban interstate.

OK

- Both. AASHTO and on some fatigue studies we have used weight station data

OR

- We use current traffic volume tables published by the Transportation Research Section of the Oregon DOT. If we collect rain flow strain data, we use the counts off the data set.

PA

- We use both.

SD

- We use estimated traffic counts form our state inventory.

TN

- N/A

TX

- We use in-house traffic counts and apply the appropriate factors in analysis outlined in "Fatigue Evaluation of Existing Steel Bridges".

UT

- AASHTO

VT

- We use the number of cycles that are in AASHTO

VA

- Not answered

WA

- WSDOT utilizes AASHTO. The number of cycles is an administrative decision. Generally set at 2,000,000+ cycles for truck and 500,000 cycles for lane loading.

WV

- AASHTO

WI

- Not used

WY

- AASHTO

⇒ **Do you use AASHTO's Fatigue Guides Specifications for determining allowable fatigue stress ranges?**

AK
- Yes.

AR
- Yes

CA
- Not widely used, but sometimes on a case by case basis.

CT
- In some cases. We also use methods developed by John Fisher.

DE
- Yes.

FL
- Yes

GA
- Yes.

IN
- Not answered

IA
- No we use AASHTO Table 10.3.1A

KS
- Yes

KY
- Not answered

LA
- Yes

MD
- Yes

MI
- Yes.

NE
- No

NJ
- Yes

NC
- Yes

ND
- No, we use AASHTO standard specifications.

OK
- Yes.

OR

Yes or no. In general we use the procedures outline for estimating the stress range but do not apply the safety factors to the stress range as recommended. If the calculated stress range is significantly below the VAFL then we assume that no fatigue problems will occur with the member in question under current loading. If it is near or above the VAFL we use a LEFM approach and calculated the life or appropriate inspection period. Most of our use of safety factors in fatigue analyses comes at the end of the analysis. Much judgment is used.

- We do this only after analyzing and field testing many bridges. This gives us the needed confidence to apply our own safety factors. Of course the redundancy of the structure and inspection quality will also affect the safety factors used.

PA

- Yes, with some modifications.
- We include a Pennsylvania traffic factor (see attached P.A. 5-4)

SD

- Yes

TN

- If analysis were done, we would look both at the standard specifications and the guide specifications for fatigue evaluation of existing bridges.

TX

- Yes.

UT

- Yes

VT

- No, we utilize the information that is provided in the AASHTO bridge specifications.

VA

- Not answered

WA

- WSDOT does not utilize the fatigue guide specifications. Current practice utilizes the 1992 AASHTO standard specifications Table 10.3.1A

WV

- Yes

WI

- Yes

WY

- Wyoming uses AASHTO standard specifications for highway bridges.

4. **What are the repair methods you follow for fatigue cracks?**

AK

- Stop drilling. Cover plates terminated with bolted connection.

AR

- Cut hole at end of crack
- Remove transverse member when possible
- Bolted splice repair

CA

- Drill 1" diameter arrest holes; single cracks less than say 6"-7" long may be welded; multiple/large cracks require plate replacement; starting to use rigid connections from stiffener to bottom flange.

CT

- Peening of coverplate welds prior to cracking
- Bolting
- Welding (where appropriate)
- Removal of portions of connections.

DE

- Arrest cracks by drilling holes at ends. Use splices to restore structure strength.

FL

- For tack welds-remove by grinding, drill holes to stop propagation,
- For out-of-plane bending retrofit detail.

GA

- Replace members, redesign connections, drill holes at the tip of the fatigue crack to arrest its growth.

IN

- Drill holes to stop propagation.
- Place splice plates either side of crack.

IA

- Out-of-plane web cracks: Drill hole at crack tip, retrofit connection to prevent web flexing or remove part of connection stiffener to reduce flexural stresses.
- In-plane flange/web cracks: bolted splices

KS

- Girder repairs by bolted splice plates.
- Out-of-plane bending and tears at stiffeners are drilled out.
- Stiffeners are bolted to flanges.

KY

- Bolted plates, grinding and drilling holes.

LA

- Identify limits of cracks and drill holes
- Use a bolted connection to replace bad detail.

MD

- Retrofits for the intermediate connection plates:

- If the cracks are in the weld material only, we grind out that weld material and perform dye penetration tests to ensure the crack has been removed. Then, a plate bolted to the flange is welded to the end of the stiffener so the connection plate is rigidly connected to the flange.
- If the crack goes into the base metal, we drill out the crack and perform dye penetration tests to make sure the entire crack is removed. Then the same repairs are made as mentioned above.

MI

- Bolt plate across the fatigue crack.

MN

- Not answered.

NE

- Out-of-plane bending stresses at floorbeams separators in girder webs are alleviated by providing a rigid connection to the flange by bolting angles to the transverse stiffener and tension flange.
- If out-of-plane bending stress is caused by diagonal wind bracing, which can be removed, we have removed the bracing to eliminate the stresses.
- In plane bending is repaired by using splice plates across the cracked portion of the girder.
- In the above mentioned we also drill a 7/8" dia. hole at the crack ends.
- Cracks from copes in floor beams are either drilled or left alone depending on their severity and whether they are propagating or not.

NJ

- Peening of weld toes.
- Arrest crack propagation by drilling holes at the tip of the crack
- Use of bolted splices and connections.

NC

- Drilling holes to terminate cracks. Bolted retrofit of coverplate termination. Cut out welds and repair.

ND

- No, experience

OK

- Drilling holes at crack ends. If crack is inside weld-grinding weld off. We replace cracked component if crack is very large. Weld or bolt repairs.

OR

The following must first be identified.

- Identify the driving force that is causing the cracking. This includes loading source, i.e. thermal loads, direct live load, and indirect live load, and any stress concentrations that may be present. Sometimes coring a crack and having a fractographic examination done gives good insight into the driving force.
- Identify the extent of cracking. We use various forms of NDT for this job.
- Identify the allowable limits of cracking and how long it will take to grow to this size. For this assessment we will sometimes use the Chary data from construction

or pull a small core for testing. Other times we will make a conservative estimate based on the material used in the structure.

- Once these three issues are resolved we attempt to design our repair to remove the crack tips and remove the loading that caused the problem in the first place. our methodology is fitness for purpose. As long as the former crack is prevented from further growth and the load bearing area of the member is adequate we are satisfied. Many times if we are going to make a repair anyway we will completely remove the crack and return the connection or member to its original strength which rescues fatigue sensitivity.

- Specific methods include but are not limited to the following:

  - Drill the tip(s) of the crack.
  - Remove the driving force, i.e., prevent out-of-plane distortion or reduce the stress concentration
  - Weld up the crack
  - Redesign the connection
  - Peening
  - Addition of extra members or an alternate load path
  - Leave the crack and monitor the growth
  - Decrease the stiffness of the connection
  - Replace damaged part and monitor

PA

  - We arrest propagating crack tips by drilling a hole and installing a high strength bolt in that hole.

SD

  - Drilling crack tips
  - Weld replacements
  - Do bone retrofit.
  - Peening.
  - Positive connection to reduce web gap.
  - Bolting

TN

  - For termination of stiffener welds, we reattach the stiffener to the tension flange by bolting.
  - Repair tears in coped flange/webs by welding or re-coping or strengthening with stiffeners.
  - Gussets for lateral bracing to web- relocate gussets by attaching to flanges w/bolts
  - Cracks in webs-weld, cracks in tensions flanges-bolts.

TX

  - Welding.
  - Drilling out ends of cracks

- Bolted or welded connections, i.e. stiffeners to strengthen out-of-plane bending areas.

UT

- We have used drilled holes to arrest the crack movement.
- We have used full penetration weld to repair the crack in the web.
- We have removed and rewelded the fillet welds.

VT

- We drill a 1/2" diameter hole at the tip of the crack or we rewarded by gouge and full penetration welding.

VA

- Repairs are tailored to the situation.

WA

- Long cracks are drilled an repaired with bolted cover plates. Short cracks are drilled and bolted at the crack tips(dye penetrant is used to locate crack tip)

WV

- Drill holes
- Attach connection stiffeners to girder flanges
- Remove detail material to allow more movement of web.

WI

- Drilling holes at crack tip

WY

- Small cracks may be gouged out and repaired by welding large and branching cracks usually involve removing the portion of steel connecting the crack and replacing with new material.

5. **Do you relate the repair method to the applied stress range?**

AK

- Yes.

AR

- NO

CA

No

CT

- Yes, for instance if we can weld a connection plate for a diaphragm to the flange (cat. C) to eliminate the distortion , we will, since bolting is much more expensive.

DE

- No.

FL

- No

GA

- Yes, if possible

IN

- Not answered

IA

- No.

KS

- No

KY

- N/A

LA

- No

MD

- Yes.

MI

- No.

MN

- Not answered

NE

- No

NJ

- No

NC

Yes

ND

- No experience

OK

- Yes.

OR

- For most of our high cycle stress range fatigue problems we relate the repair to the stress range or the stress intensity range. We attempt to design our repairs such that the stress intensity range at the tip of the cracks(if they are not removed) is less than 3 ksi-$in^{1/2}$. In some of the low cycle high stress fatigue problems we will use a strain based approach. Out-of-plane loading problems are usually related to displacements or stresses.

PA

- Yes

SD

- Yes

TN

- NO

TX

- No

UT

- No

VT
- Not answered.

VA
- No

WA
- No, Repairs are detailed for improved fatigue characteristics and reliability of installation.

WV
- Yes

WI
- No

WY
- No

6. **Do you exclude welding from fatigue?**

AK
- Normally not, but had on temporary basis.

AR
- Yes, cost and difficulty of weld inspection.

CA
- We will allow welding to the web areas, and will not weld flange areas(except web to flange welds). We are concerned with the generally poor quality and associated local stress problems of field welds.

CT
- No.

DE
- No

FL
- We discourage field welding. We distrust quality of field welds and welders.

GA
- Generally, we do not weld fatigue cracks. It makes for a poor quality weld and it usually refractures at the weld locations.

IN
- Yes, we prefer to do it.

IA
- Yes, if feasible.
- Unsatisfactory experience with field welding under adverse conditions.

KS
- In most cases, bolted splices are preferred. In an area of proven fatigue, why ask for trouble.

KY
- Attempt to exclude all welding from the repair method.

LA

- If it is a poor fatigue detail class, we normally will. Such as Class D or E detail.

MD

- The repair used mentioned in response to Que. #4 does use a welded connection between the plate bolted to the flange and the intermediate diaphragm connection plate. But, we do not reweld a cracked weld caused by fatigue. Unless the problem area is retrofitted, these welds just recrack.

MI

- Yes, we do not know the stress range.

MN

- Not answered.

NE

- We usually try to avoid field welding. We have used welding to repair one fractured girder and a crack in a bent plate floorbeam to girder connection angle.

NJ

- Yes- because of lack of quality control

NC

- Yes- welding could lead to further fatigue problems

ND

- No experience.

OK

- Not always. We rewelded a butt weld once. Because it appeared to be an incomplete weld originally.

OR

- In general we do not use welding for fatigue repairs but if it is suitable we do. It depends on the member or connection of concern and the ability to apply NDT after the repair. Again, we use a fitness for purpose approach.

PA

- The control of field welding bolted splices when possible.

SD

- No

TN

- No

TX

- No

UT

- No, we have applied welding to bridge the gap at the connection plates in out-of-plane deformation where it was determined that this type of repair was adequate.

VT

- We would in some instances for fear of recracking. In that instance we would probably drill a hole at end of crack and bolt on reinforcement.

VA

- No

WA

- WSDOT does not utilize welds as a repair method for fatigue cracks. Field welds are difficult to control preheat and interpass temperature in the field. Weld quality is also difficult to maintain. Embrittlement and shrinkage add stress risers to the weld area enhancing future cracking potential. Weld repairs performed under traffic are not effective.

WV

- No

WI

- No, we evaluate if it will work.

WY

- Welding is allowed in certain cases if the crack can be entirely removed and if the detail causing fatigue is retrofit to prevent future cracking.

7. **Do you evaluate the remaining life for relatively small fatigue cracks? What effect would it make on your choice of repair methods?**

AK

- We have not used this approach.

AR

- No, none

CA

- No analytical evaluation, but increased inspection frequency.

CT

- If the crack is isolated, we will monitor the bridge. If the same crack occurs at many locations, we usually evaluate the bridge. We also have developed (through the University of CT) a portable fatigue evaluation system. We use strain gages to monitor the bridge details under normal traffic. From this we can develop an actual stress range histogram. Then we use this information to analyze the detail according to the AASHTO Guide Specifications.

DE

- No, None

FL

- If fatigue cracks are found, the remaining life may be evaluated. This information may be used for REPLACE VS. REHABILITATION DECISIONS. Length of time structure is to remain in service may effect repair methods chosen.

GA

- Usually not. A remaining life analysis may help you decide to replace the structure

IN

- Not answered

IA

- No,
- No Effect

KS

- No remaining life calculations.
- No effect on choice of methods.

KY

- No. Repair methods are usually detail determined.

LA

- No

MD

- No, we do not evaluate the remaining life for relatively small fatigue cracks. For budget purposes, it could result in monitoring cracks instead of repairing.

MI

- Yes. This has no effect on the choice of repair method. The repair method is bolting the plate to the fatigue crack.

MN

- Not answered.

NE

- We do not do a formal evaluation and usually do not shorten the estimated life for small fatigue cracks. The presence of fatigue cracking will usually cause us to replace the superstructure when the structure requires widening.

NJ

- No

NC

- Yes- no significant effect.

ND

- No experience.

OK

- Sometimes. Almost none. Usually this is for our own information, since by that time we have already decided to do the repair.

OR

- We calculate the remaining life of fatigue cracks based on the LEFM approach. Assuming we have identified the current crack geometry and loading on the member we assign an allowable final crack geometry. We make this selection based on either experience or toughness measurements on the material in question. The vast majority of our structures are fabricated from steel that will fail in a ductile manner under the loading and temperatures they experience. Because of this a LEFM assessment is only

reasonably valid for cracks that are small with respect to the dimensions of the member. Thus we will select a maximum allowable crack length of say 2 or 3 inches and base the remaining fatigue life LEFM as opposed to an stress life or strain life approach.

- We compare the number of stress cycles required to grow the crack to the maximum selected size with the ADTT. From this we can decide how soon we need to make a repair or if temporary repairs are needed.

PA

- Yes, it depends on the structure, ADTT, location etc.,

SD

- No

TN

- No, we would repair by welding or arrest growth by drilling holes at crack tip.

TX

- No.

UT

- We have not evaluated structures remaining life based on fatigue life approach.

VT

- No, None

VA

- No

WA

- WSDOT does not evaluate the remaining life of small fatigue cracks. Small cracks are watched for growth if they are deemed non-critical.

WV

- No
- None

WI

No

WY

- No

8. **What is your state's opinions about welding on tension flange and termination of welding in tension zone?**

AK

- Attempt to avoid. Use mechanical termination. When unavoidable we follow AASHTO.

AR

- Try to avoid, however, allow welding when AASHTO fatigue requirements permit and the weld is properly inspected.

CA

- We do not allow welds/welded repairs on the tension flange; we evaluate the type of weld and detail in the tension zone of girder webs and secondary elements and approve it on a case-by-case basis.

CT

- If the element of the bridge is designed according to AASHTO, we allow the weld. John Fisher stated that if you design according to the AASHTO standard Specifications, the detail will not crack.

DE

- Do not permit welding on tension flanges

FL

- Details may be welded on tension flange, but stress range for appropriate detail most be met. We do not allow utility attachments to be installed with welding.

GA

- We currently weld to the tension flange for some shear connections and for gusset plates for diaphragms. This seems to be all right. We do not terminate cover plates in tension zones or end longitudinal stiffeners or bottom lateral gusset plates in the tension areas of webs.

IN

- Not answered.

IA

- Avoid if possible.

KS

- On new structures, Kansas prefers to weld intermediate stiffeners to both flanges when the stiffeners are used as connecting plates for cross frames. The flange stress is investigated for fatigue. Otherwise, keeping all transverse welding out of tension zones is preferable.

KY

- We prefer not to field weld to any tension flanges or tension zones.

LA

- We try to avoid stress Category D and E details.

MD

- Welding to the tension flange is allowed but in accordance with AASHTO's requirements (allowable stress range, stress Category)

MI

- No welding is done in the tension flange.

MN

- Not answered.

NE

- On our new structures we are welding the transverse stiffeners to the tension flange at separators if the allowable fatigue stress range in not exceeded. If the

stress range is exceeded we weld the transverse stiffener to a plate that is bolted through the tension flange.

NJ

- We use bolted connection on tension flanges
- *Note: Since fatigue detail Categories D, E, E' are of major concern, we minimize them at the design stage.*

NC

- We have not experienced fatigue problems due to welding stiffeners etc. to tension areas, so no opinion one way or the other.

ND

- we avoid all tension welding.

OK

- With the exception of some very Low ADT bridges, welding to tension flanges is strictly forbidden.

OR

- In new design it would be considered poor detailing practice and probably replaced with a bolted connection. For a retrofit it may be considered if the anticipated stress range is below that of the VAFL for fatigue Category C (thin stiffeners). We would select a bolted connection over a field weld. On existing fracture critical structures with such connections we might consider peening of the welds.

PA

- Not allowed.

SD

- Current details allow welding to the tension flange for diaphragm stiffener to flange connections.

TN

- We avoid welding to tension flanges if feasible. If not we would use a Category C and check allowable. If Category C can not be achieved we would go to great lengths to bolt the termination of the weld in tension areas.

TX

- Welding in tension zones and flanges is done only when necessary, i.e. cross bracing on curved girders, etc. All welding in tension is in accordance with the AASHTO "Standard Specifications for Highway Bridges".

UT

- We concur with AASHTO's ruling for positive connection of transverse connection plate to tension flange. It seems to reduce the out-of-plane distortion.

VT

- We do weld connection plates to tension flanges, but hold weld back 1" from edge of flange. We do not weld bearing stiffeners to tension flange over piers where the stress is high. We run cover plates to within 5' of end of rolled beams so that we can terminate them in a low stress area.

VA

- Follow the specs.(AASHTO Sec. 10)

WA

- Welding on tension flanges is permitted provided the appropriate AASHTO fatigue Category and details are utilized.

WV

- Provided calculated stress range does not exceed allowable for Category C, we would weld.

WI

- Do not weld on tension flange except for transverse stiffener connections.

WY

- Intermediate stiffeners are welded to tension flange.

4.5 Brief Comments on the Various Responses

Most of the responses obtained from surveying the different states are applicable to Nevada steel bridges. The responses to each question are reviewed based on the collective information obtained from the survey. This is convenient in case of immediate need of collective information on fatigue evaluation and crack repair strategies for steel bridges.

Most of the states have experienced fatigue problems in their steel bridges. The main fatigue problems experienced are in-plane load induced fatigue, out-of-plane distortion induced fatigue, high cycles-low amplitude vibrations/distortions, and fracture due to impact damage. Among these problems, out-of-plane distortion induced fatigue is the pre-dominant. Most of these fatigue problems are associated with Category D, E, and E' type details. In some cases, Category B and C type details are also subjected to severe fatigue cracking.

To rehabilitate steel bridges that experienced fatigue cracks, it is important to identify the types and causes of the fatigue cracks. Most of the states take periodic visual

inspection as the first step in resolving in-plane load induced and out-of-plane distortion induced fatigue problems. Non-destructive testing, use of strain gauges to check stress ranges, analysis of traffic data, research history of the problems, and good engineering judgment are the frequent solutions in evaluating the main fatigue problems. However, there are not any specific evaluation procedures for fatigue problems. Some states limit the stresses by using more rigid connections through bolting or welding or by eliminating the members driving the out-of-plane bending.

Structural analysis procedure is also one of the important parameter for fatigue evaluation. Most of the states use 2-D structural analysis for fatigue evaluation and repair. Few states use 3-D finite element analysis for this purpose. In fatigue evaluation, most of the states use the AASHTO HS20 Truck. Only few of the states use their own Permit Trucks, such as T-3, T352, T3-3, HS25, P13, etc. Most of the states use AASHTO criteria for the number of truck passages. Only a few of them use weigh station data for this purpose. In determining allowable fatigue stress ranges, most of the states use AASHTO's Standard Specifications, and few use Fatigue Guides Specifications.

Repair of fatigue cracks depends on the actual fatigue problems, its size and shape. The most common solution for repair of fatigue cracks is arresting the propagation of cracks by drilling smooth holes at crack ends. Some of the specific methods for repair of fatigue cracks are:

- Drilling holes at the tips of the cracks and installing a high strength bolt in that place.

- Removal of driving force, i.e. reduction of the stress concentration or prevention of out-of-plane distortion.
- Weld up the crack and redesign the connection to previous strength.
- Peening
- Addition of extra members or an alternate load path.
- Leaving the crack and monitoring the crack growth.
- Decreasing the stiffness of the connection, replacing the damaged part, and monitoring the situation.

Most of the states do not relate the fatigue repair methods to the applied stress ranges. A few relate them for high cycle stress range problems. It is seen from the survey that it is appropriate to exclude welding from fatigue repair because of poor quality and associated local stress problems of field welding. It is difficult to control preheat and interpass temperatures in the field. Weld quality is also difficult to maintain. Embrittlement and shrinkage add stress raisers to the weld area, enhancing future cracking potential. Furthermore, weld repairs performed under dynamic loading (traffic) are not effective.

Some states evaluate the remaining life for relatively small fatigue cracks. This depends on the structure, ADTT, and location. This evaluation helps them in replace vs. rehabilitation decision options. However, the presence of fatigue cracking usually causes them to replace the superstructure when the structure requires widening.

Most of the states prefer to avoid welding on the tension flange and the termination of welding in tension zone. In unavoidable situations, they allow welding that AASHTO fatigue requirements permit and that are properly inspected.

Chapter 5

Summary and Recommendations

5.1 Summary

The primary objective of this research was to identify and recommend to the Nevada Department of Transportation appropriate fatigue evaluation and repair strategies for steel bridges. To accomplish this objective, fatigue parameter: applied stress ranges were investigated for the following wide range of variables to determine their sensitivity on the overall fatigue evaluation.

1. Mathematical models: 2-D or 3-D
2. Bridge geometry: Skew angle, girder spacing, and depth
3. Type and area of cross frames and lateral bracing
4. Types of loading: Legal and permit

2-D and 3-D analytical results obtained from the above mentioned parametric analysis of the Rose Creek Overpass, IR80-HU3.4, in this research, lead to the following conclusions.

1. The results of 2-D and 3-D structural analyses for different cases of right bridges is given below.

   1.1. Closely spaced bridges ($S \leq 5.83$ ft.): 3-D analysis gave approximately 50% higher values of applied stress ranges than 2-D analysis.

1.2. Normally spaced bridge ($10 \leq S \leq 14$ ft.): 2-D structural analysis gave 50% higher values of applied stress ranges than 3-D analysis.

1.3. Widely spaced bridge ($S \geq 17.5$ ft.): 3-D analysis gave 25% higher values of stress ranges than 2-D analysis.

2. 2-D analysis for a right bridge gave approximately 50%, 75%, and 170% higher values of applied stress ranges than the 3-D analysis for bridge having skew angles 0°, 30°, and 60° respectively.

3. From the results of the 3-D structural analysis for different cases of the Rose Creek bridge, the following conclusions can be drawn.

3.1. An increase in the skew angle results in a decrease in the applied stress ranges. Increasing the skew angle from 0° to 30° resulted in a 15% decrease in the stress ranges, while increasing the skew angle from 0° to 60° resulted in a 40% decrease in the stress ranges.

3.2. In cases of right bridge, a Single HS20 Truck Load would apply the smallest magnitude of stress range, while a Single P13 Truck Load would apply the highest stress ranges. The stress ranges produced by multi-lane HS20 Truck and Lane Loads would be almost equal.

3.3. Increasing girder spacing and depth would decrease the applied stress ranges.

3.4. The variation of the applied stress range and the axial forces related to bridge stiffness are given below.

3.4.1. The applied stress range value did not vary with the cross frame configurations. However, as skew angle increases, cross frames

attracted more axial forces. X Type configurations attracted almost double the axial forces of K Type configurations. As girder spacing increases, the axial forces in the cross frame decreases due to the decrease in stiffness.

3.4.2. Cross frame cross sectional area did not have any effect on the applied stress ranges. However, an increase in the cross-sectional area causes an increase in the axial forces in the members. Doubling the cross-sectional area would result in a 100% increase in the axial forces.

3.5. The presence and absence of lateral bracing did not show any variation on the values of the applied stress ranges. As skew angle increases, the forces in the lateral bracing increase.

3.6. Vertical deflections of girders were not affected by the different cross frame configurations or cross sectional areas.

The fatigue parameters affecting the allowable stress ranges: redundancy of load path, number of stress cycles, and types of details, were also briefly addressed in this research. Following are conclusions drawn about the allowable stress ranges.

1. The number of equivalent stress cycles per HS20 and P13 Truck passages are equal to 1.5 and 1.1, respectively, for the representative bridge.
2. Fatigue damage results from the average, or typical, rather than the extreme condition of loading. High frequencies of occurrence of low stress ranges are more damaging than low frequencies of occurrence of higher stress ranges. A Single HS20 Truck Load is the most damaging load.

A survey of 50 states, the Commonwealth of Puerto Rico, and the U.S. Department of Transportation, regarding fatigue evaluation procedures and fatigue cracking repair methods was carried out. Based on the responses obtained from 32 states, the following observations can be observed.

1. Most of the states have experienced fatigue problems in their steel bridges. Out-of-plane distortion induced fatigue associated with Category D, E, and E' type details is pre-dominant.
2. Periodic visual inspection is the first step in resolving in-plane load induced and out-of-plane distortion induced fatigue problems. Nondestructive testing, use of strain gauges to check stress ranges, analysis of traffic data, history of problems, and good engineering judgment are the frequent solutions in evaluating fatigue problems.
3. 2-D structural analysis is the most common tool in fatigue structural analysis. Most of the states use the AASHTO HS20 Truck and its criteria for the number of truck passages for fatigue evaluation. For determining allowable fatigue stress ranges, most of the states use AASHTO's Standard Specifications and a few use the Fatigue Guide Specifications.
4. The most common solution for repair of fatigue cracks is arresting the propagation of the cracks by drilling smooth holes at the crack ends. Installation of high strength bolts in drilled holes, removal of the driving force, redesign of the connection, peening, addition of extra members or an alternate load path, decrease the stiffness of the connection, replacement of the damaged part, and monitoring are remedies for repair of cracks.

5. It is rare to relate the fatigue repair methods to the applied stress ranges. It is appropriate to exclude welding from crack repair.
6. Some states evaluate the remaining life for relatively small fatigue cracks. This depends on the structure, ADTT, and location. This helps in replace vs. rehabilitation decisions.
7. Most of the states prefer to avoid welding in tension zones and the termination of welding in tension zones.

5.2 Recommendations

Following are the recommendations to NDOT based on the research study of the representative bridge and the survey of other states regarding fatigue evaluation procedures and repair method for steel bridges.

1. NDOT can still use a 2-D structural analysis procedure for fatigue design of steel bridges. However, in cases of closely spaced and widely spaced right bridges, it is appropriate to use a 3-D structural analysis procedure.
2. Skewed bridges are not as susceptible to in-plane fatigue problems as right bridges. The 2-D structural analysis leads to a conservative evaluation of stress ranges when the girder spacing is $10 \leq S \leq 14$ ft. However, forces in cross frame become significant and may lead to severe distortion-induced fatigue cracking.
3. For the design of right steel bridges, it is not necessary to quantify cross frame configurations and changes in cross sectional area as main parameters for fatigue concerns. However, it is appropriate to use K Type cross frames.

4. NDOT should use a Single HS20 Truck Load for fatigue loading and should evaluate for over two million cycles. Allowable stresses for fatigue should be checked with the value obtained from the LRFD Specification Section 6.6.1.2.5-1.
5. Lateral bracing should be considered in design of skewed bridges since these members attract more forces as bridge skewness increases.

References

1. American Association of State Highway and Transportation officials, 1992. "Standard Specification for Highway Bridges," 15th edition, Washington, D.C.
2. American Association of State Highway and Transportation officials, 1994. "LRFD Bridge Design Specifications," 1st edition, Washington, D.C.
3. Gregory, E. N., Slater, G., and Woodley, C. C, 1989. "Welded Repair of Cracks in Steel Bridge Members," NCHRP Report 321, Washington D.C.
4. Caltrans, 1987. "Bridge Design Specifications," Division of Structures, , Sacramento, CA.
5. Nevada Department of Transportation, 1991. "Bridge Design and Procedures Manual," Bridge Manual No: 82, Carson City, NV.
6. American Institute of Steel Construction, Inc., 1994. "Simon Systems User Manual," Version 7.00, Chicago, Illinois.
7. Telos Technologies, Inc., 1987-1993. "CBridge The Syracuse University Three-Dimensional Horizontally Curved Girder Bridge Analysis Program," Syracuse, NY.
8. Miner, M. A., 1945. "Cumulative Damage in Fatigue," Transcations of the American Society of Mechanical Engineers, Vol. 67.
9. Schilling, C. G., and Klippstein, K. H., 1978. "New Method for Fatigue Design of Bridges,"Journal of Structural Division, ASCE, Vol. 104, No.ST3, Proc. Paper 13618, pp.425-438.
10. Moses, F., Schilling, C. G., and Raju, K. S., 1987. "Fatigue Evaluation Procedures for Steel Bridges," NCHRP Report 299, Washington D.C.

11. Schilling, C. G., et al., 1978. "Fatigue of Welded Steel Bridge Members Under Variable-Amplitude Loadings," NCHRP Report 188, Washington D.C.

12. Schilling, C. G., 1984. "Stress Cycles for Fatigue Design of Steel Bridges," Journal of Structural Division, ASCE, Vol. 110 No. ST 6, , pp 1222-1232.

13. Schiling, C. G., 1982. "Highway Structures Design Handbook, Chapter I/6 -Fatigue, Section II - Fatigue Stresses," United States Steel Corporation, Pittsburgh, PA.

14. Keating, P. B., 1987. "High Cycles Fatigue Behavior of Welded Details Under Variable Amplitude Loading, Ph D thesis submitted to Lehigh University.

Table 2.1 Type of steel used and variation of girder section along longitudinal direction.

	Span 1		Span 2			Span 3	
Items	0'-65'	65'-95'	0'-30'	30'-100'	100'-130'	0'-30'	30'-95'
Steel Used	A36	A441	A441	A36	A441	A441	A36
Top Flange	12"x5/8"	Tapering up from 12"x1.5" to 28"x1.5"	Tapering down from 28"x1.5" to 12"x13/16"	12"x13/16"	Tapering up from 12"x13/16" to 28"x1.5"	Tapering down from 28"x1.5" to 12"x5/8"	12"x5/8"
Bottom Flange	18"x1.5"	Tapering up from 18"x1.5" to 28"x1.5"	Tapering down from 28"x1.5" to 22"x1.5"	22"x1.5"	Tapering up from 22"x1.5" to 28"x1.5"	Tapering down from 28"x1.5" to 18"x1.5"	18"x1.5"
Web	48"x5/16"	48"x3/8"	48"x3/8"	48"x5/16"	48"x3/8"	48"x3/8"	48"x5/16"

Table 2.2 Area of cross section of secondary members

Type of Member	Area of inclined member (in^2)	Area of horizontal member (in^2)
Lateral Bracing	N/A	2.6
Intermediate Cross Frames	1.93	1.93
Pier and Abutement Cross Framses	2.6	5.5

Table 2.3 Weight and deck thickness for different girder sections

Design of bridge for girder spacing (S) and girder depth (D)	Average weight of girder section	Thickness of concrete deck	Maximum live load deflection	Section modulus of the girder sections at		
Types	(lb./ft.)	(in.)	(in.)	0.5 L1 (in^3)	Interior supports (in^3)	0.5 L2 (in^3)
S = (5.83 ft.) *D = (4 ft)**.	142	7.25	0.97	1,186	1,196	1,188
S = (11.67 ft.) * *D = (4 ft.)**	177	8.5	0.93	1,646	2,465	1,956
S = (17.5 ft.) *D = (4 ft.)**	266	11.25	0.81	2,504	3,330	2,871
D = (2 ft.) *S = (11.67 ft.)**	458	8.5	1.38	2,247	2,647	2,820
D = (4 ft.)* *S = (11.67 ft.)**	177	8.5	0.93	1,646	2,465	1,956
D = (6 ft.) *S = (11.67 ft.)**	194	8.5	0.50	2,675	2,889	2,678

* = existing

Table 2.4 Bridge with X Type cross frame of A, a = 30, S = 11.67 ft and D = 4 ft

	Axial Force in member (kips)								
Diaphragm	1	2	3	4	5	6	7	8	9
1	-62	56	-27	-58	58	25	-57	61	22
2	-22	22	11	-21	21	10	-22	22	9
3	22	-22	9	21	-21	-10	22	-22	11
4	61	-57	22	59	-58	25	57	-41	-30

Table 2.5 Bridge with X Type cross frame of 2A, a = 30, S = 11.67 ft and D = 4 ft

	Axial Force in member (kips)								
Diaphragm	1	2	3	4	5	6	7	8	9
1	-104	108	47	-107	108	43	-109	113	37
2	-46	46	21	-43	43	18	-46	46	17
3	45	-45	17	43	-43	-18	46	-46	21
4	113	-110	37	109	-108	43	109	-116	-50

Table 2.6 Bridge with X Type cross frame of A, a = 60, S = 11.67 ft and D = 4 ft

	Axial Force in member (kips)								
Diaphragm	1	2	3	4	5	6	7	8	9
1	-55	38	-23	-49	49	17	-48	52	16
2	-20	20	-9	-18	18	7	-18	18	-8
3	17	-17	7	17	-17	-9	14	-14	-9
4	15	-34	48	35	-19	-40	52	-58	-24

Table 2.7 Bridge with X Type cross frame of 2A, a = 60, S = 11.67 ft and D = 4 ft

	Axial Force in member (kips)								
Diaphragm	1	2	3	4	5	6	7	8	9
1	-96	95	-36	-85	86	25	-88	93	24
2	-41	41	-15	-37	37	12	-36	30	-16
3	31	-31	11	33	-33	-17	41	-41	16
4	28	-38	83	61	-24	-72	95	-102	38

Table 2.8 Bridge with K Type cross frame of A, a = 30, S = 11.67 ft and D = 4 ft

	Axial Force in member (kips)								
Diaphragm	1	2	3	4	5	6	7	8	9
1	31	-35	-29	33	-33	27	35	-31	24
2	12	-11	11	11	-11	11	11	-12	10
3	-12	11	10	11	11	11	-11	12	11
4	-31	35	-24	-33	34	27	-36	21	-31

Table 2.9 Bridge with K Type cross frame of 2A, a = 30, S = 11.67 ft and D = 4 ft

	Axial Force in member (kips)								
Diaphragm	1	2	3	4	5	6	7	8	9
1	61	-68	-50	65	65	48	67	-63	25
2	25	-22	21	22	-22	-20	22	-24	18
3	24	22	18	-22	22	-20	-22	25	-22
4	-65	67	-14	-65	65	48	68	63	-53

Table 2.10 Bridge with K Type cross frame of A, a = 60, S = 11.67 ft and D = 4 ft

	Axial Force in member (kips)								
Diaphragm	1	2	3	4	5	6	7	8	9
1	30	-29	-24	28	-27	17	28	-29	20
2	12	-9	-11	6	-8	8	8	-8	-9
3	-8	8	-10	-9	9	7	-9	12	-12
4	-32	22	26	-21	30	-22	-29	31	25

Table 2.11 Bridge with K Type cross frame of 2A, a = 60, S = 11.67 ft and D = 4 ft

	Axial Force in member (kips)								
Diaphragm	1	2	3	4	5	6	7	8	9
1	45	-51	44	51	-51	-27	50	-61	37
2	26	-19	-24	19	-18	-13	18	-16	-18
3	-15	18	-21	-18	18	-14	-18	26	-24
4	-67	35	51	-51	62	45	-39	54	-39

Table 2.12 Bridge with K Type cross frame of 2A, a = 30, S = 11.67 ft and D = 2 ft

	Axial Force in member (kips)								
Diaphragm	1	2	3	4	5	6	7	8	9
1	21	-23	-20	22	-22	19	23	-21	-16
2	13	-12	9	12	-12	8	12	-12	-9
3	-12	12	-9	-12	12	9	-12	13	9
4	-22	23	16	-22	22	18	-24	22	-21

Table 2.13 Bridge with K Type cross frame of 2A, a = 60, S = 11.67 ft and D = 2 ft

	Axial Force in member (kips)								
Diaphragm	1	2	3	4	5	6	7	8	9
1	21	-21	-17	20	-19	12	21	-18	12
2	11	-9	-9	9	-9	7	9	-9	-6
3	-5	5	-8	-5	8	-11	-8	12	-12
4	-29	17	25	-16	25	-18	-24	20	16

Table 2.14 Bridge with K Type cross frame of A, a = 30, S = 11.67 ft and D = 6 ft

	Axial Force in member (kips)								
Diaphragm	1	2	3	4	5	6	7	8	9
1	22	-24	-21	23	-23	20	24	-22	-18
2	11	-10	10	11	-11	-9	11	-11	9
3	-11	10	9	-11	10	-9	-10	11	-10
4	-22	23	19	23	23	20	24	22	22

Table 2.15 Bridge with K Type cross frame of A, a = 60, S = 11.67 ft and D = 6 ft

	Axial Force in member (kips)								
Diaphragm	1	2	3	4	5	6	7	8	9
1	23	-20	-19	20	-20	-15	20	-22	17
2	11	-9	-10	9	-9	8	9	-9	-7
3	6	8	-17	-8	8	-7	-8	12	-12
4	-33	19	32	-20	22	-19	-24	22	-16

Table 2.16 Bridge with K Type cross frame of A, a = 30, S = 17.5 ft and D = 4 ft

	Axial Force in member (kips)					
Diaphragm		2	3	4	5	6
1	19	24	23	-26	-19	-20
2	8	-8	8	8	8	7
3	-8	8	-6	-8	8	8
4	-19	26	-20	-26	19	23

Table 2.17 Bridge with K Type cross frame of A, a = 60, S = 17.5 ft and D = 4 ft

	Axial Force in member (kips)					
Diaphragm	1	2	3	4	5	6
1	18	-23	19	24	-14	-18
2	8	-6	-8	6	-6	-6
3	-6	6	5	-6	8	-8
4	-14	24	18	-24	18	18

Table 2.18 Bridge with K Type diaphragm of A, a =30, S = 5.83 ft and D = 4 ft.

	Axial force in member (kips)																	
Diaphragm	1	2	3	4	5	6	7	8	9	10	11	12	13	14	15	16	17	18
Exterior 1	48	-48	-31	43	-43	-25	41	-41	23	41	-41	22	43	-44	23	46	-50	22
Interior 2	28	-25	-12	25	-24	11	24	-23	11	23	-25	10	24	-25	10	26	-27	8
Interior 3	-27	26	9	-25	24	10	-24	24	10	23	23	11	-23	23	10	-24	27	-11
Exterior 4	-48	48	21	-43	42	23	-41	40	21	-40	40	23	-43	42	-25	-45	49	-31

Table 2.19 Bridge with K Type diaphragm of A, a =60, S = 5.83 ft and D = 4 ft.

	Axial force in member (kips)																	
Diaphragm	1	2	3	4	5	6	7	8	9	10	11	12	13	14	15	16	17	18
Exterior 1	51	-30	-38	32	-30	14	30	-29	-11	28	-32	14	31	-35	14	34	41	14
Interior 2	24	-15	-22	16	-14	7	14	-14	15	14	-15	7	15	-15	-6	14	-11	-14
Interior 3	-11	14	-14	-14	15	5	-15	14	7	-14	14	-5	-14	15	-7	-15	-20	-22
Exterior 4	-40	34	-14	-35	31	13	-31	28	14	28	30	-11	-30	32	-14	-30	51	-38

Table 2.20 Bridge with X Type cross frame of A, S = 11.67 ft and D = 4 ft.

	Axial force in intermediate cross frame member (kips),											
Skew Angle	1	2	3	4	5	6	7	8	9	10	11	12
a = 0°	-5	-10	10	11	-10	-12	-12	21	5	10	-10	11
a = 30°	5	-12	13	14	10	-12	-12	26	5	13	13	14
a = 60°	-10	-23	28	24	-18	-11	-11	50	-10	28	-24	24

Table 2.21 Bridge with X Type cross frame of A, S = 11.67 ft and D = 4 ft.

	Axial force in member of lateral bracing (Kips)																								
a	1	2	3	4	5	6	7	8	9	10	11	12	13	14	15	16	17	18	19	20	21	22	23	24	25	26
0°	-23	-18	-17	-21	-15	15	-15	20	15	15	-15	16	15	14	-15	-15	17	-16	-19	-17	-19	25				
30°				-61	13	-20	-14	25	19	-20	-22	20	21	-23	-21	20	26	-16	-22	30	-13	25	43			
60°							11	-59	-16	25	17	36	-42	46	-46	45	45	-50	52	-35	32	24	-17	-57	-15	11

Table 3.1 Detail category constant, A

DETAIL CATEGORY	CONSTANT, A TIMES 10^8
A	250.0
B	120.0
B'	61.0
C	44.0
C'	44.0
D	22.0
E	11.0
E'	3.9
M164 (A325) Bolts in Axial Tension	17.1
M253 (A490) Bolts in Axial Tension	31.5

Table 3.2 Calculations of equivalent number of cycles

Number	Primary cycle Moment Range M_{rp}	Moment range M_{ri}	M_{ri}/M_{rp}	$[M_{ri}/M_{rp}]^3$
1	1515.2	1515.2	1.000	1.000
2	1515.2	127.2	0.084	0.006
3	1515.2	616.2	0.407	0.067
		The equivalent number of cycles, $N_{ec,p} = 1.073 \approx 1.1$		

Table 3.3 Calculation of percentage damage and effective stress range

Straight original bridge having K-Type Cross Frames (Area = A)							
Interval	ADTT	n	# of Cycles (N) Equ (5)	$\frac{N}{\Sigma N} = (\alpha)$	Stress Interval (S_{ri}), ksi	$(\alpha)x(S_{ri})^3$	% Damage
1	3	1.1	$9.03x10^4$	$2.39x10^{-5}$	13.34	0.57	0.14
2	4	1.1	$12.04x10^4$	$3.18x10^{-4}$	13.34	0.76	0.19
3	5	1.1	$15.05x10^5$	$3.98x10^{-3}$	13.34	0.95	0.24
4	2000	1.5	$8.21x10^7$	$2.17x10^{-1}$	7.11	77.99	19.52
5	3000	1.5	$1.23x10^8$	$3.25x10^{-1}$	7.11	116.99	29.29
6	4000	1.5	$1.64x10^8$	$4.33x10^{-1}$	7.11	155.99	39.05
7	15	1	$4.11x10^5$	$1.09x10^{-3}$	12.86	2.32	0.58
8	18	1	$4.93x10^5$	$1.31x10^{-3}$	12.86	2.78	0.70
9	20	1	$5.48x10^5$	$1.45x10^{-3}$	12.86	3.09	0.77
10	60	1	$1.64x10^6$	$4.34x10^{-3}$	13.57	10.84	2.72
11	70	1	$1.92x10^6$	$5.08x10^{-3}$	13.57	12.65	3.18
12	80	1	$2.19x10^6$	$5.79x10^{-3}$	13.57	14.48	3.63
			$\Sigma N=3.77x10^8$	$\Sigma\left(\frac{N}{\Sigma N}\right)=1$		Σ =399.39	$\Sigma = 100$
Effective Stress Range, $S_r = (\Sigma\alpha_i S^3_{ri})^{1/3} = (399.39)^{1/3} = 7.37$ ksi							

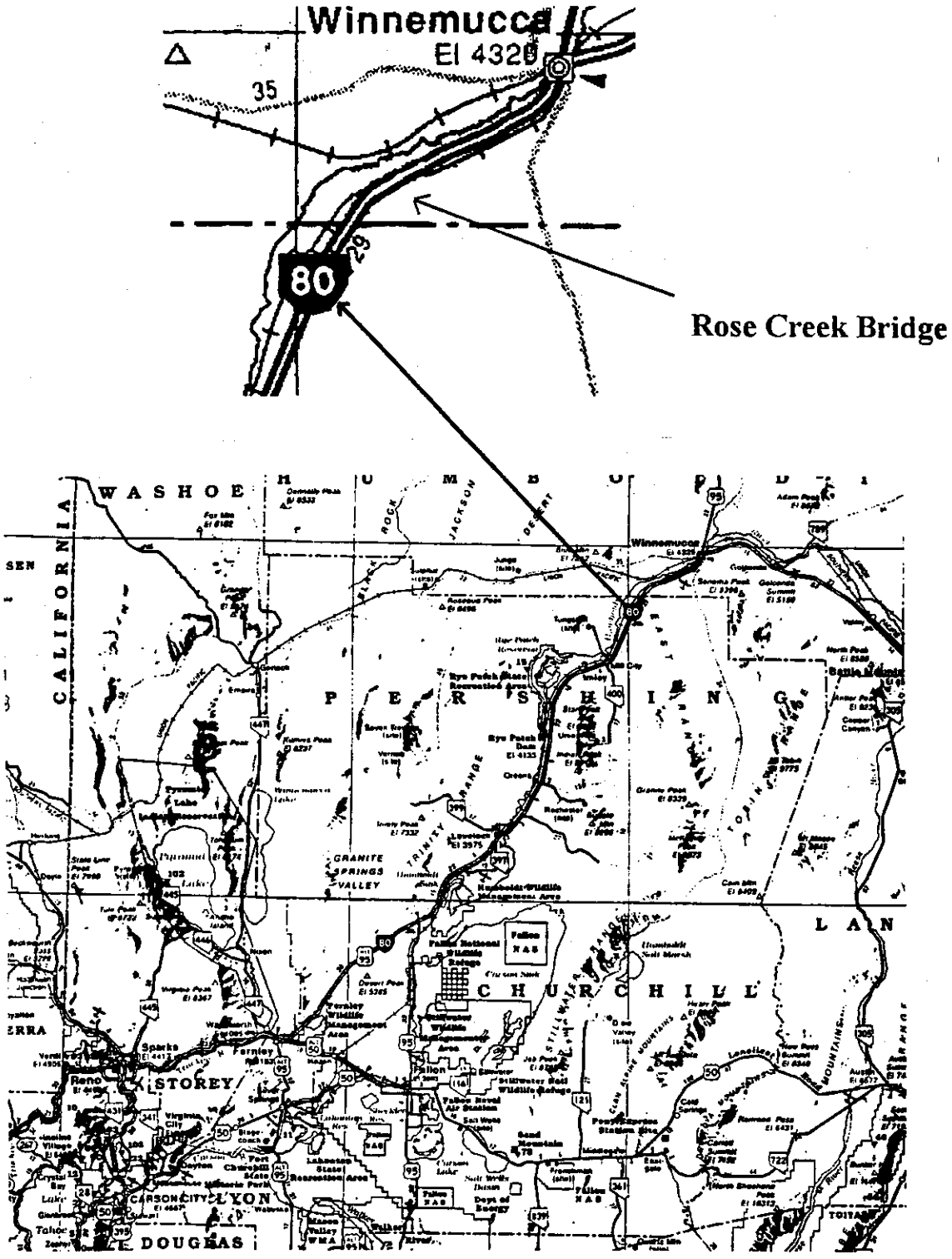

Figure 2.1 Location map of the Rose Creek Bridge

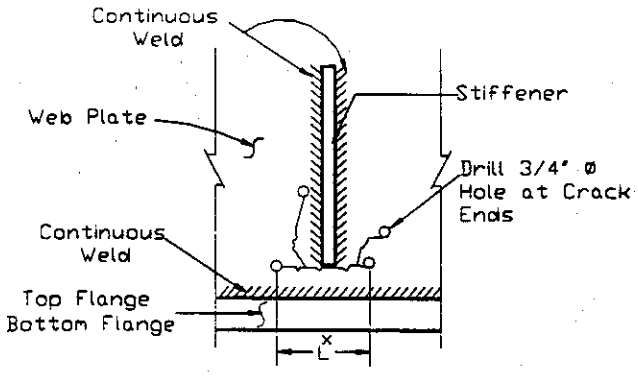

TYPE 1

(WEB CRACK ABOVE WELD)

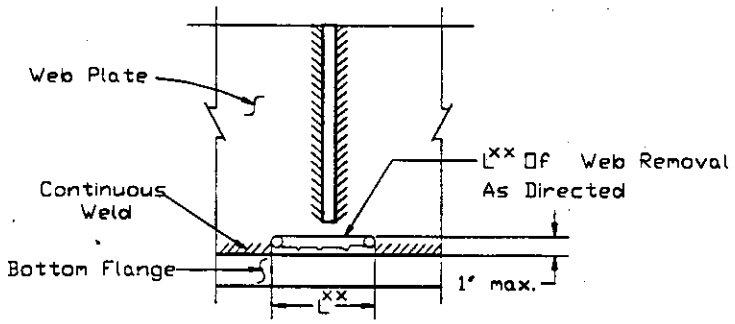

TYPE 2

(CRACK IN WEB-FLANGE WELD)

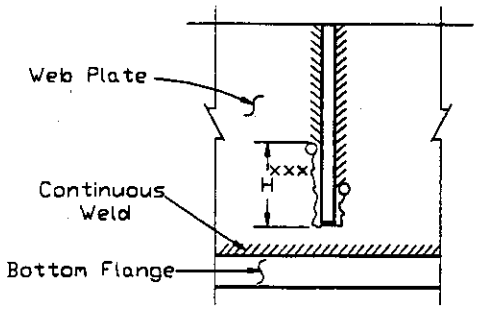

TYPE 3

(CRACK STIFFENER WELD)

Figure 2.2 Typical fatigue cracks and their locations

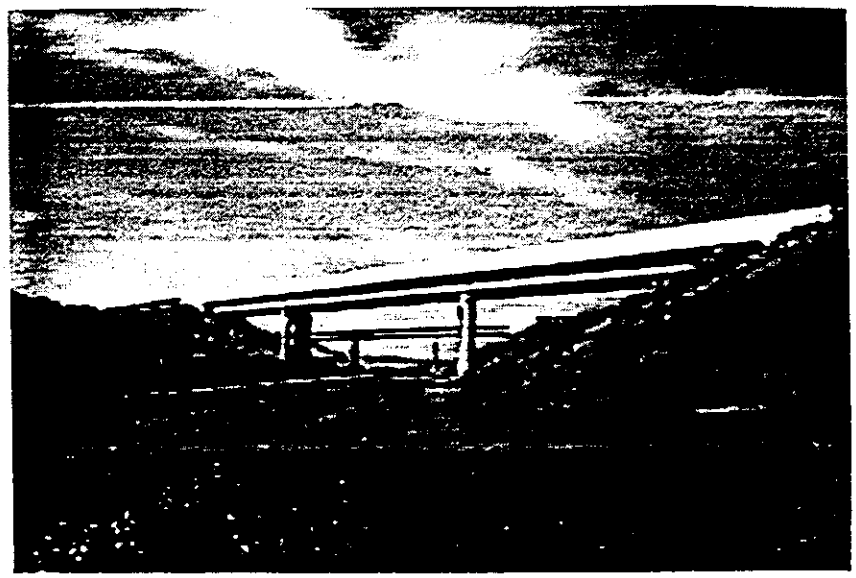

Figure 2.3 Elevation of Rose Creek Bridge

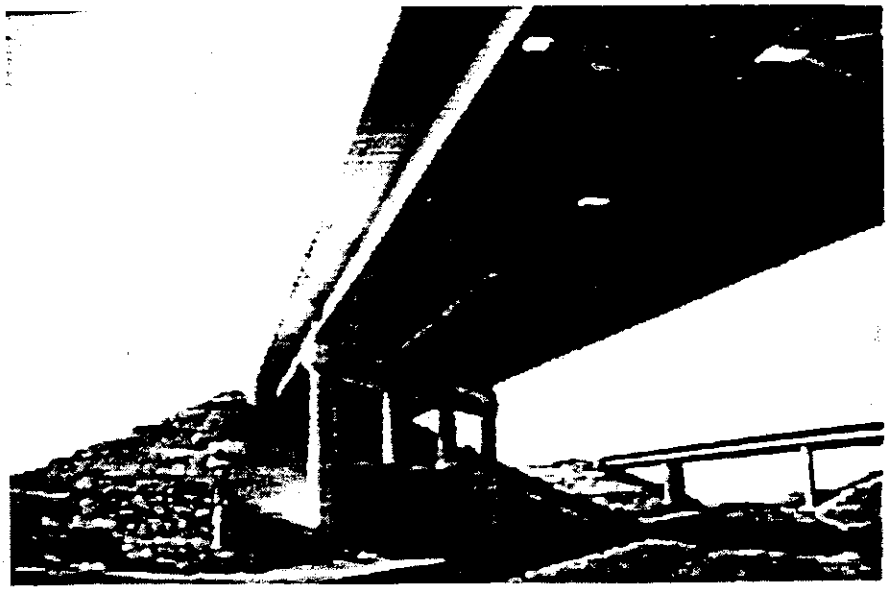

Figure 2.4 View of girders and piers

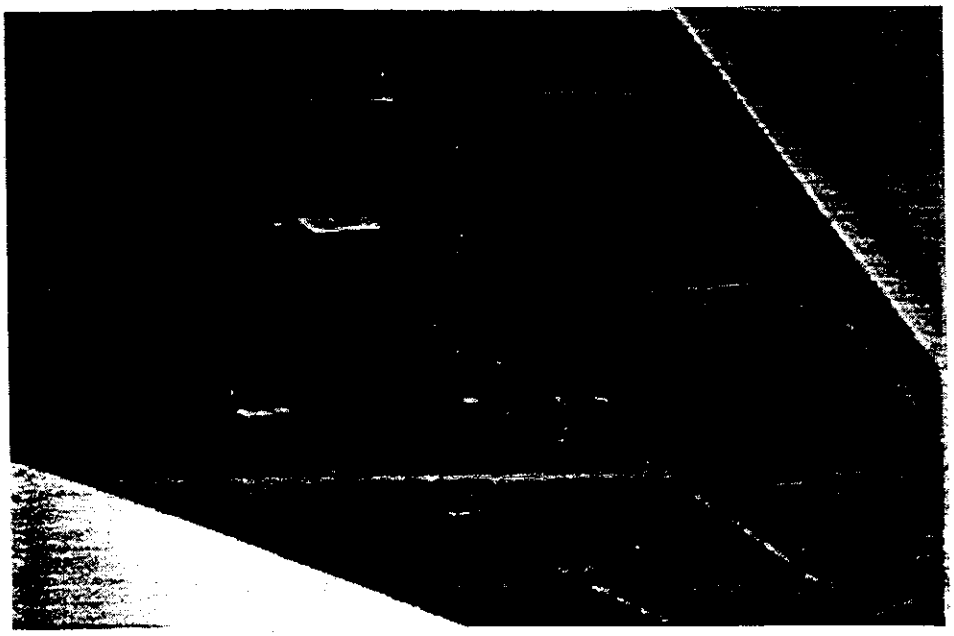

Figure 2.5 Close-up of plate girders and cross frames

Figure 2.6 Close-up of lateral bracings and their connection to plate girders

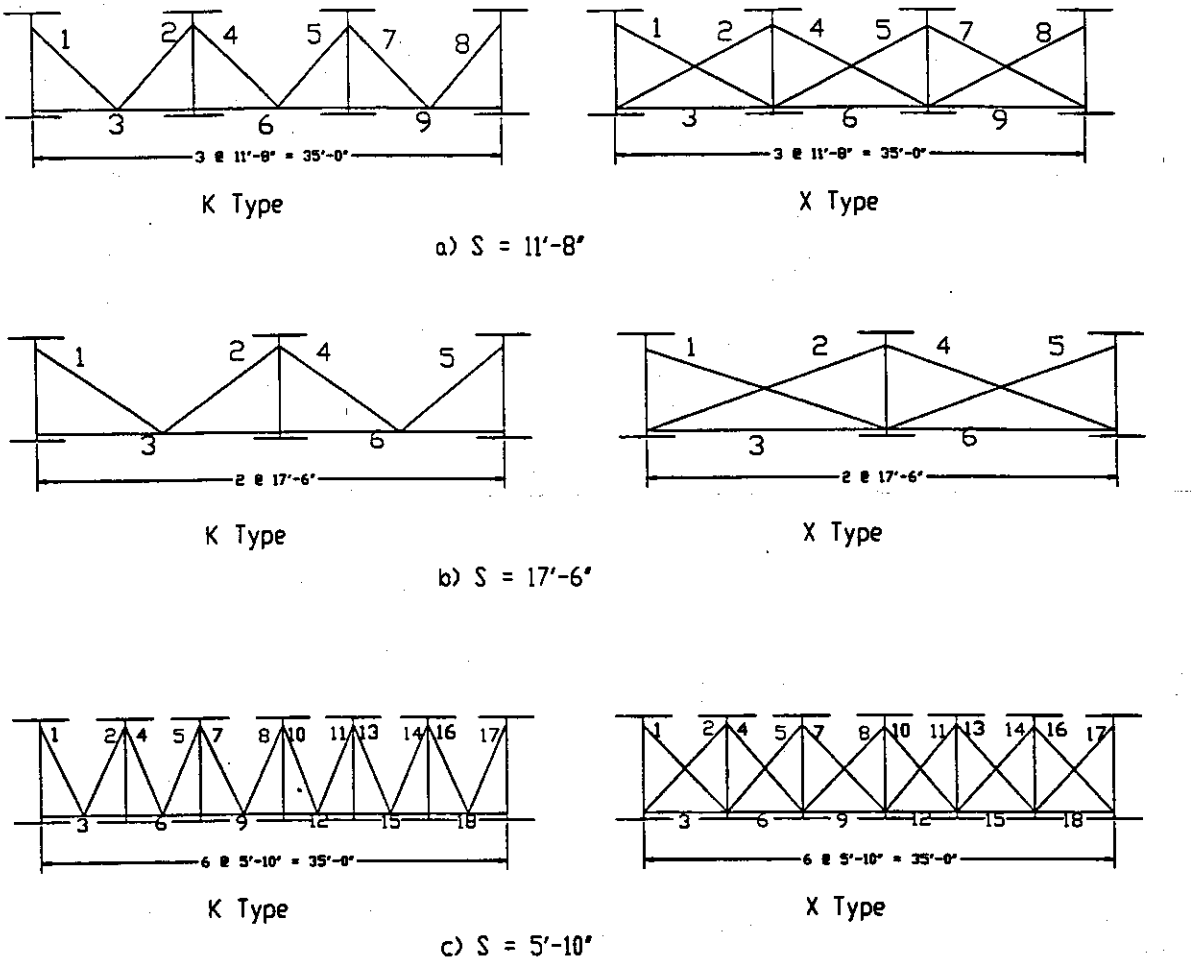

Figure 2.7-a Cross frame (diaphragm) configurations at supports

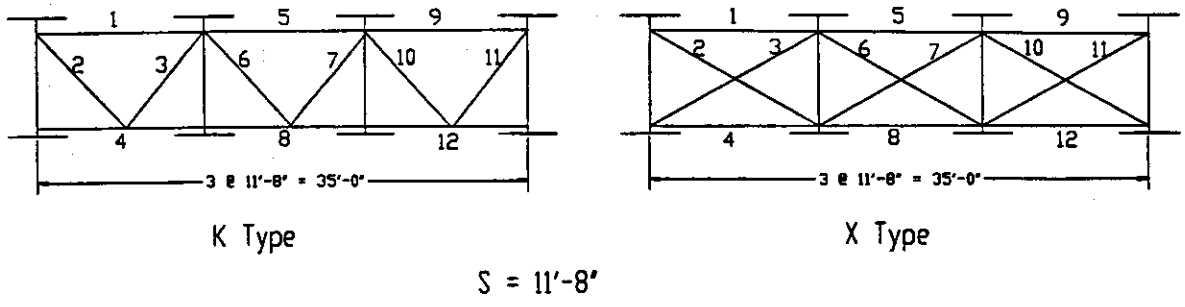

Figure 2.7-b Intermediate cross frame configurations

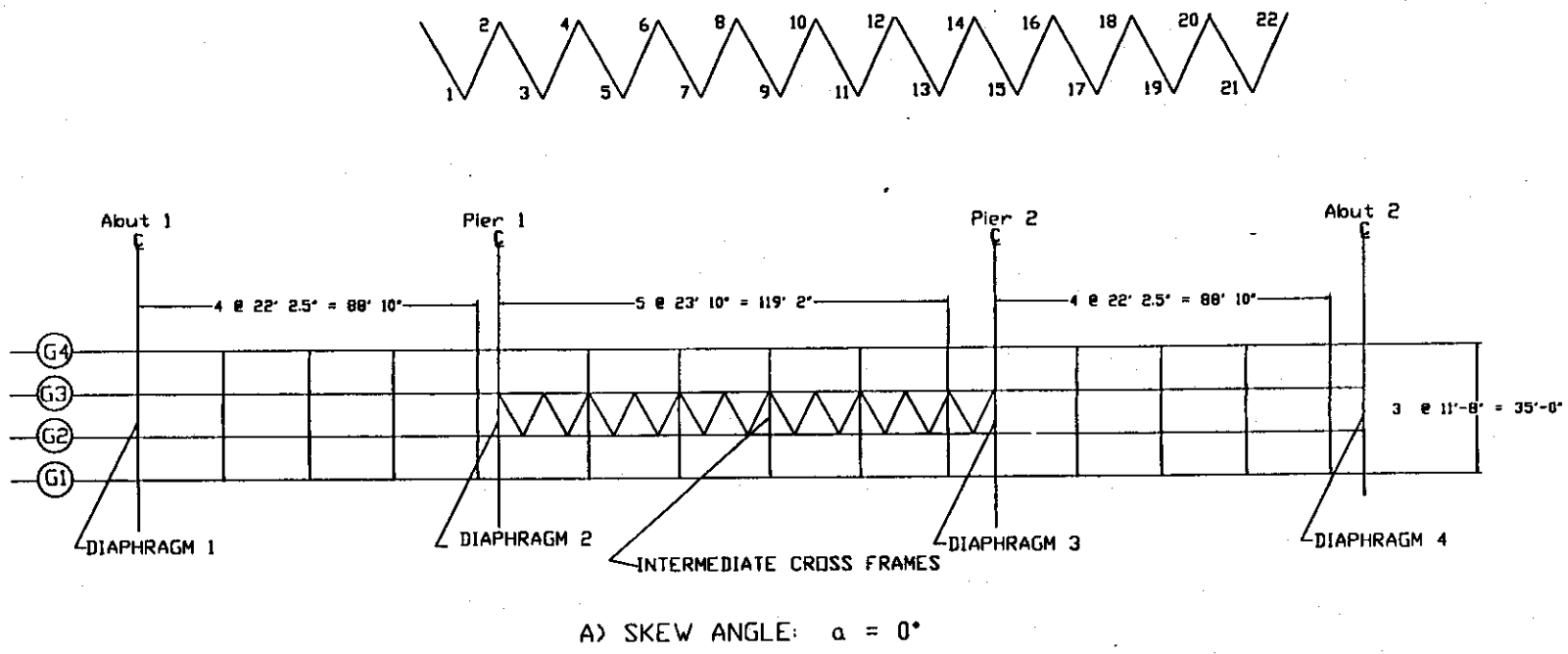

Figure 2.8-a Location of supports, diaphragms, intermediate cross frames, and lateral bracing of the straight bridge.

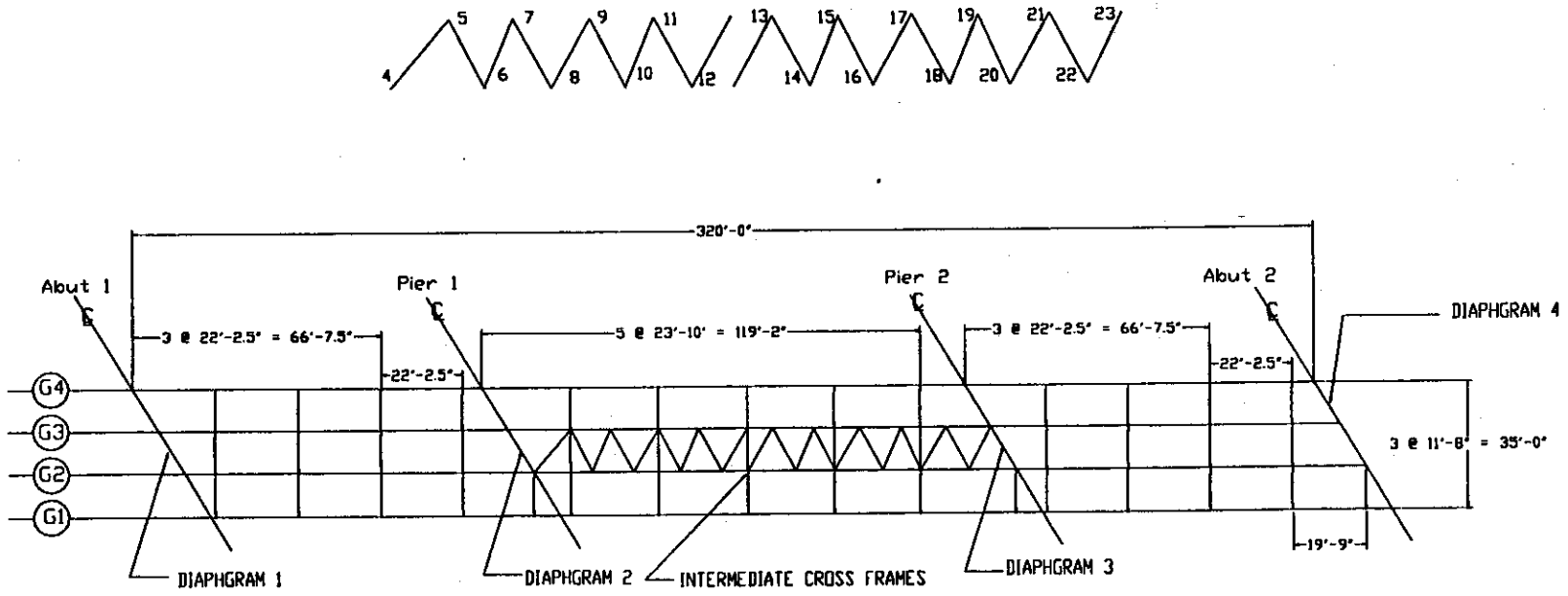

B) SKEW ANGLE: $\alpha = 30°$

Figure 2.8-b Location of supports, diaphragms, intermediate cross frames, and lateral bracing of 30^0 skewed bridge.

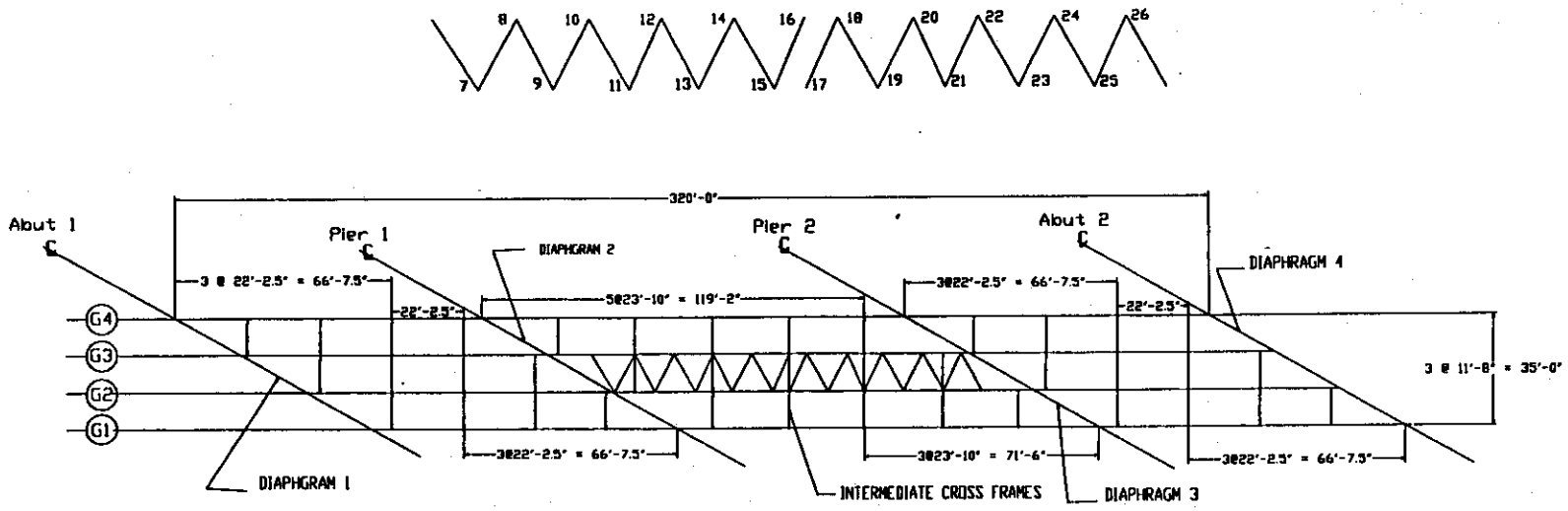

C) SKEW ANGLE: $\alpha = 60°$

Figure 2.8-c Location of supports, diaphragms, intermediate cross frames, and lateral bracing of 60^0 skewed bridge.

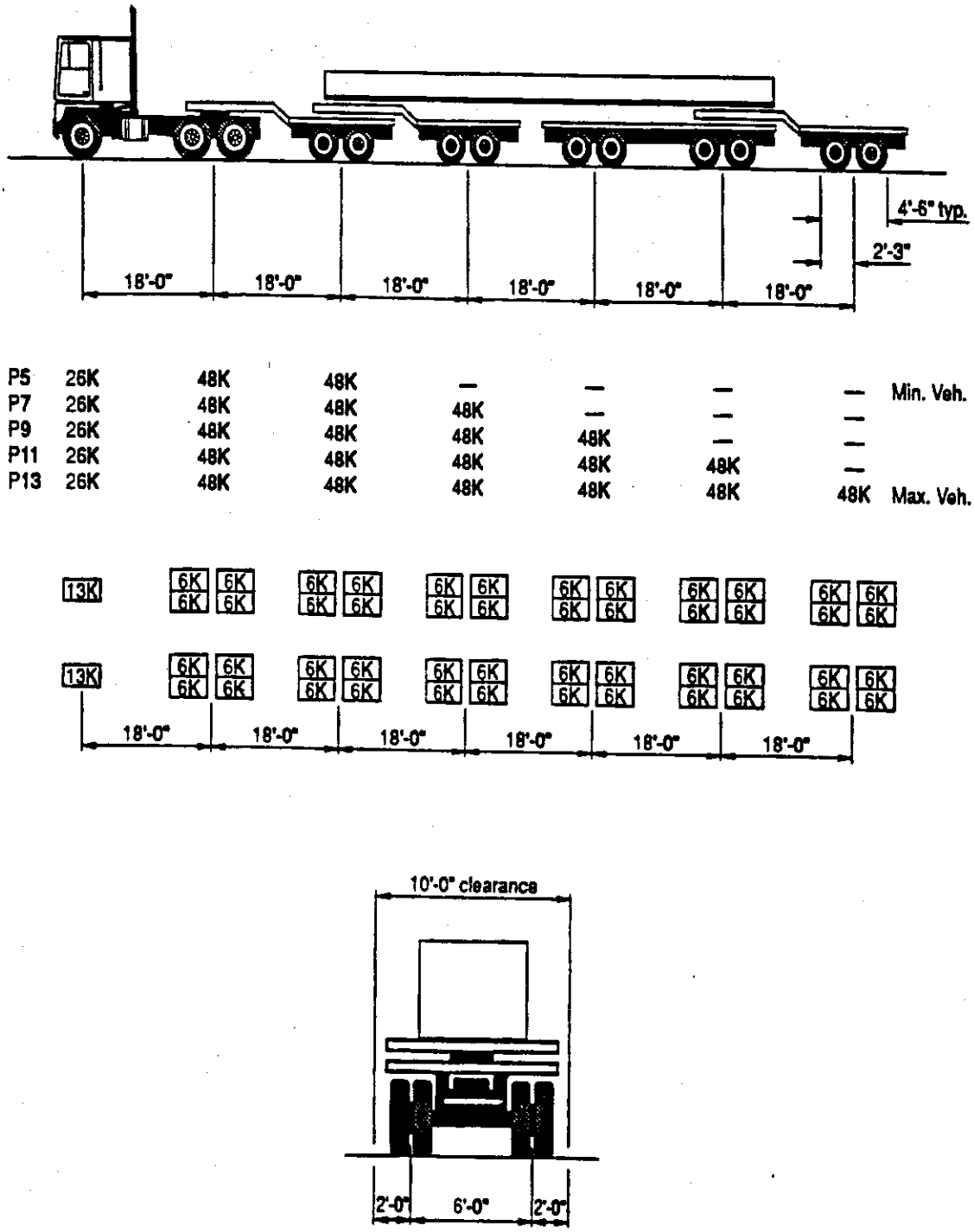

Figure 2.9 California Permit Truck Load (Nevada overload)

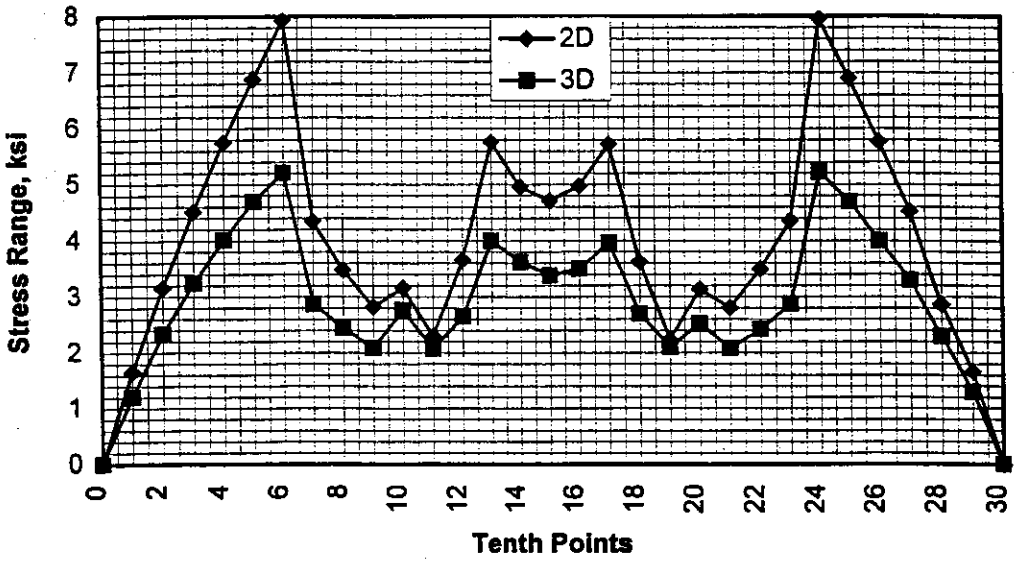

Figure 2.10-a Stress range diagram at top flange due to a Single HS20 Truck Load
(S = 11.67 ft. & D = 48 in.)

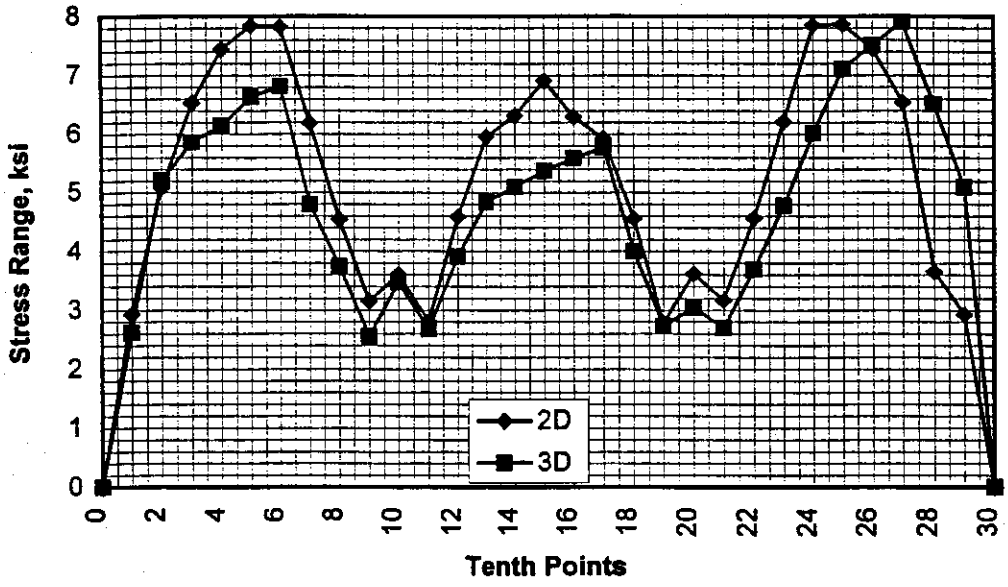

Figure 2.10-b Stress range diagram at bottom flange due to a Single HS20 Truck Load
(S = 11.67 ft. & D = 48 in.)

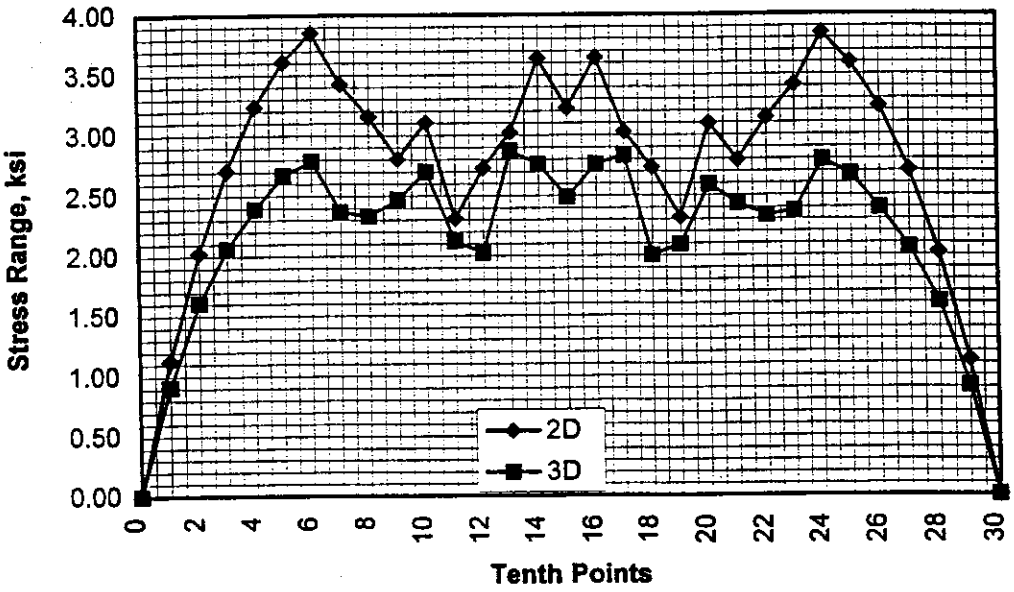

Figure 2.11-a Stress range diagram at top flange due to a Single HS20 Truck Load (D = 24 in.)

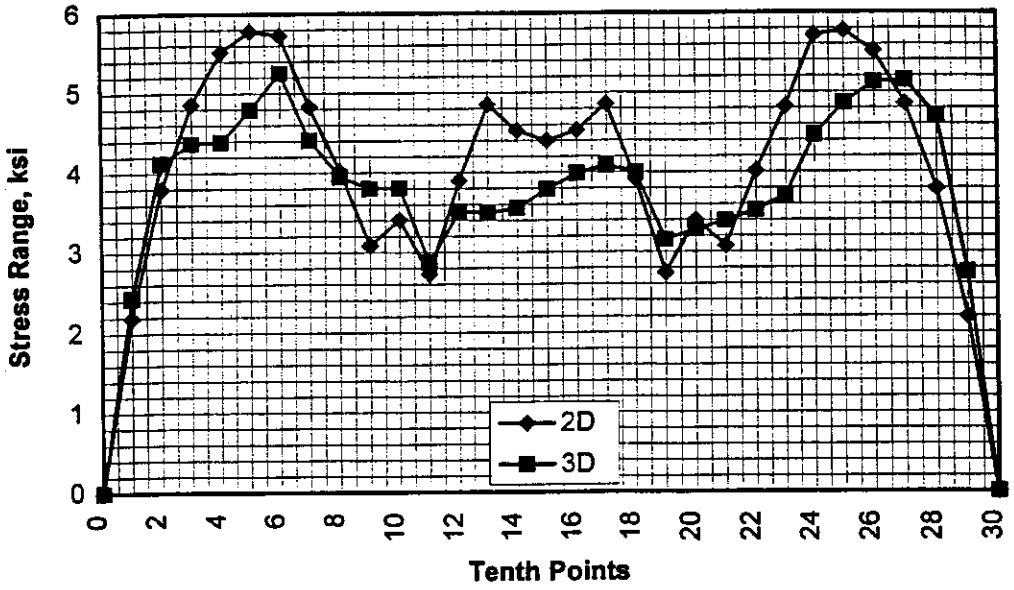

Figure 2.11-b Stress range diagram at bottom flange due to a Single HS20 Truck Load (D = 24 in.)

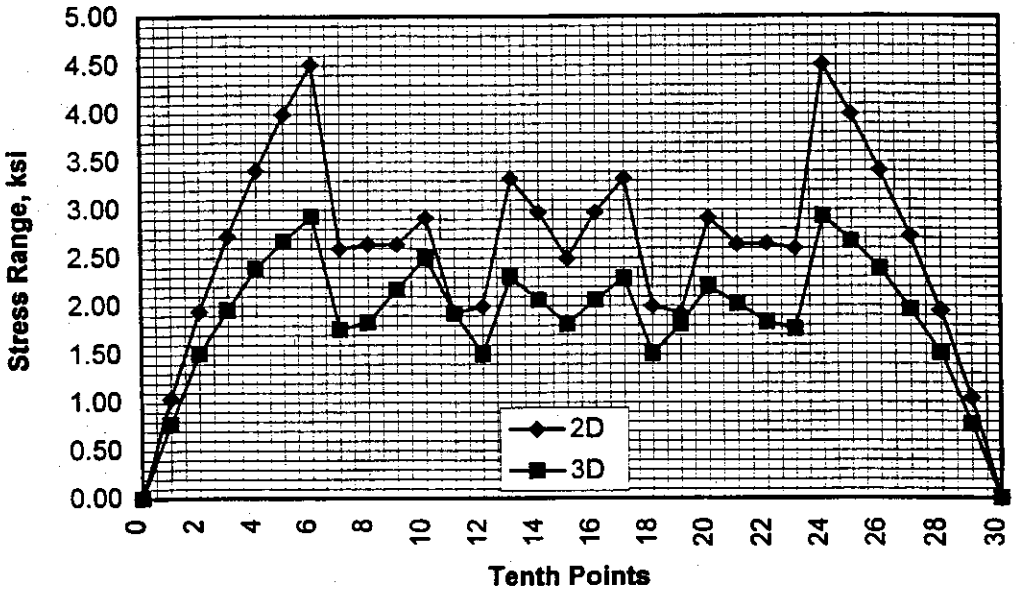

Figure 2.12-a Stress range diagram at top flange due to a Single HS20 Truck Load (D = 72 in.)

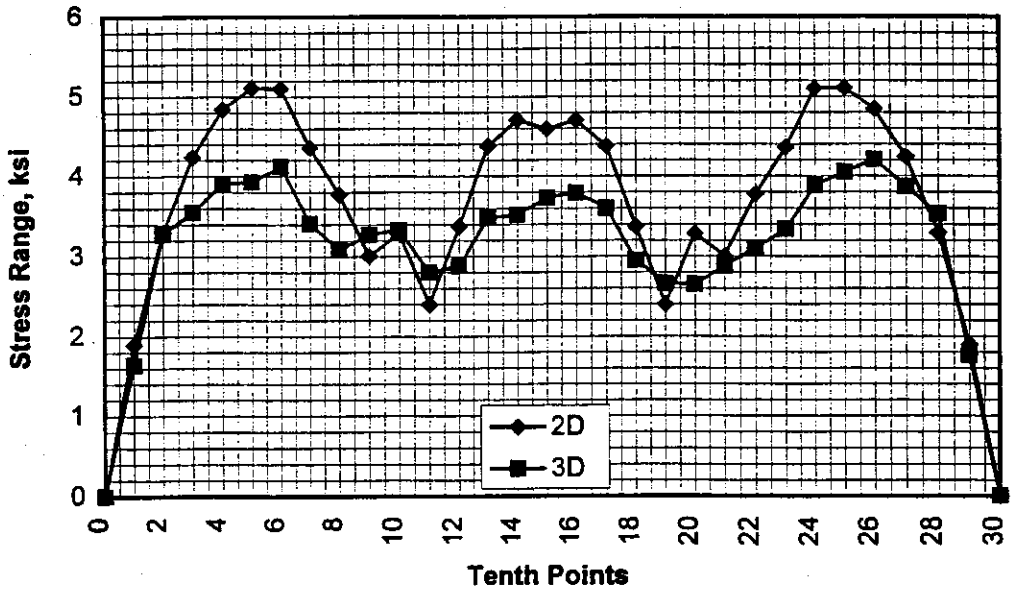

Figure 2.12-b Stress range diagram at bottom flange due to a Single HS20 Truck Load (D = 72 in.)

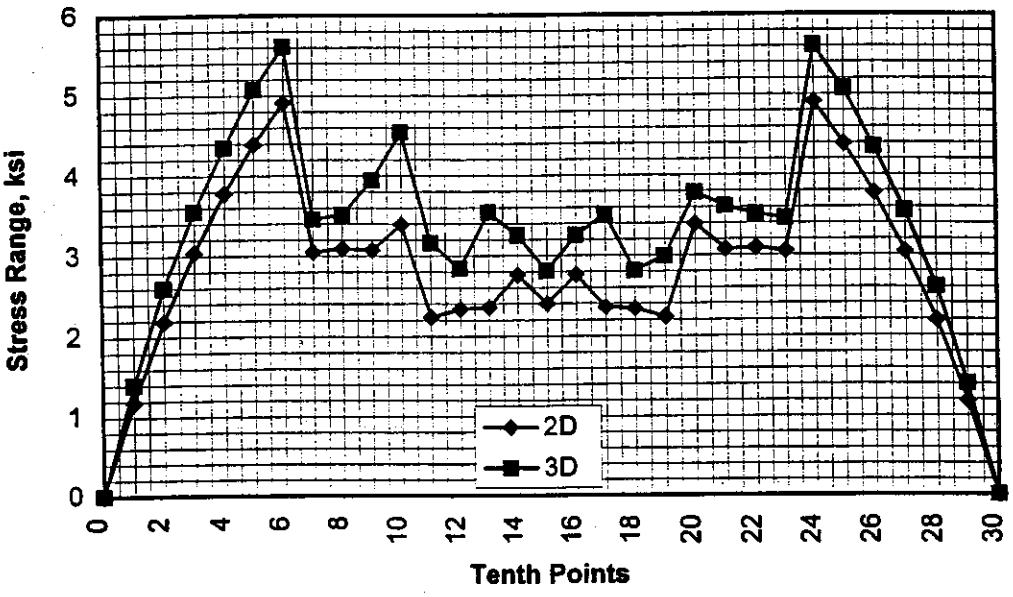

Figure 2.13-a Stress range diagram at top flange due to a Single HS20 Truck Load (S = 5.83 ft.)

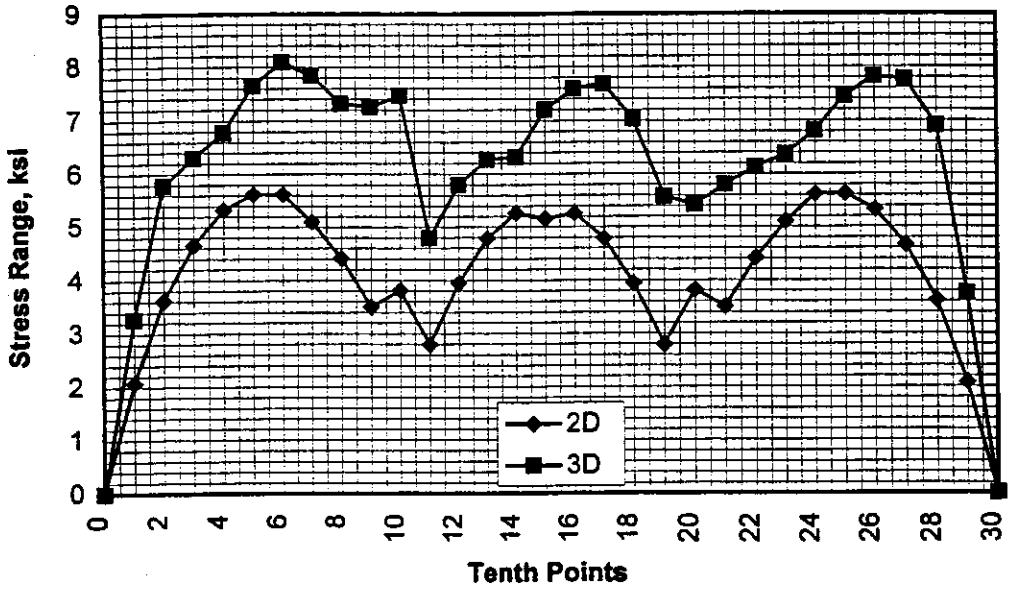

Figure 2.13-b Stress range diagram at bottom flange due to a Single HS20 Truck Load (S = 5.83 ft.)

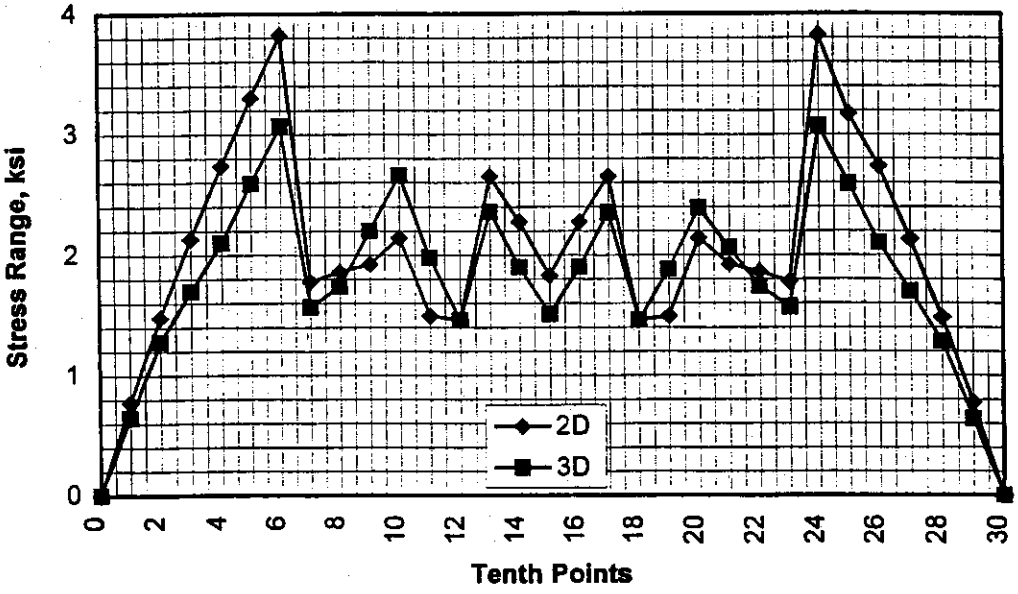

Figure 2.14-a Stress range diagram at top flange due to a Single HS20 Truck Load (S = 17.5 ft.)

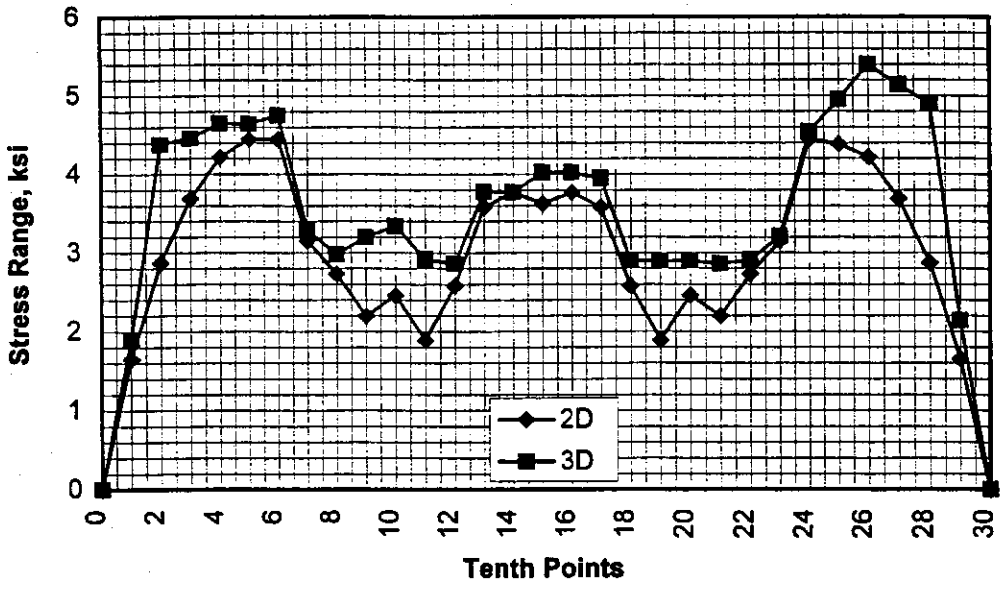

Figure 2.14-b Stress range diagram at bottom flange due to a Single HS20 Truck Load (S = 17.5 ft.)

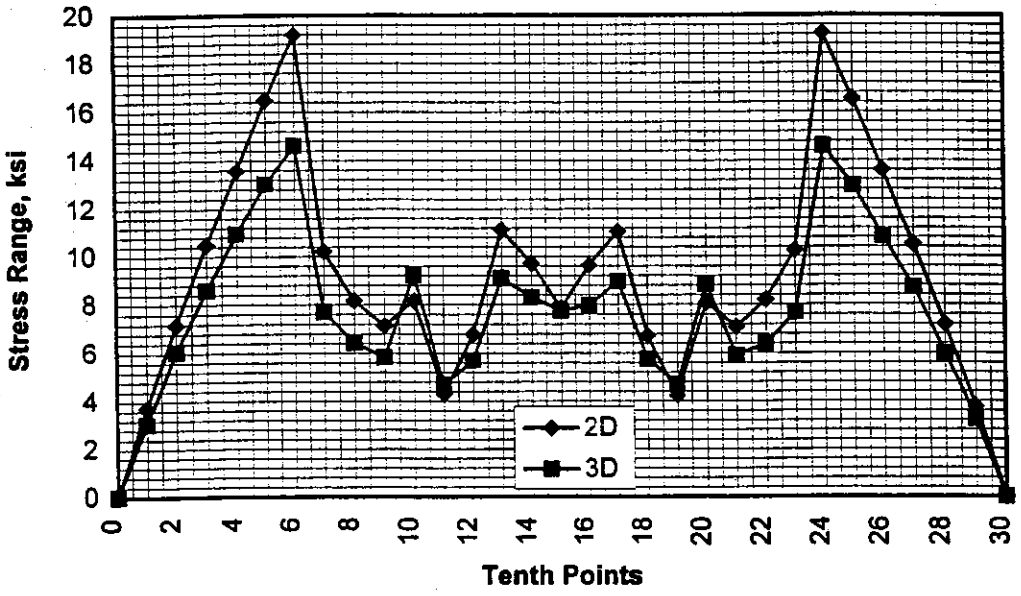

Figure 2.15-a Stress range diagram at top flange due to a Single P13 Truck Load
(S = 11.67 ft. & D = 48 in.)

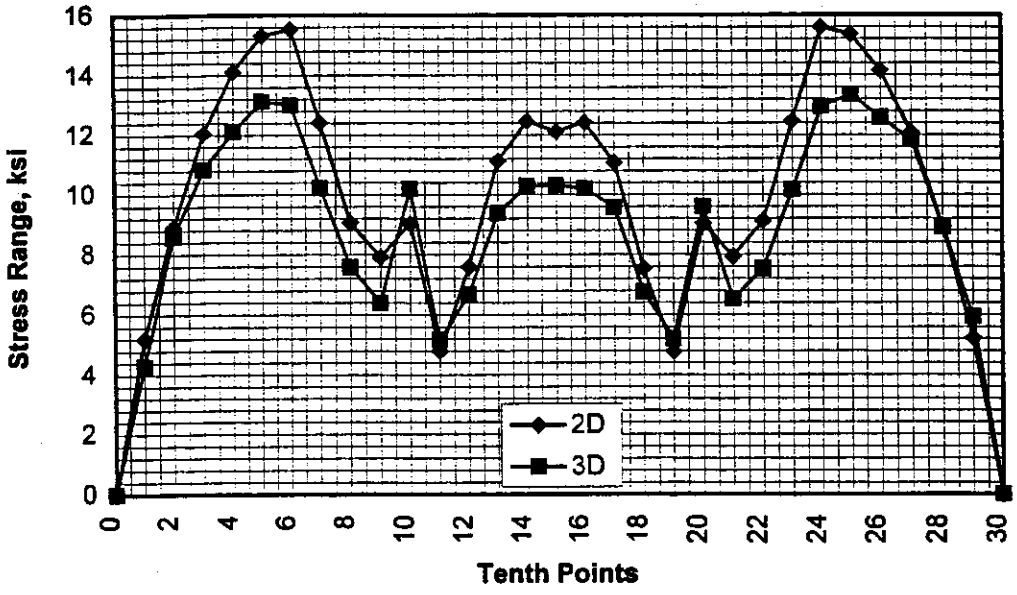

Figure 2.15-b Stress range diagram at bottom flange due to a Single P13 Truck Load
(S = 11.67 ft. & D = 48 in.)

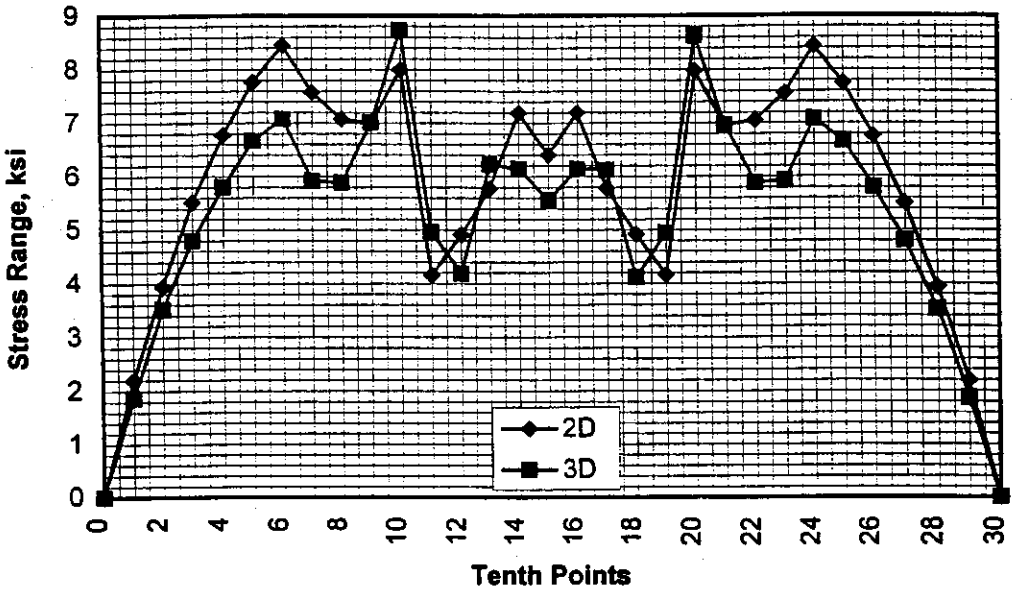

Figure 2.16-a Stress range diagram at top flange due to a Single P13 Truck Load (D = 24 in.)

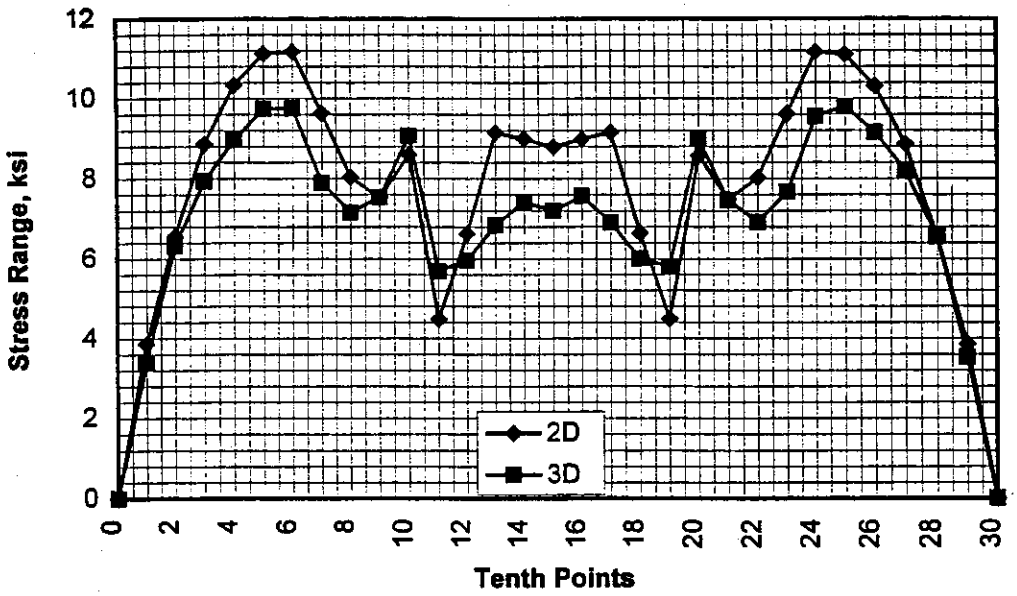

Figure 2.16-b Stress range diagram at bottom flange due to a Single P13 Truck Load (D = 24 in.)

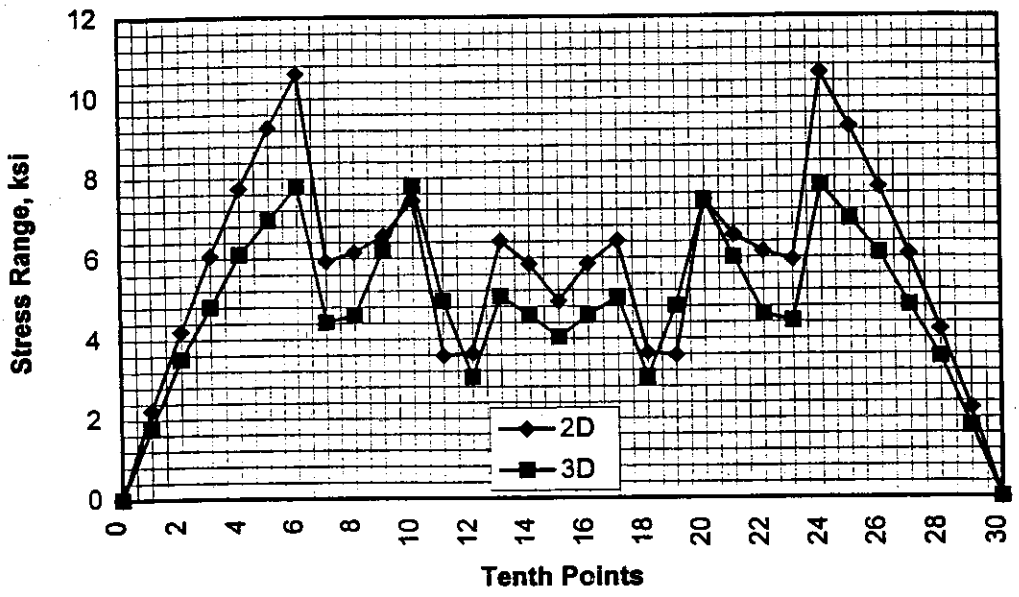

Figure 2.17-a Stress range diagram at top flange due to a Single P13 Truck Load (D= 72 in.)

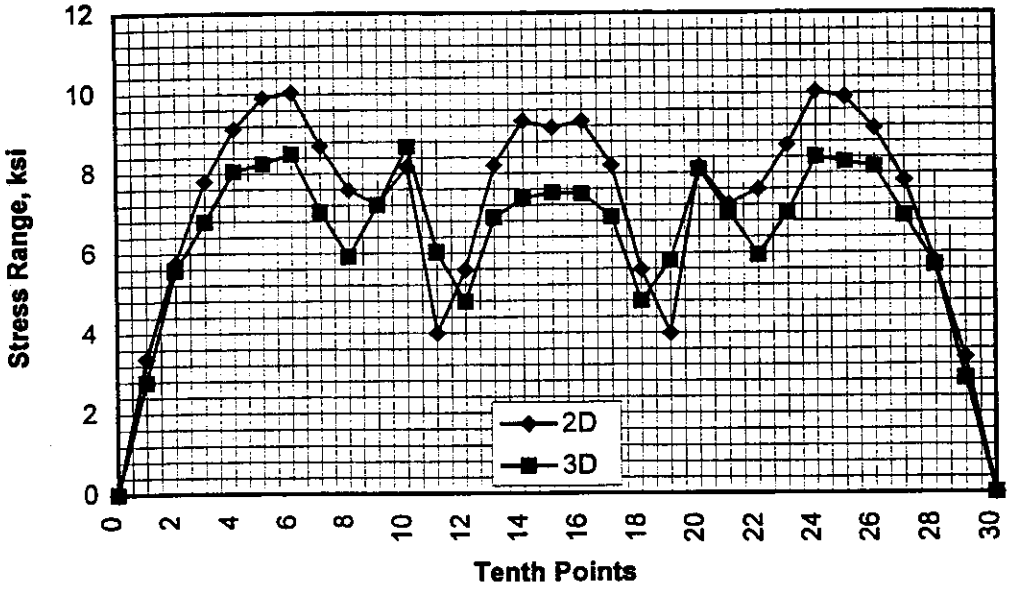

Figure 2.17-b Stress range diagram at bottom flange due to a Single P13 Truck Load (D= 72 in.)

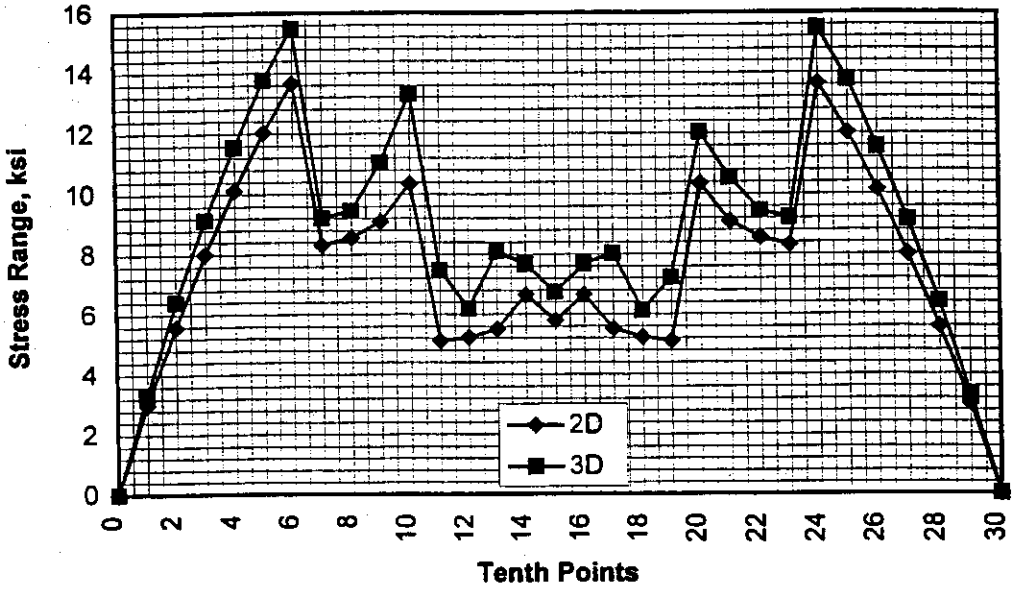

Figure 2.18-a Stress range diagram at top flange due to a Single P13 Truck Load (S = 5.83 ft.)

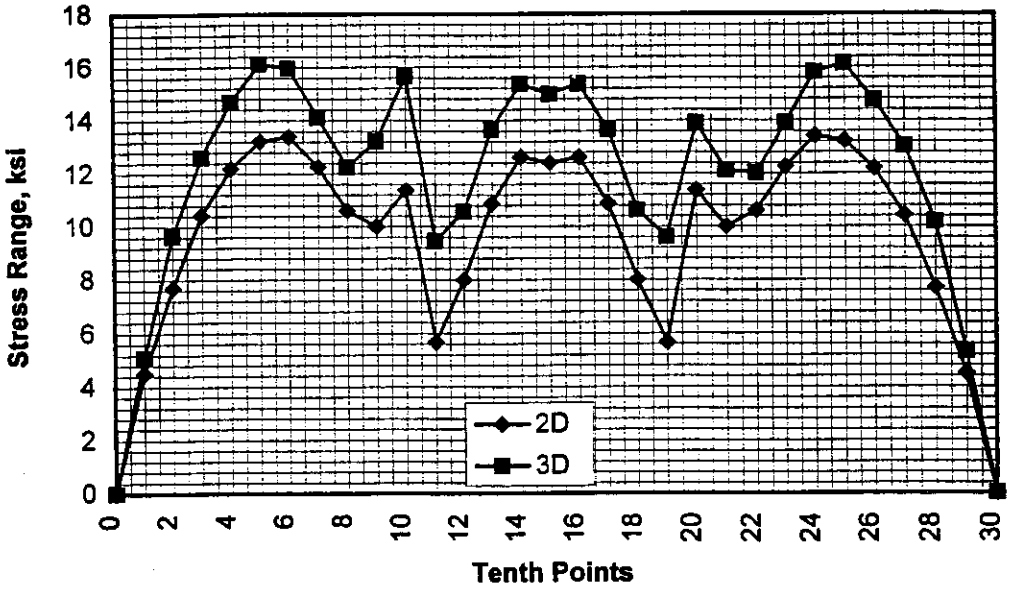

Figure 2.18-b Stress range diagram at bottom flange due to a Single P13 Truck Load (S = 5.83 ft.)

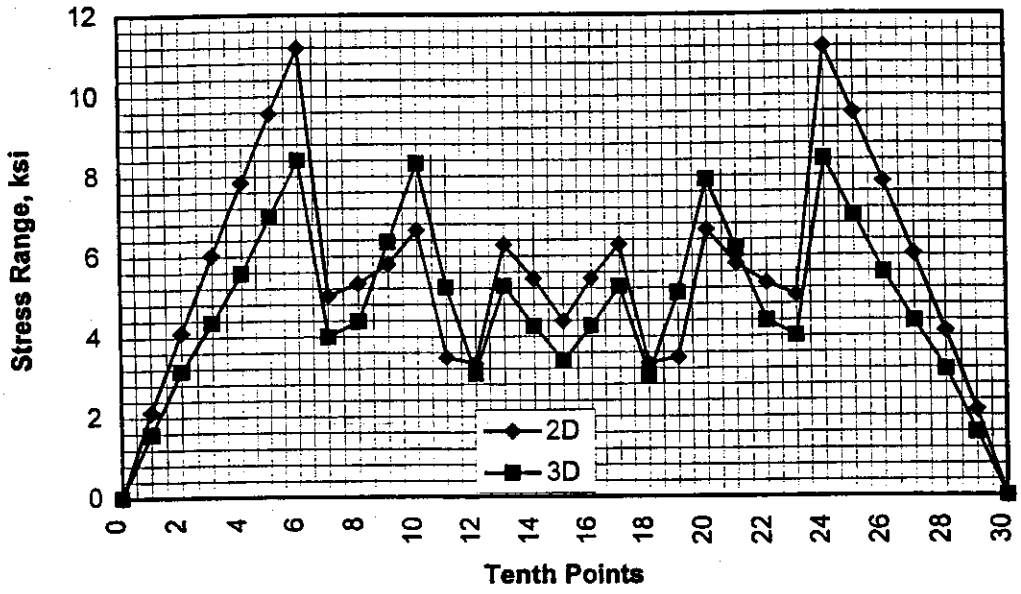

Figure 2.19-a Stress range diagram at top flange due to a Single P13 Truck Load (S = 17.5 ft.)

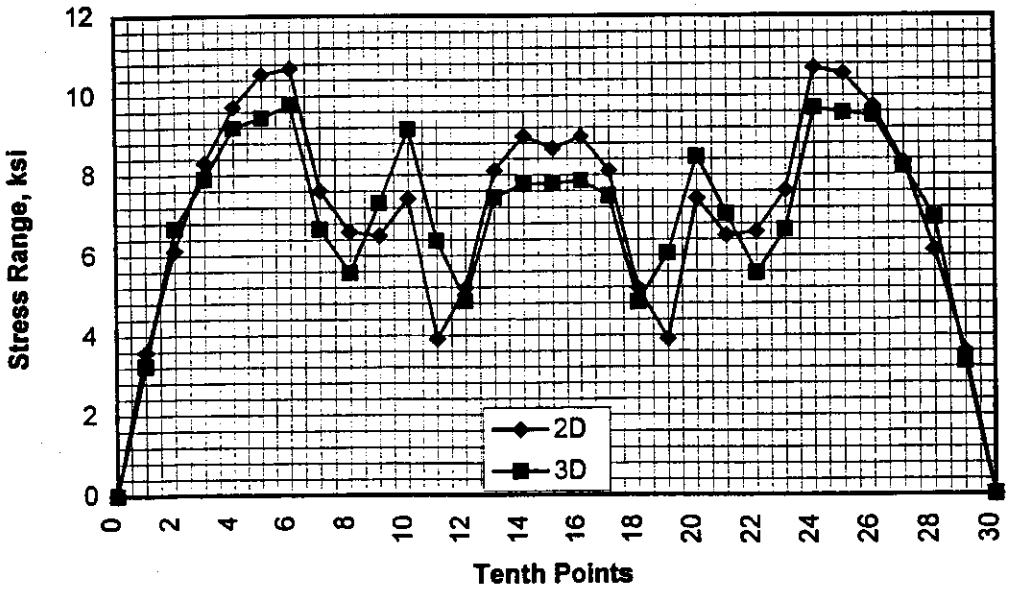

Figure 2.19-b Stress range diagram at bottom flange due to a Single P13 Truck Load (S = 17.5 ft.)

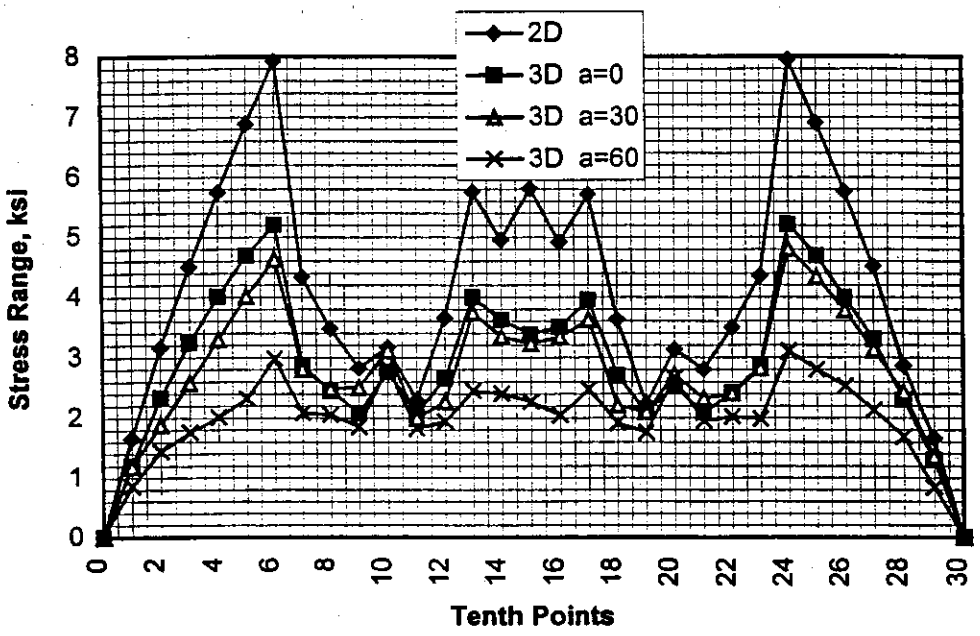

Figure 2.20-a Stress range diagram at top flange of girder G2 due to a Single HS20 Truck Load (S = 11.67 ft. & D = 48 in.)

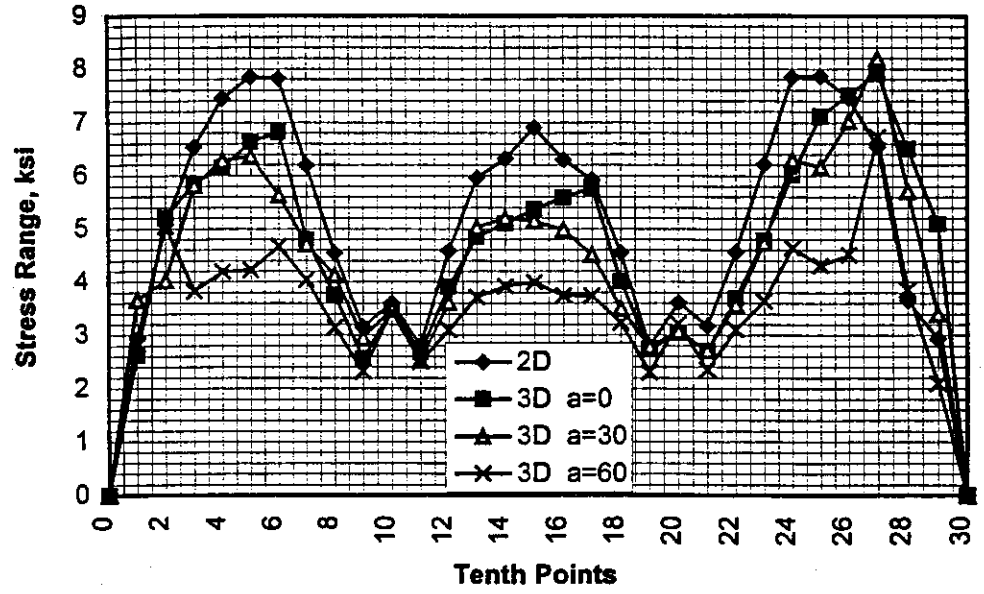

Figure 2.20-b Stress range diagram at bottom flange of girder G2 due to a Single HS20 Truck Load (S = 11.67 ft. & D = 48 in.)

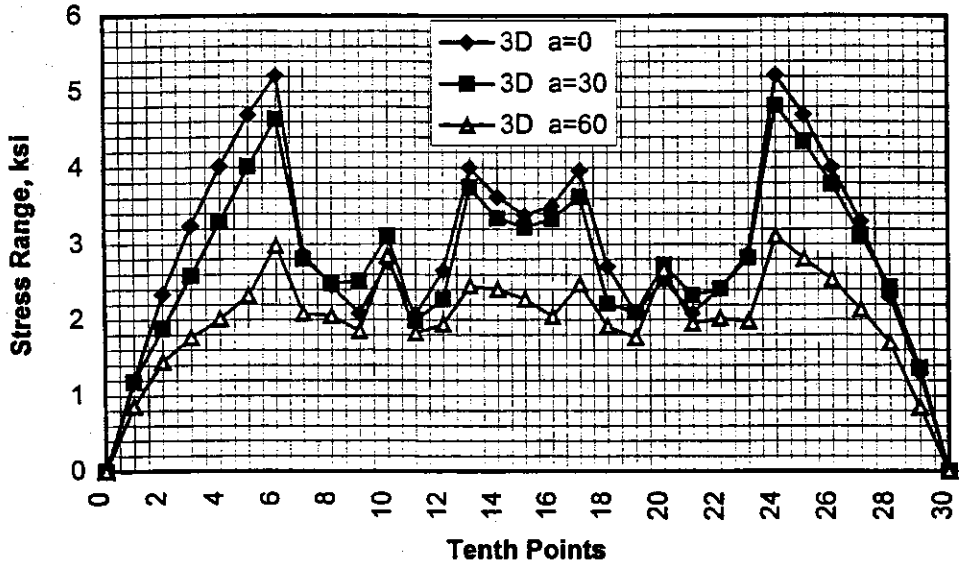

Figure 2.21-a Stress range diagram at top flange of girder G2 due to a Single HS20 Truck Load (S = 11.67 ft. & D = 48 in.)

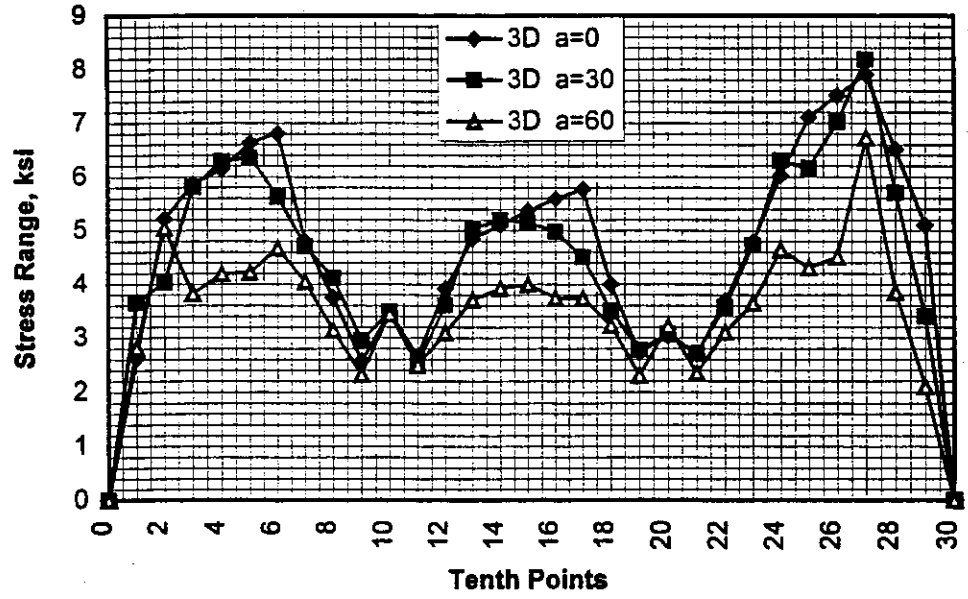

Figure 2.21-b Stress range diagram at bottom flange of girder G2 due to a Single HS20 Truck Load (S = 11.67 ft. & D = 48 in.)

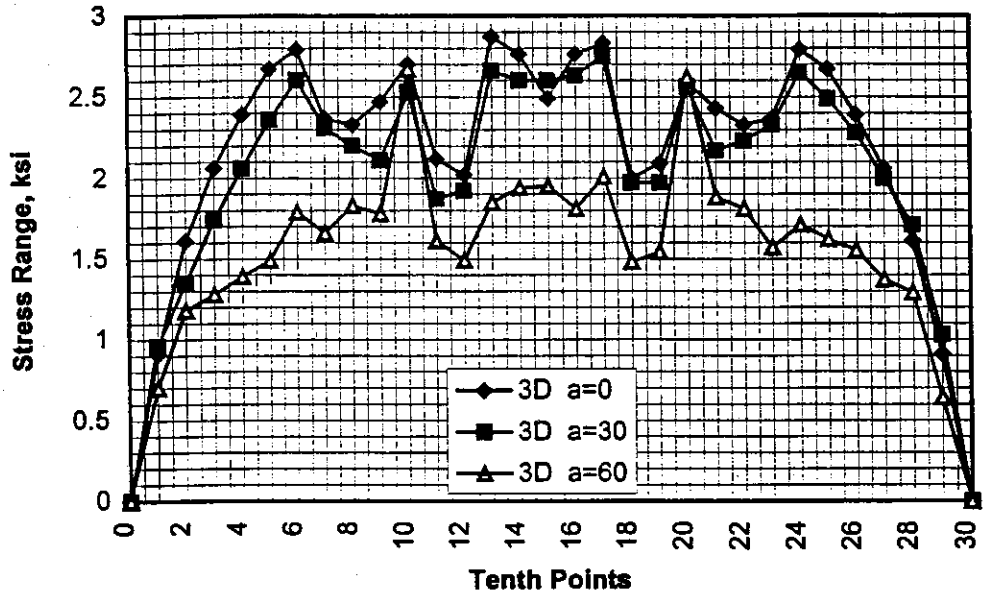

Figure 2.22-a Stress range diagram at top flange of girder G2 due to a Single HS20 Truck Load (D = 24 in.)

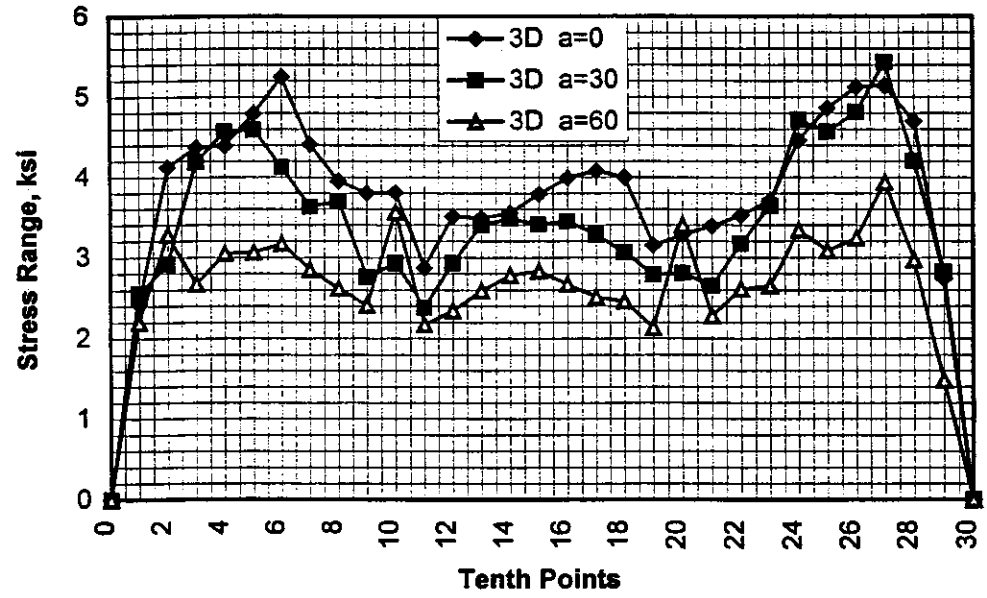

Figure 2.22-b Stress range diagram at bottom flange of girder G2 due to a Single HS20 Truck Load (D = 24 in.)

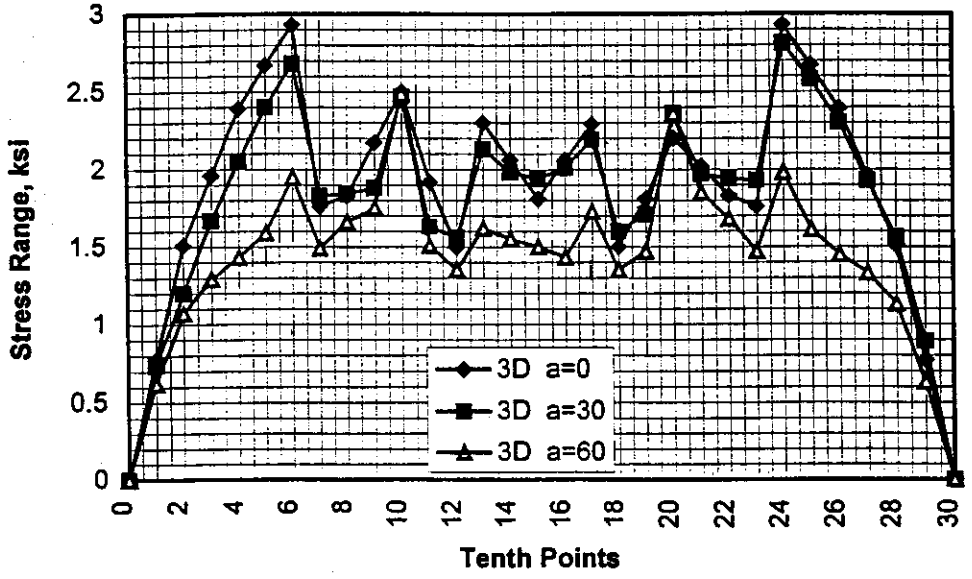

Figure 2.23-a Stress range diagram at top flange of girder G2 due to a Single HS20 Truck Load (D= 72 in.)

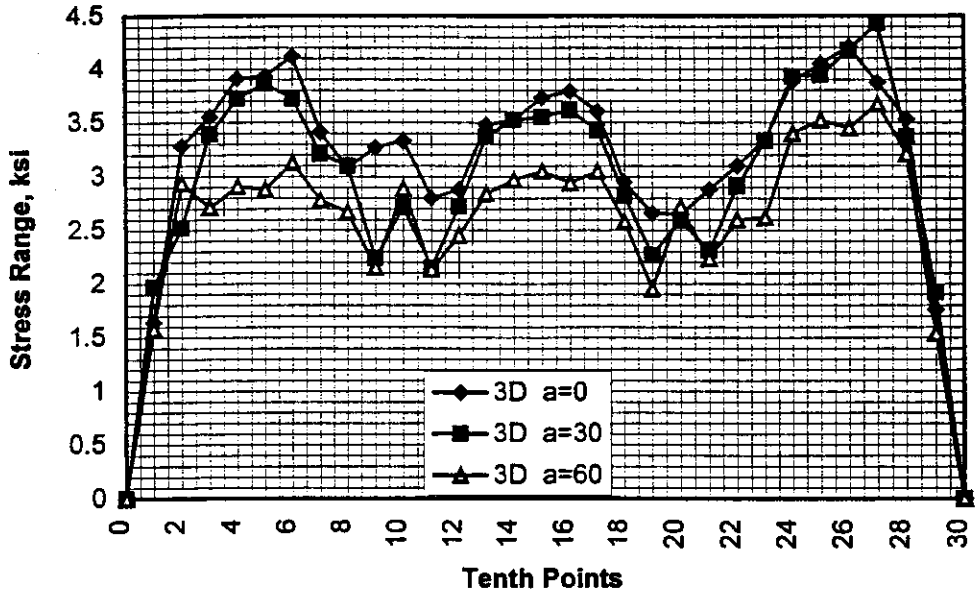

Figure 2.23-b Stress range diagram at bottom flange of girder G2 due to a Single HS20 Truck Load (D= 72 in.)

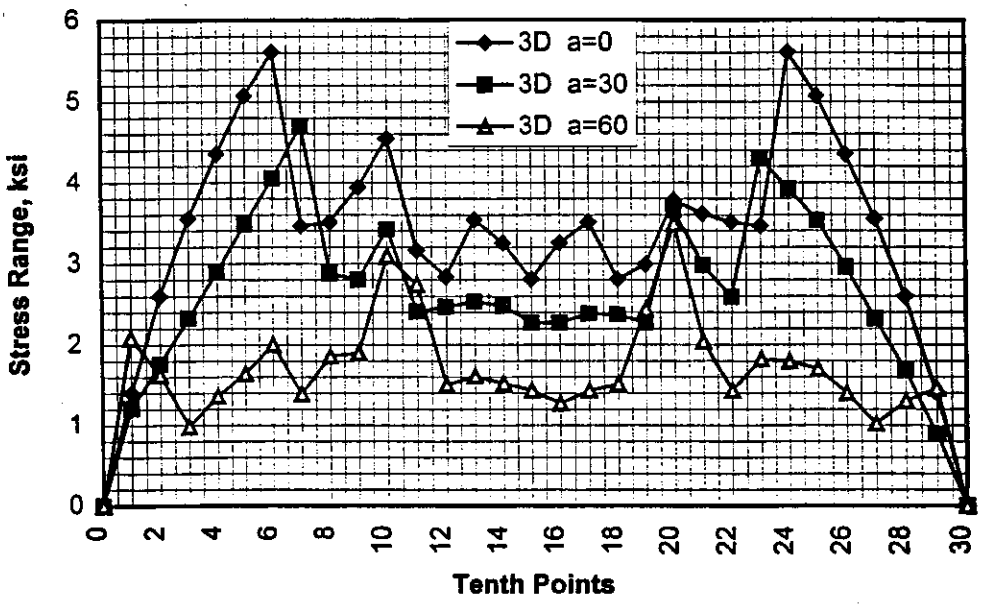

Figure 2.24-a Stress range diagram at top flange of girder G2 due to a Single HS20 Truck Load (S = 5.83 ft.)

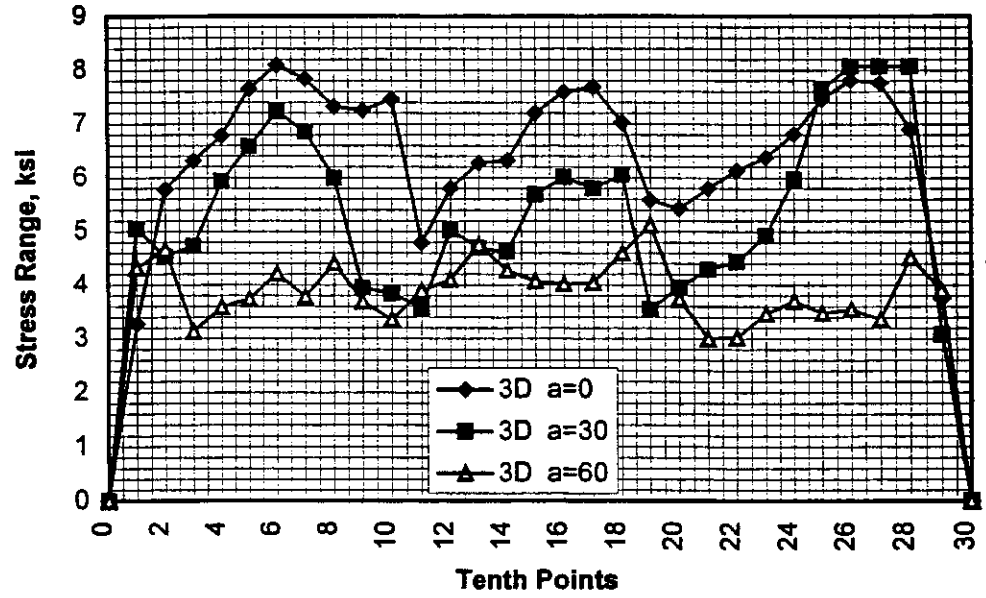

Figure 2.24-b Stress range diagram at bottom flange of girder G2 due to a Single HS20 Truck Load (S = 5.83 ft.)

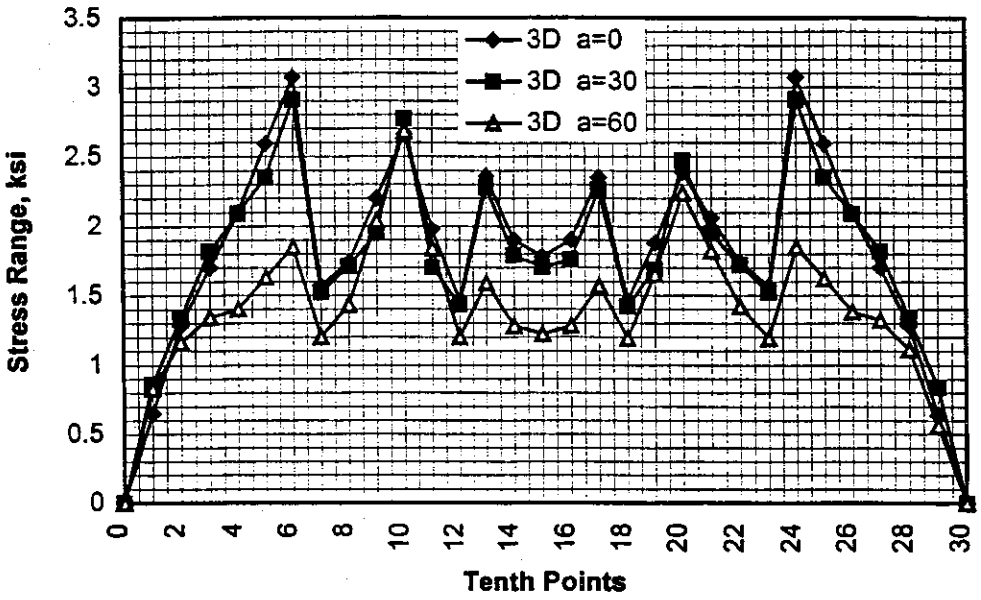

Figure 2.25-a Stress range diagram at top flange of girder G2 due to a Single HS20 Truck Load (S = 17.5 ft.)

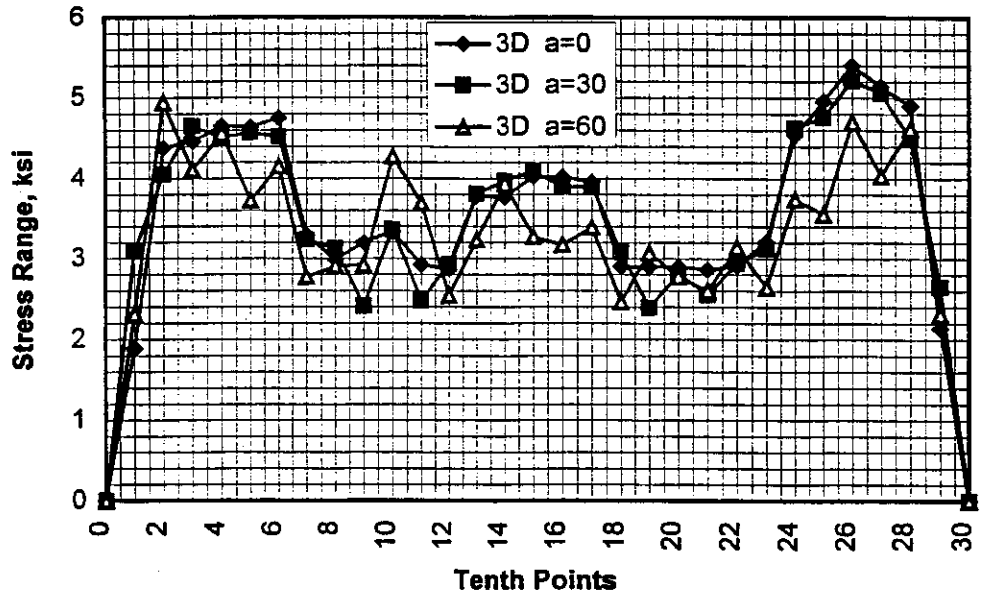

Figure 2.25-b Stress range diagram at bottom flange of girder G2 due to a Single HS20 Truck Load (S = 17.5 ft.)

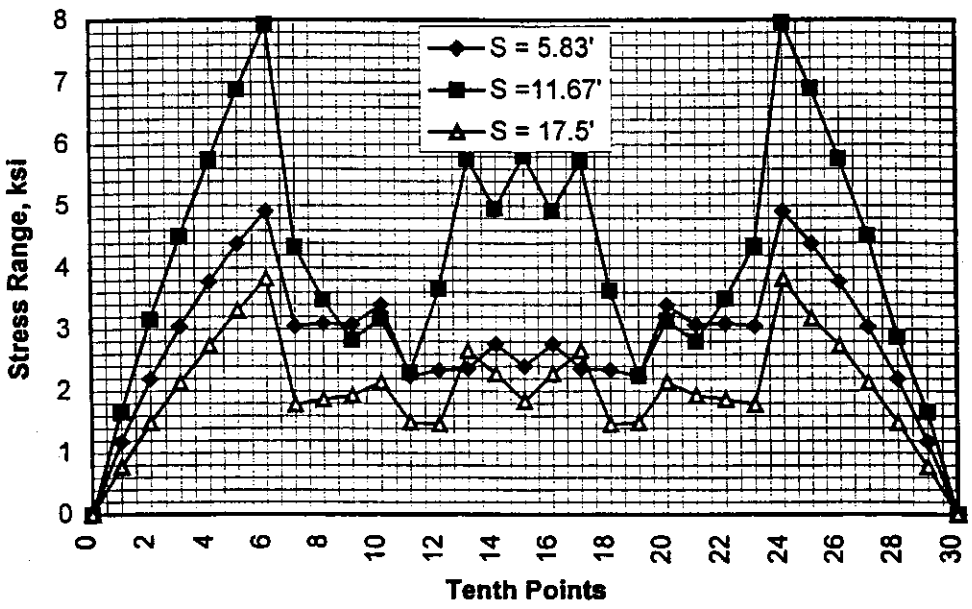

Figure 2.26-a Stress range diagram at top flange of girder G2 due to a Single HS20 Truck Load (Right bridge, 2D)

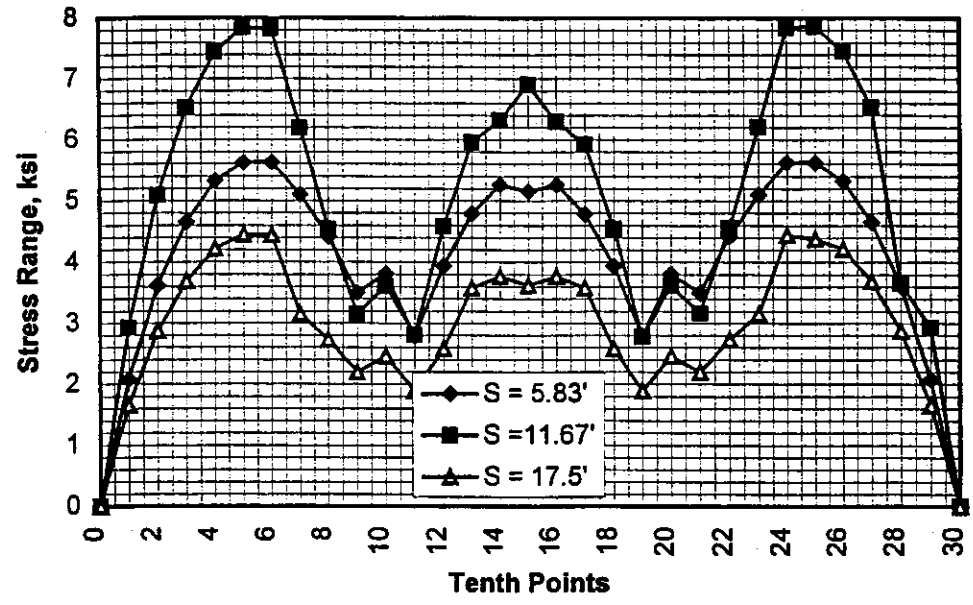

Figure 2.26-b Stress range diagram at bottom flange of girder G2 due to a Single HS20 Truck Load (Right bridge, 2D)

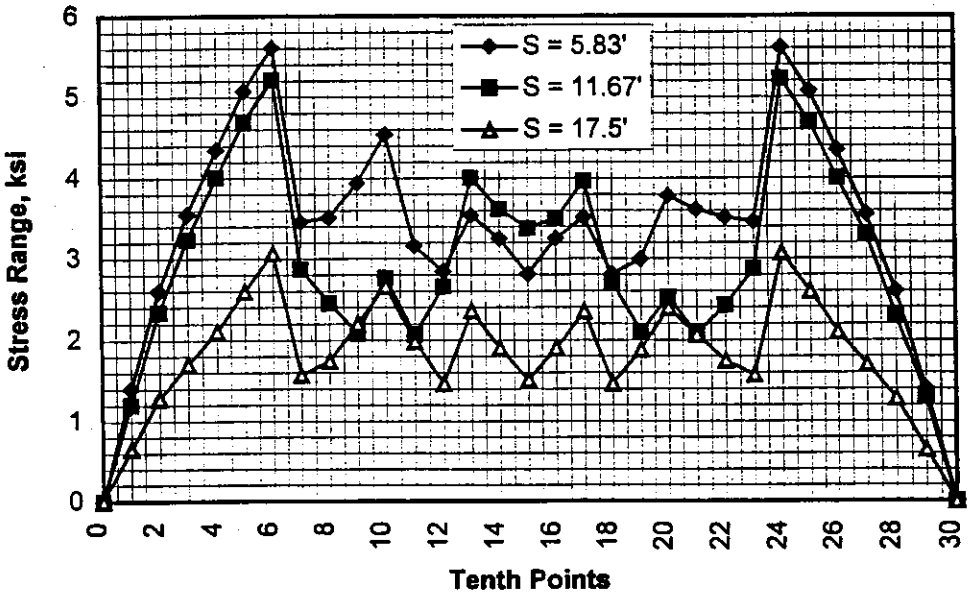

Figure 2.27-a Stress range diagram at top flange of girder G2 due to a Single HS20 Truck Load (Right bridge)

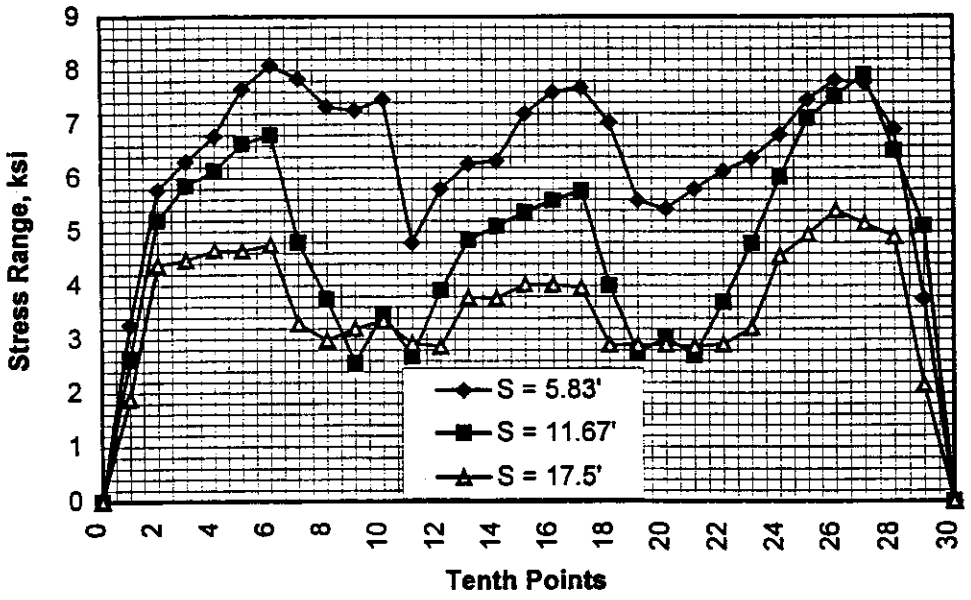

Figure 2.27-b Stress range diagram at bottom flange of girder G2 due to a Single HS20 Truck Load (Right bridge)

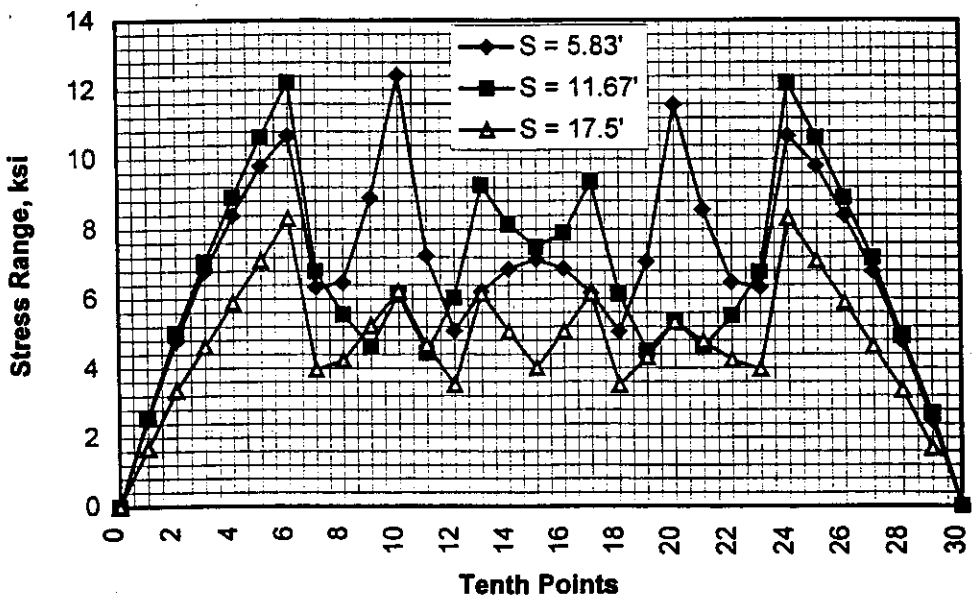

Figure 2.28-a Stress range diagram at top flange of girder G2 due to Multi-HS20 Truck Load (Right bridge)

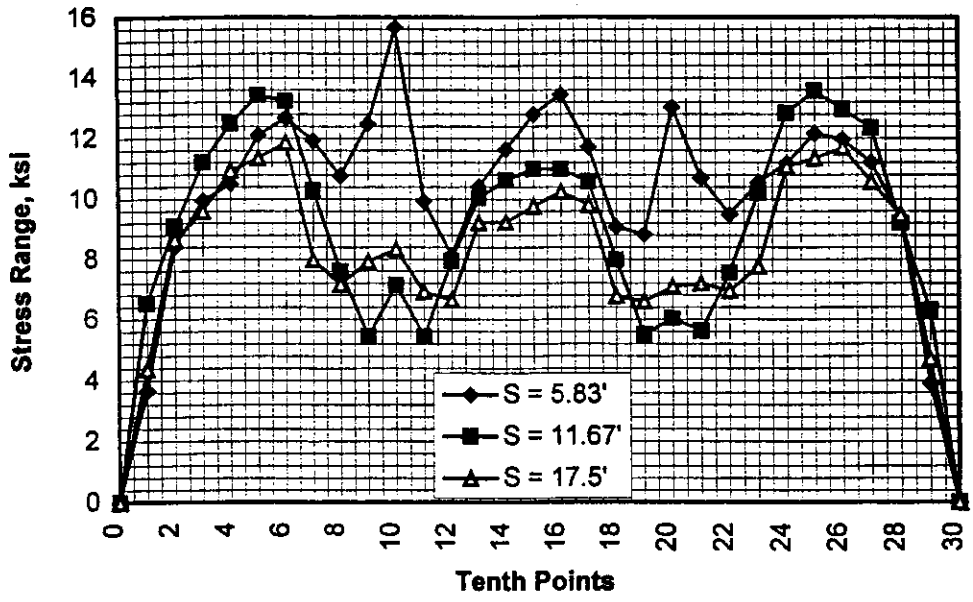

Figure 2.28-b Stress range diagram at bottom flange of girder G2 due to Multi-HS20 Truck Load (Right bridge)

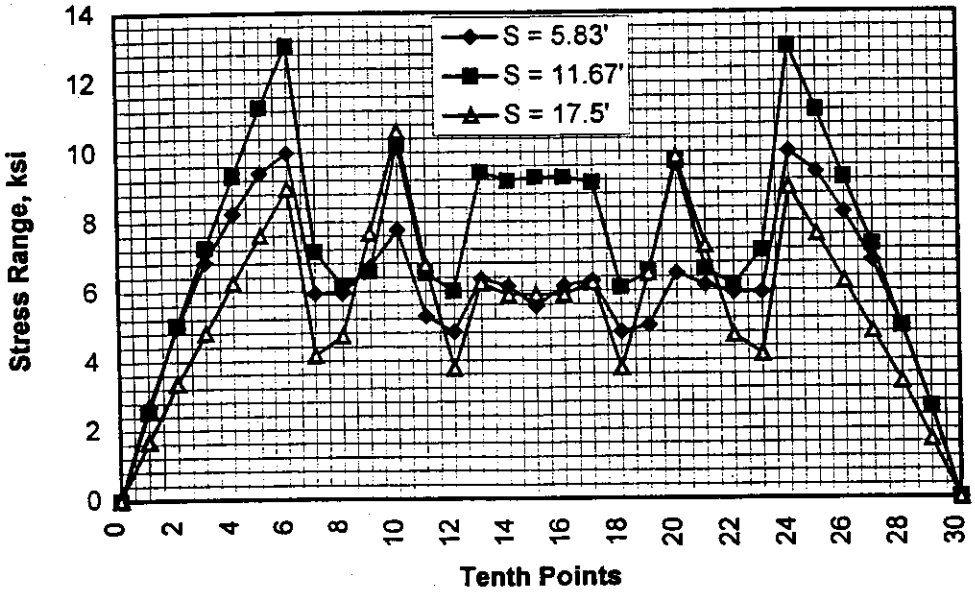

Figure 2.29-a Stress range diagram at top flange of girder G2 due to Multi-Lane Load (Right bridge)

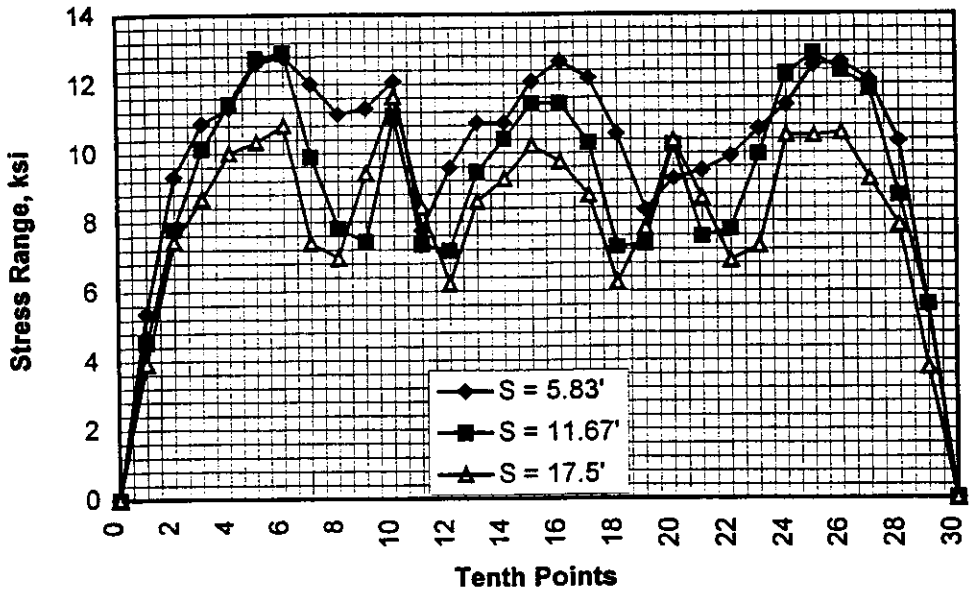

Figure 2.29-b Stress range diagram at bottom flange of girder G2 due to Multi-Lane Load (Right bridge)

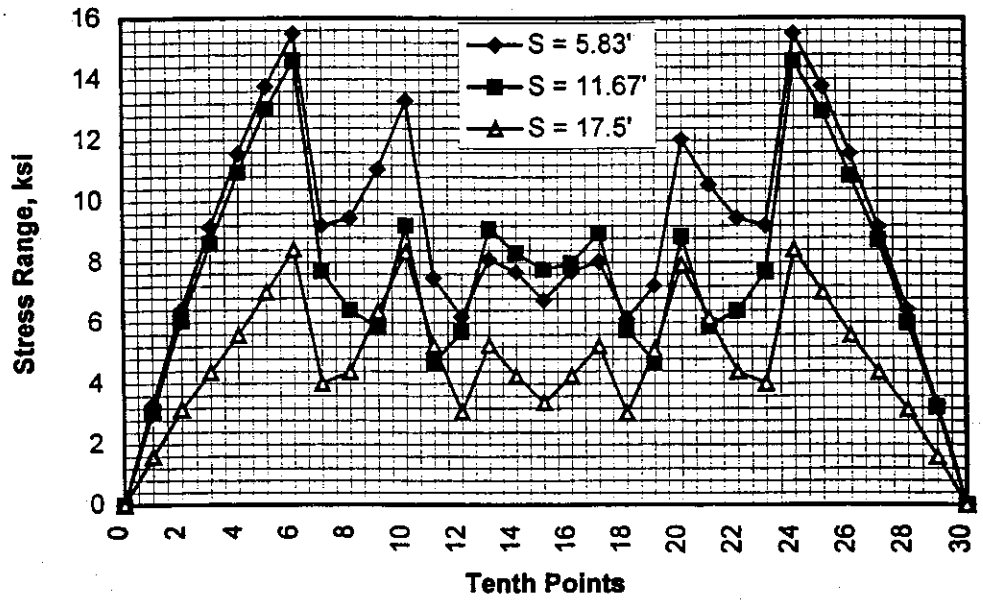

Figure 2.30-a Stress range diagram at top flange of girder G2 due to a Single P13 Truck Load (Right bridge)

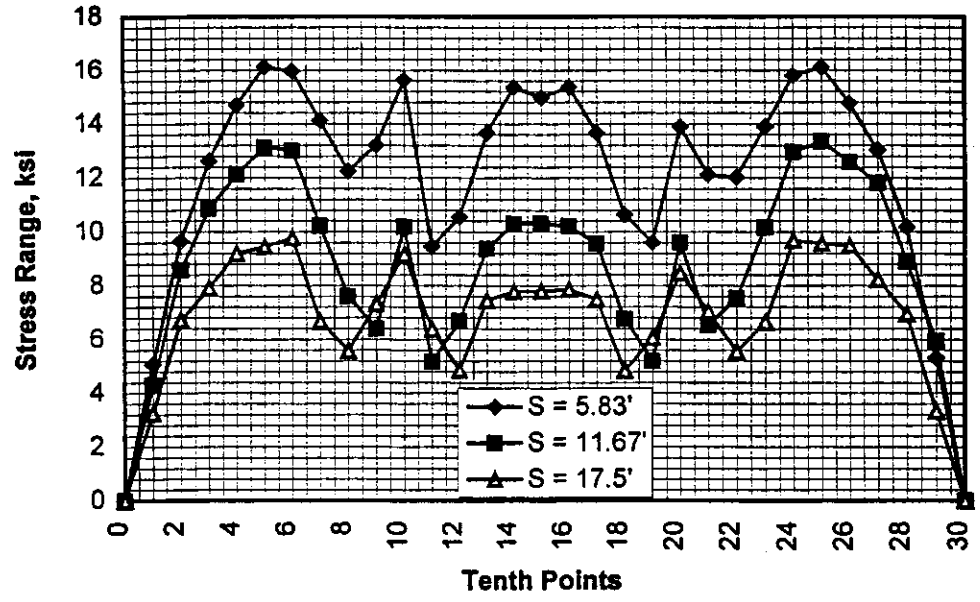

Figure 2.30-b Stress range diagram at bottom flange of girder G2 due to a Single P13 Truck Load (Right bridge)

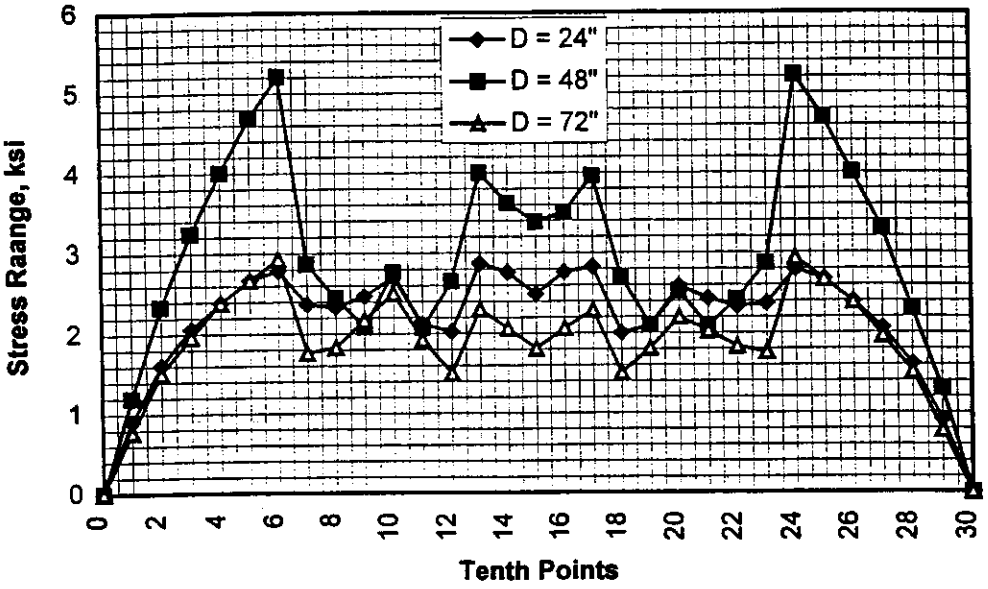

Figure 2.31-a Stress range diagram at top flange of girder G2 due to a Single HS20 Truck Load (Right bridge)

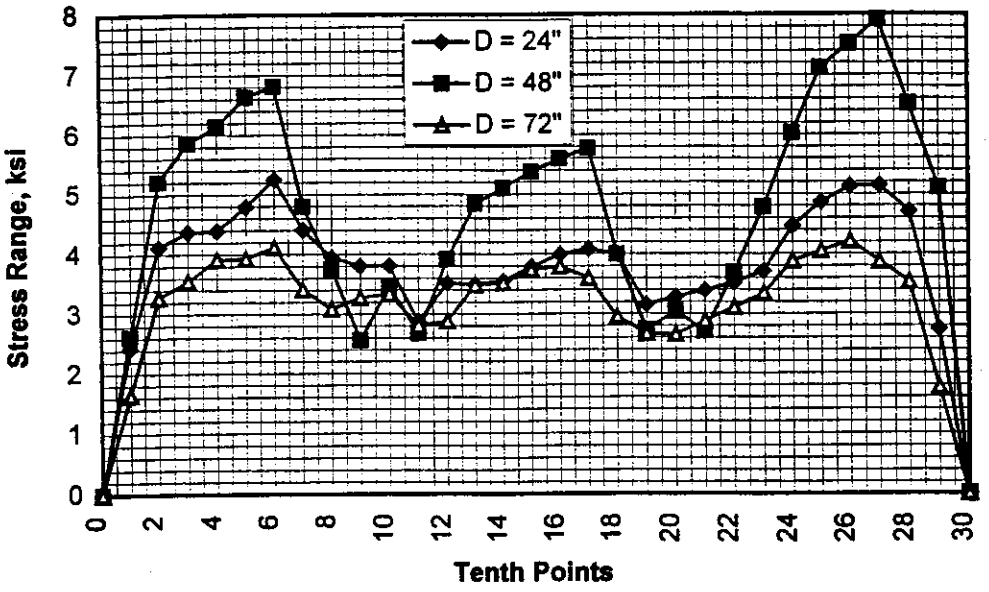

Figure 2.31-b Stress range diagram at bottom flange of girder G2 due to a Single HS20 Truck Load (Right bridge)

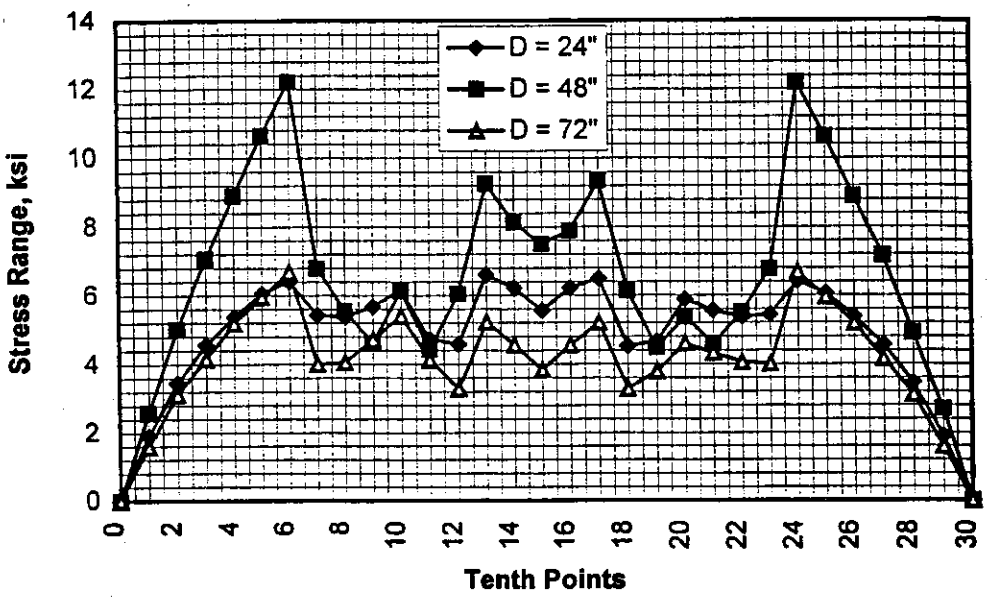

Figure 2.32-a Stress range diagram at top flange of girder G2 due to Multi- HS20 Truck (Right bridge)

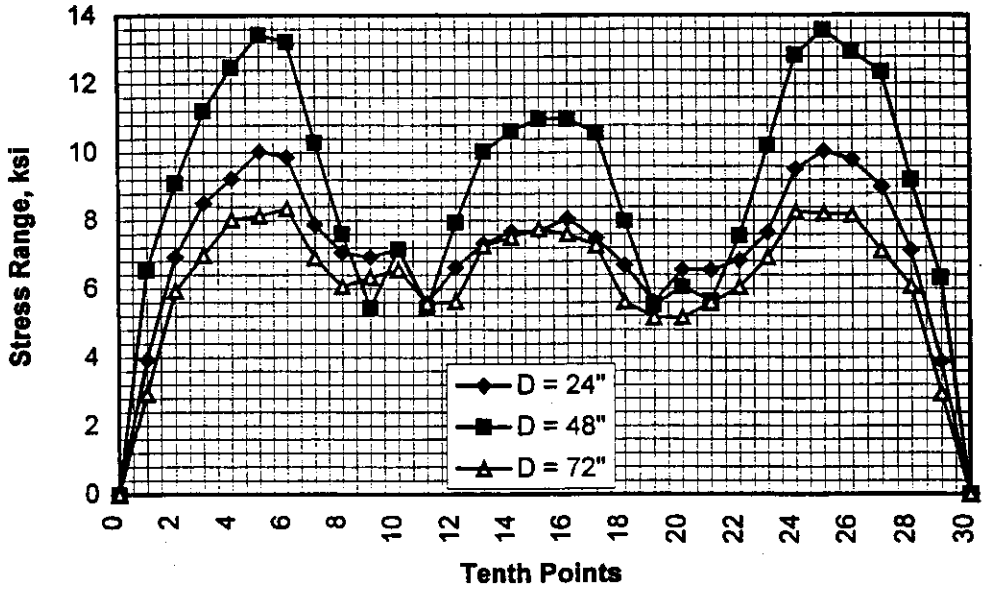

Figure 2.32-b Stress range diagram at bottom flange of girder G2 due to Multi- HS20 Truck (Right bridge)

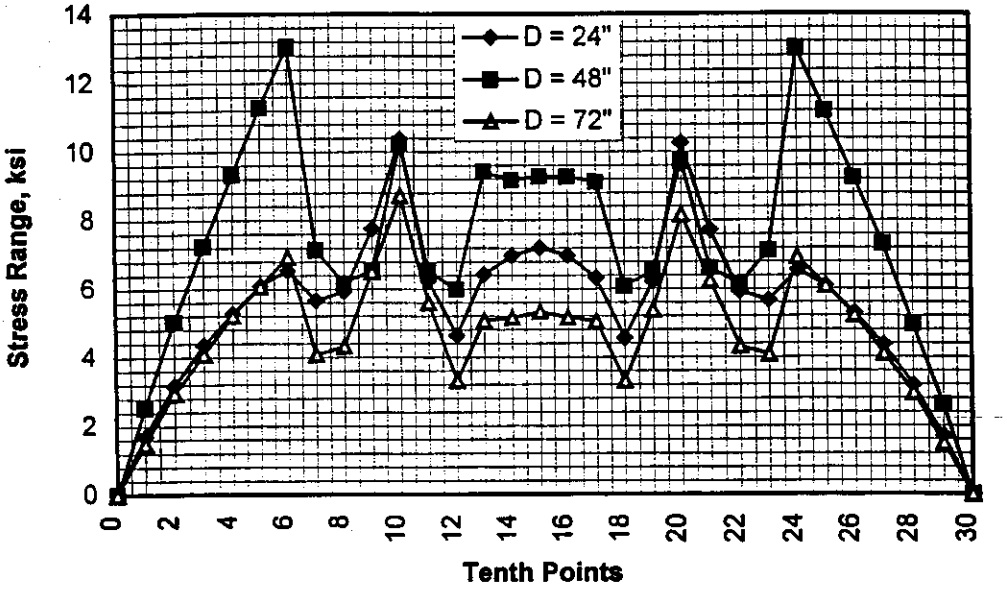

Figure 2.33-a Stress range diagram at top flange of girder G2 due to Multi-Lane Load (Right bridge)

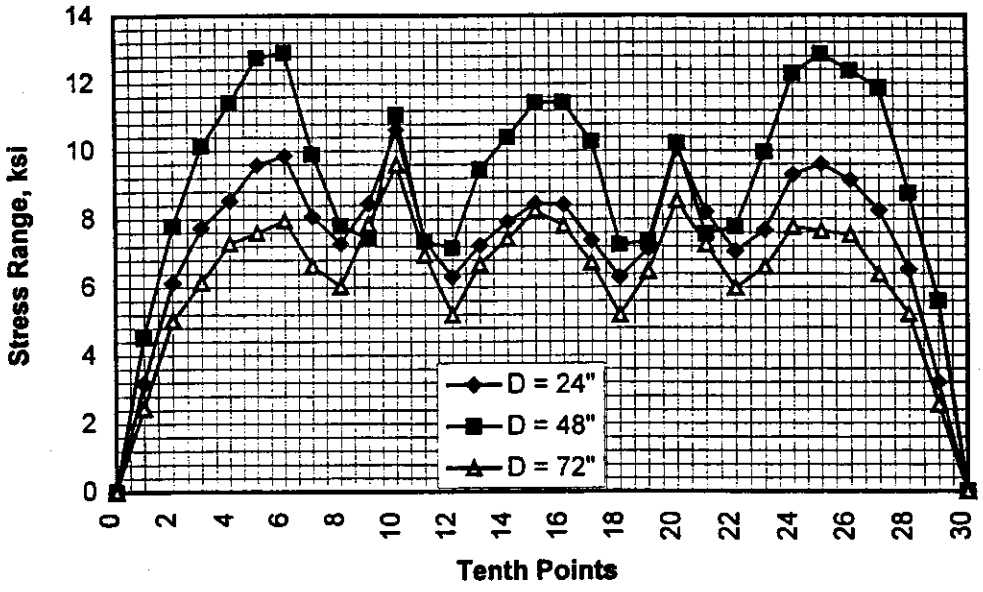

Figure 2.33-b Stress range diagram at bottom flange of girder G2 due to Multi-Lane Load (Right bridge)

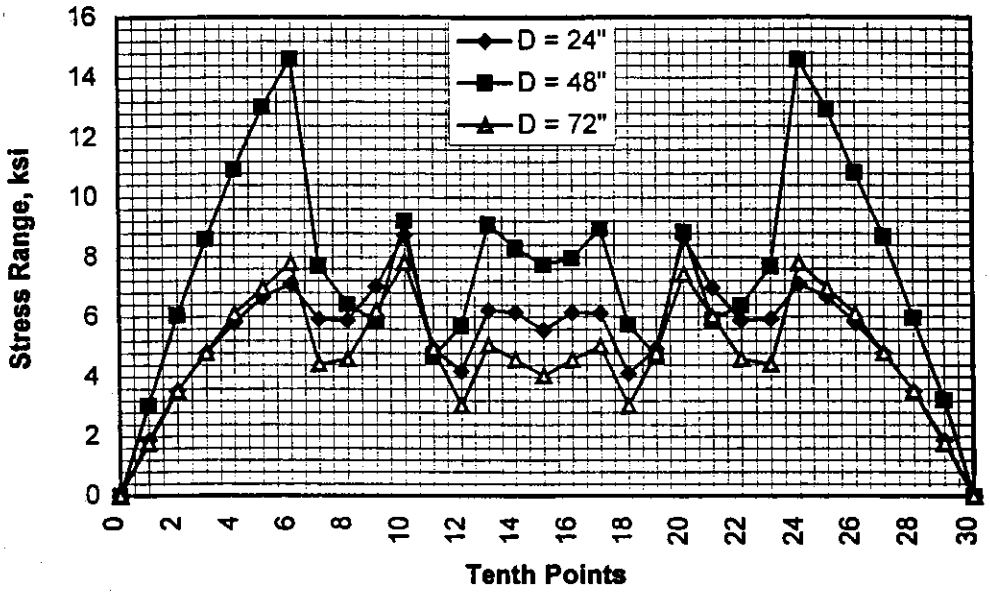

Figure 2.34-a Stress range diagram at top flange of girder G2 due to a Single P13 Truck Load (Right bridge)

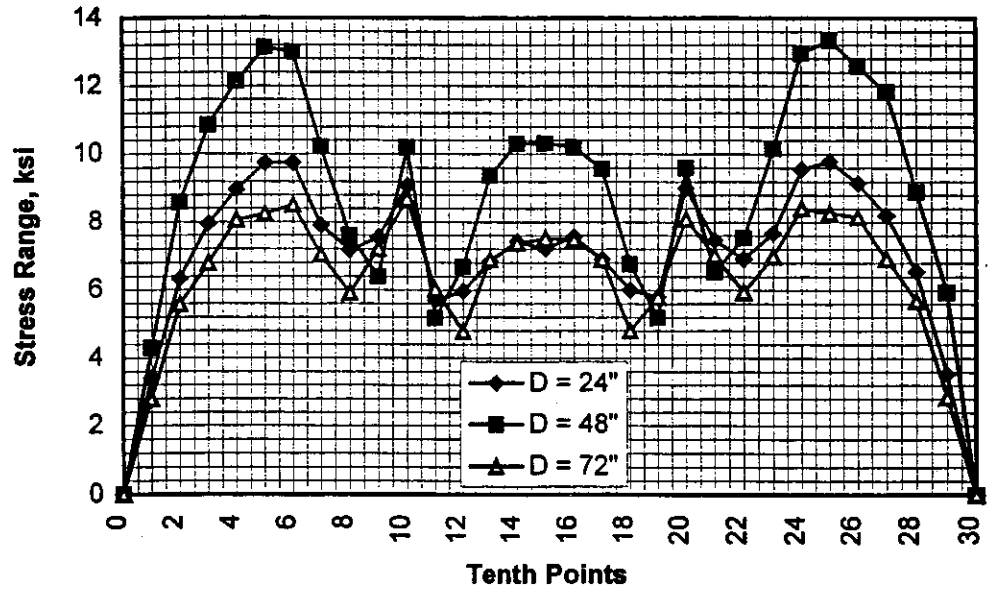

Figure 2.34-b Stress range diagram at bottom flange of girder G2 due to a Single P13 Truck Load (Right bridge)

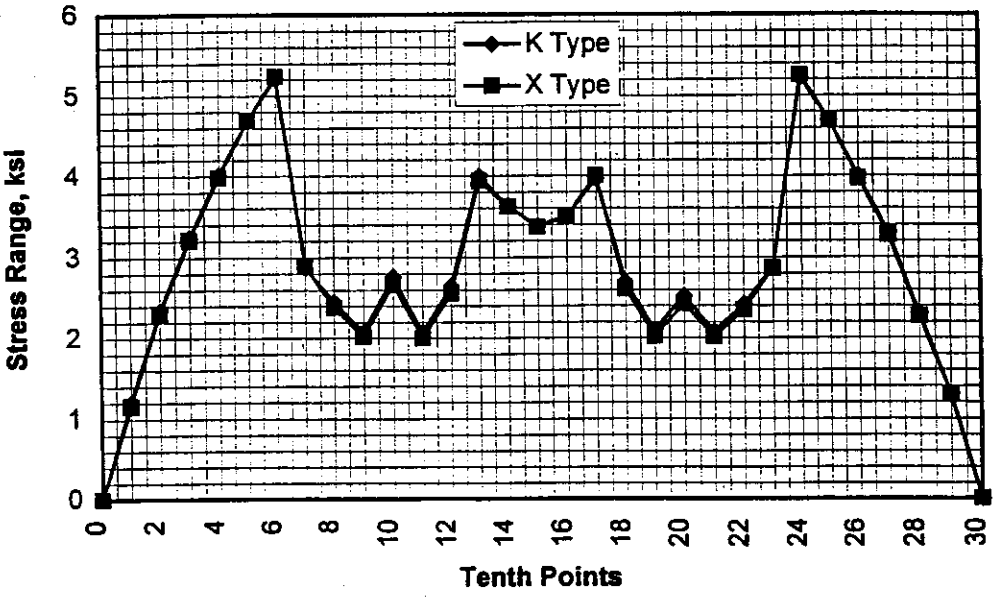

Figure 2.35-a Stress range diagram at top flange of girder G2 due to a Single HS20 Truck Load (a = 0°)

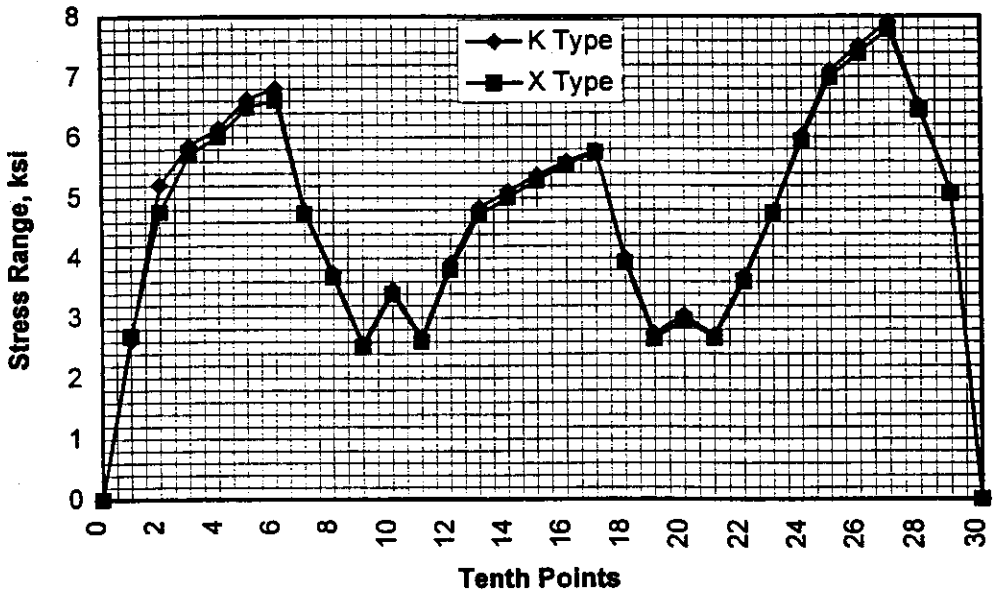

Figure 2.35-b Stress range diagram at bottom flange of girder G2 due to a Single HS20 Truck Load (a = 0°)

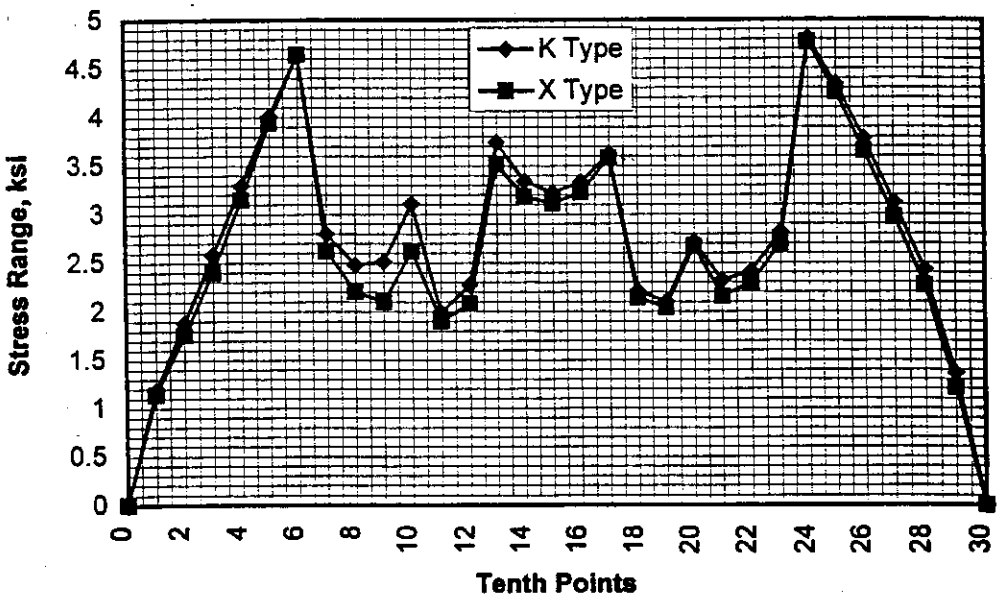

Figure 2.36-a Stress range diagram at top flange of girder G2 due to a Single HS20 Truck Load (a = 30°)

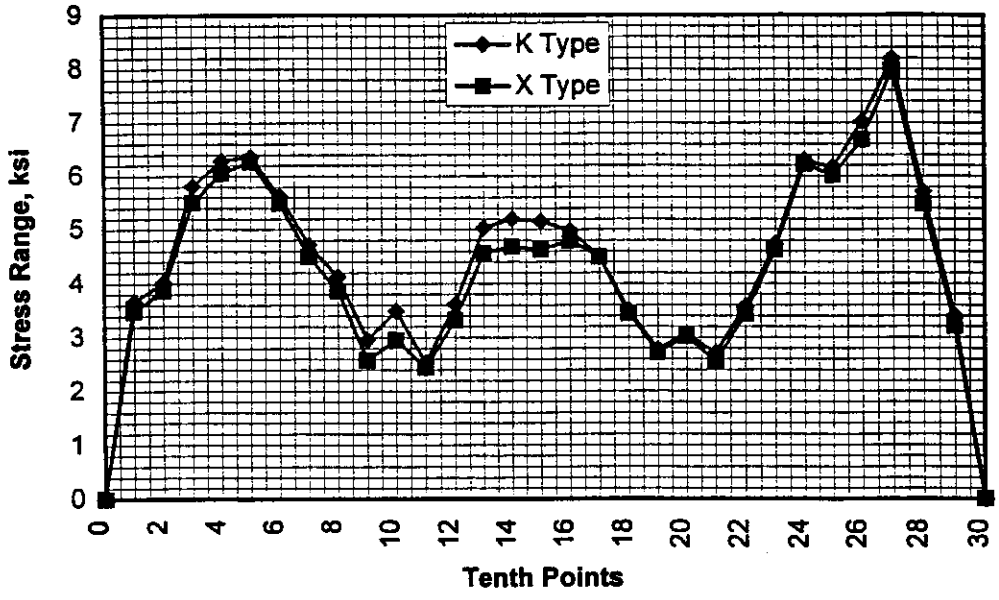

Figure 2.36-b Stress range diagram of bottom flange of girder G2 due to a Single HS20 Truck Load (a = 30°)

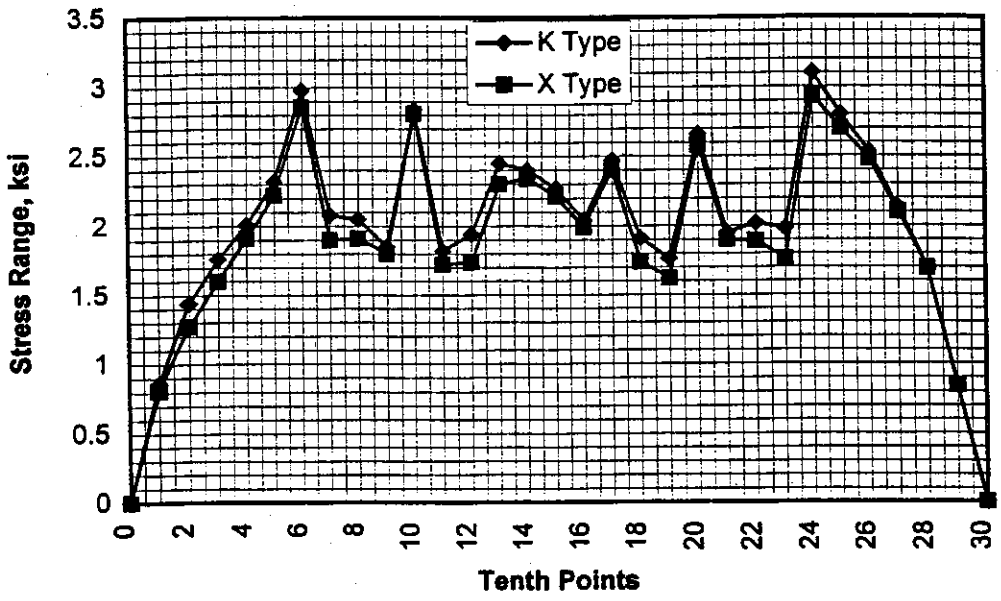

Figure 2.37-a Stress range diagram at bottom flange of girder G2 due to a Single HS20 Truck Load (a = 60°)

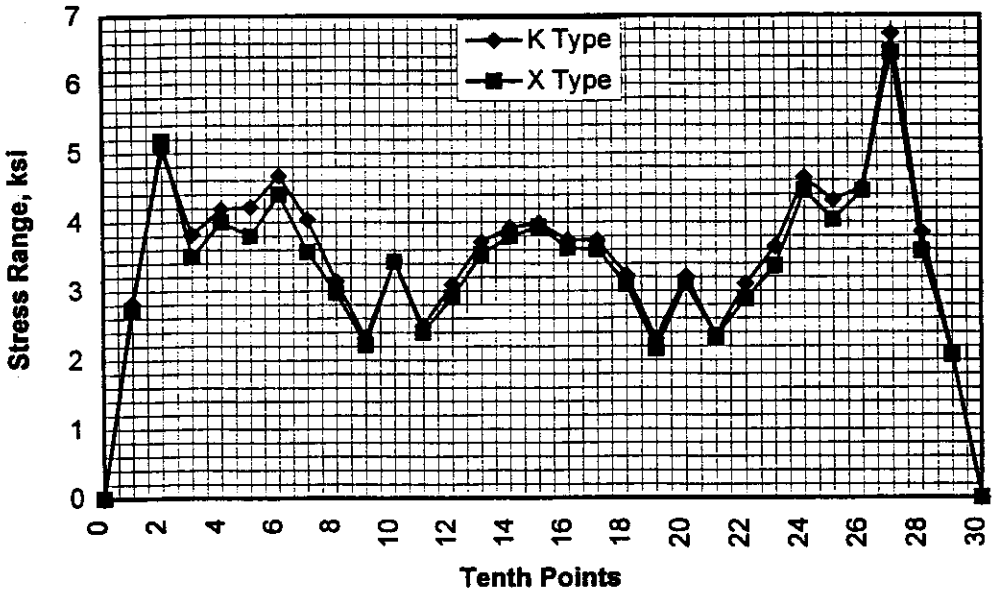

Figure 2.37-b Stress range diagram at bottom flange of girder G2 due to a Single HS20 Truck Load (a = 60°)

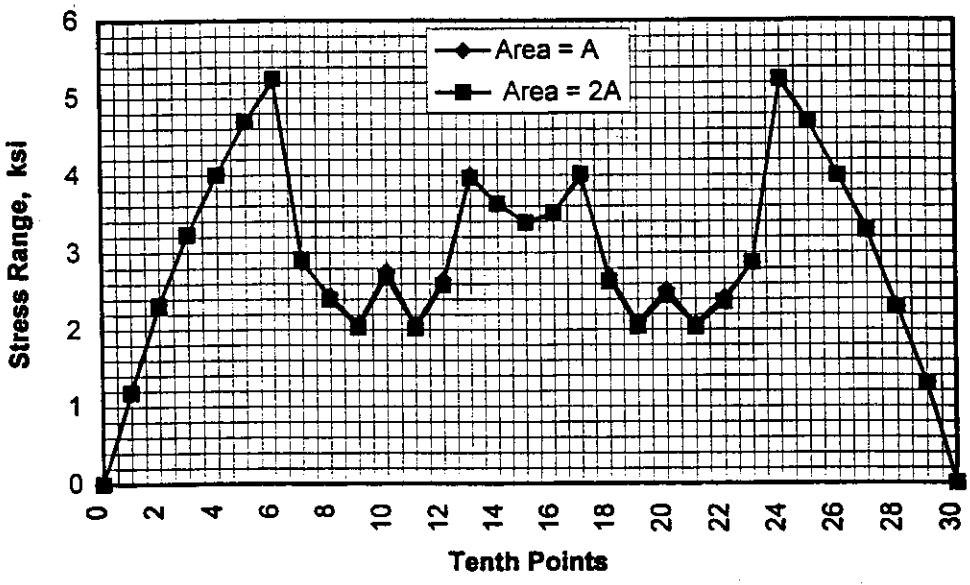

Figure 2.38-a Stress range diagram at top flange of girder G2 due to a Single HS20 Truck Load (Right bridge, K Type cross frames)

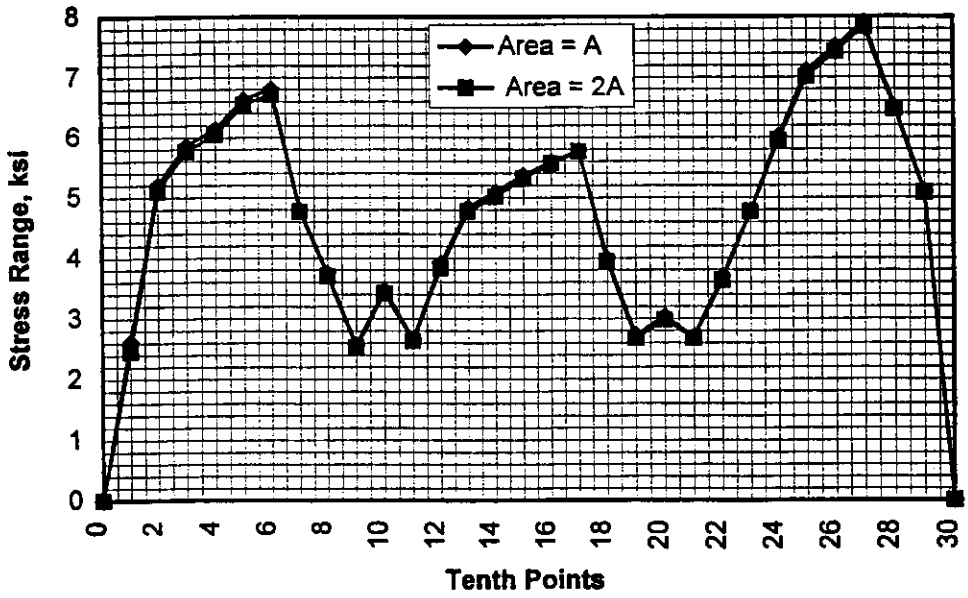

Figure 2.38-b Stress range diagram at bottom flange of girder G2 due to a Single HS20 Truck Load (Right bridge, K Type cross frames)

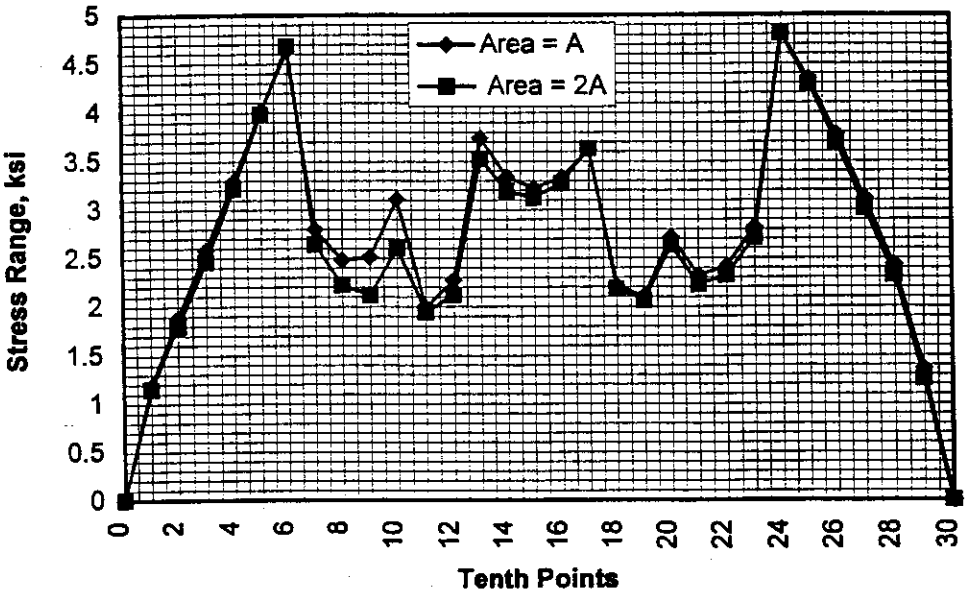

Figure 2.39-a Stress range diagram at top flange of girder G2 due to a Single HS20 Truck Load (a = 30°, K Type cross frames)

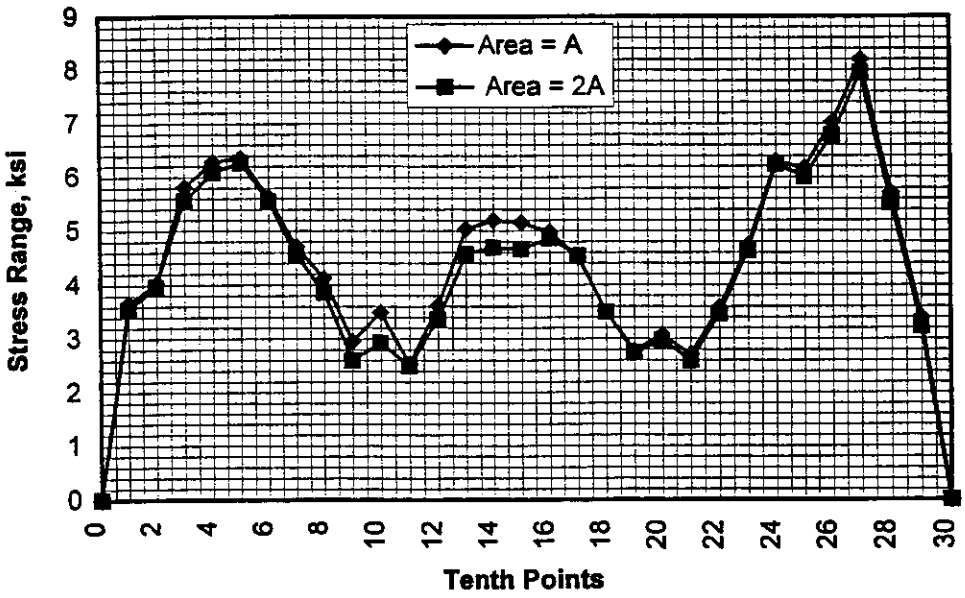

Figure 2.39-b Stress range diagram at bottom flange of girder G2 due to a Single HS20 Truck Load (a = 30°, K Type cross frames)

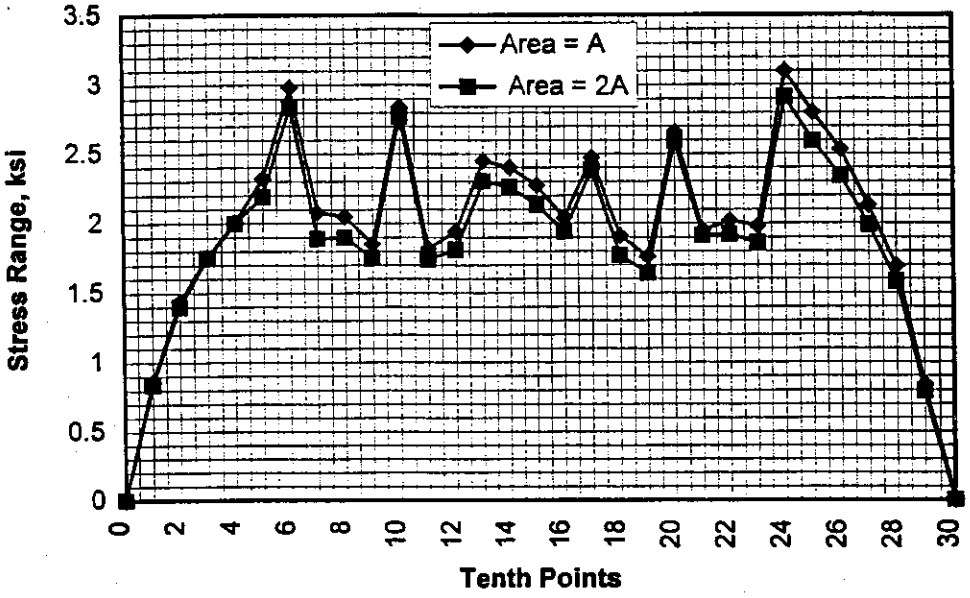

Figure 2.40-a Stress range diagram at top flange of girder G2 due to a Single HS20 Truck Load (a = 60°, K Type cross frames)

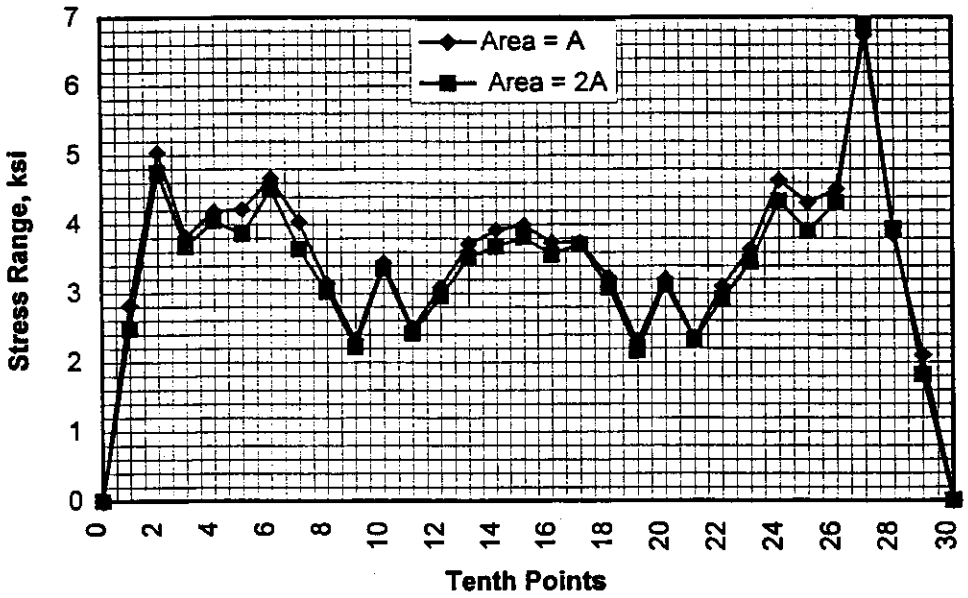

Figure 2.40-b Stress range diagram at bottom flange of girder G2 due to a Single HS20 Truck Load (a = 60°, K Type cross frames)

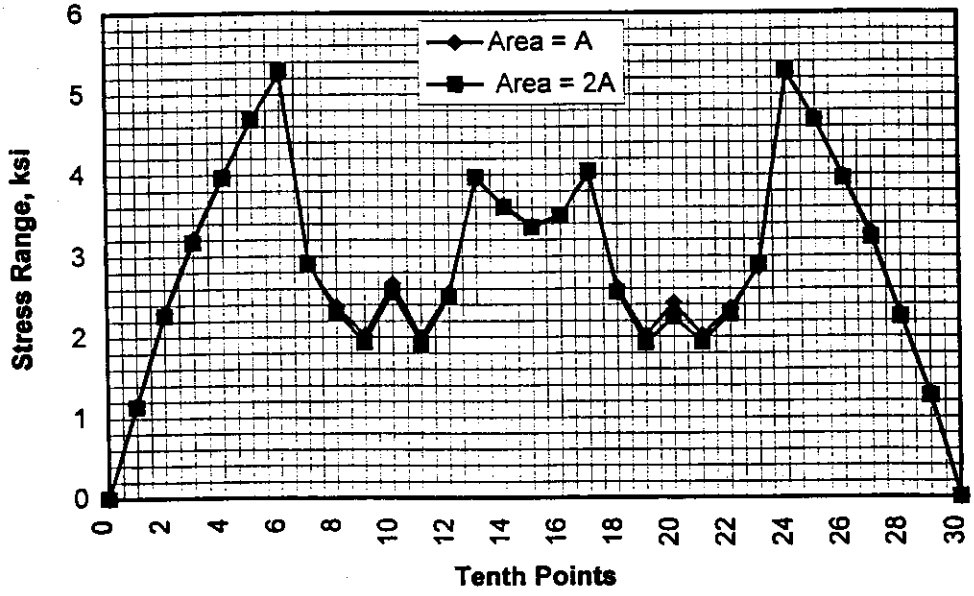

Figure 2.41-a Stress range diagram at top flange of girder G2 due to a Single HS20 Truck Load (Right bridge, X Type cross frames)

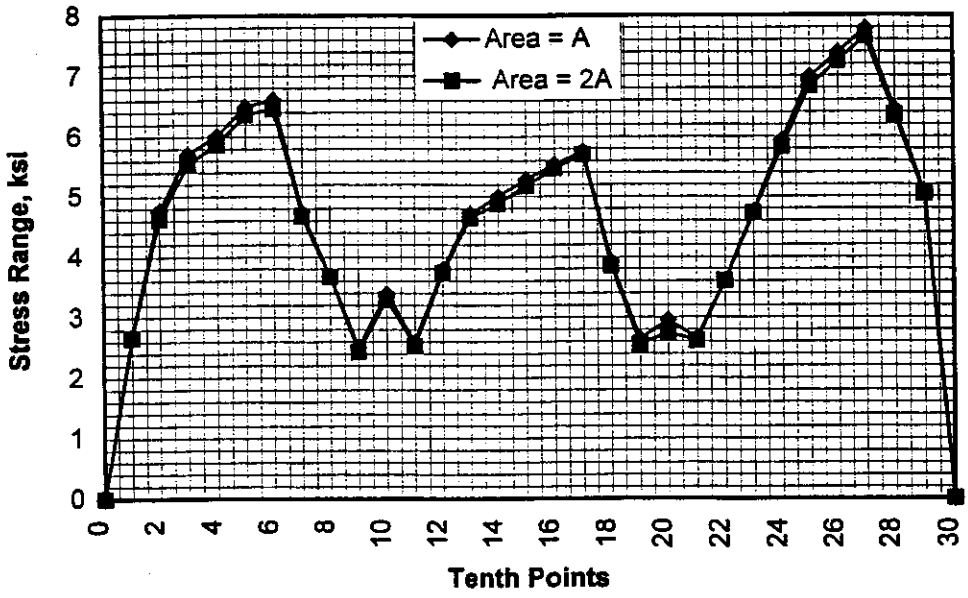

Figure 2.41-b Stress range diagram at bottom flange of girder G2 due to a Single HS20 Truck Load (Right bridge, X Type cross frames)

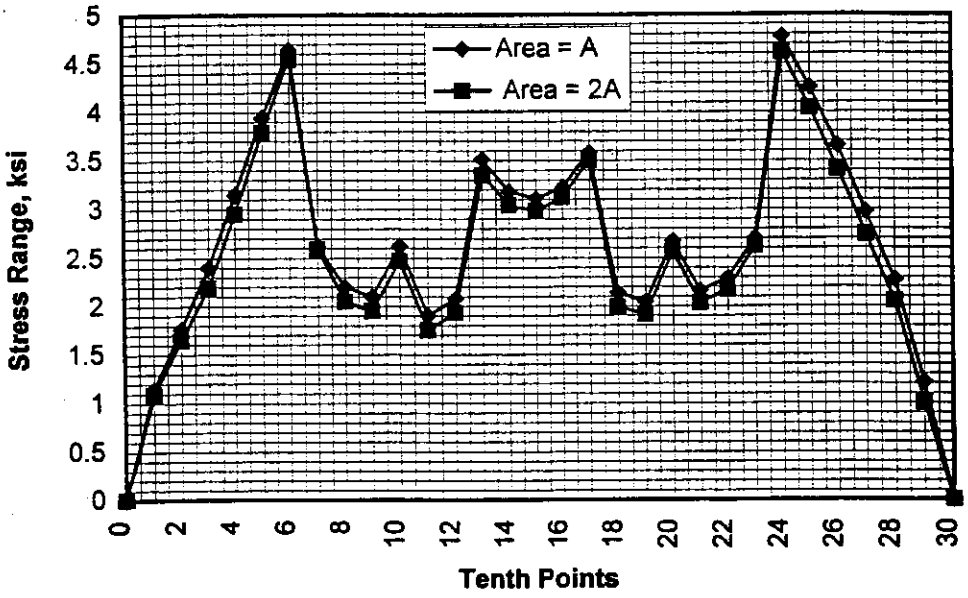

Figure 2.42-a Stress range diagram at top flange of girder G2 due to a Single HS20 Truck Load (a = 30°, X Type cross frames)

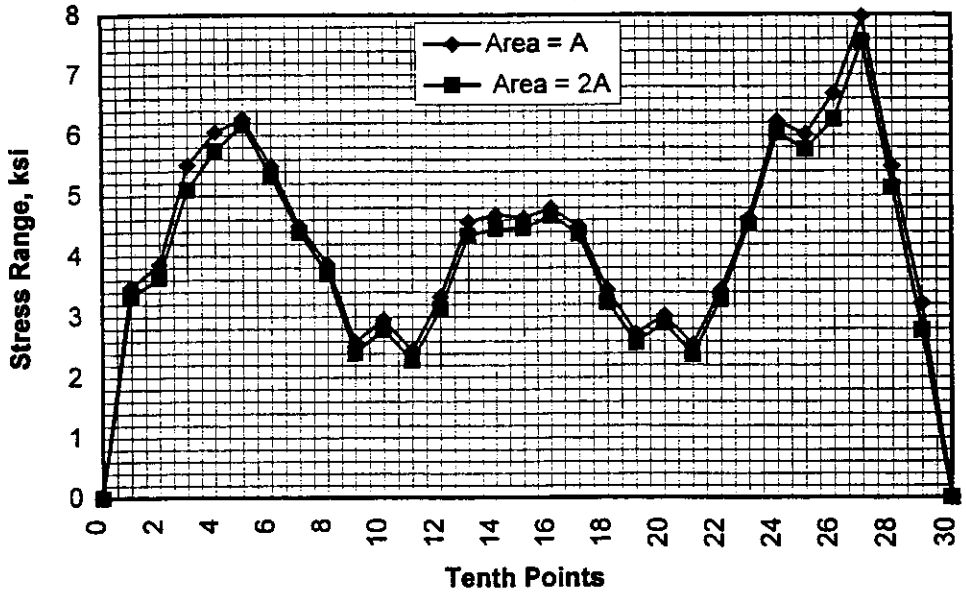

Figure 2.42-b Stress range diagram at bottom flange of girder G2 due to a Single HS20 Truck Load (a = 30°, X Type cross frames)

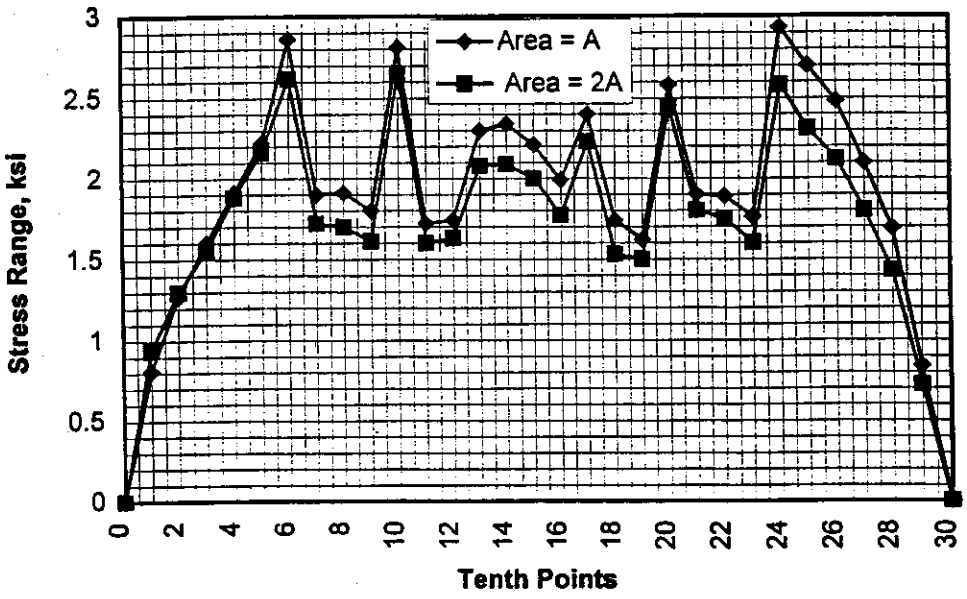

Figure 2.43-a Stress range diagram at top flange of girder G2 due to a Single HS20 Truck Load (a = 60°, X Type cross frames)

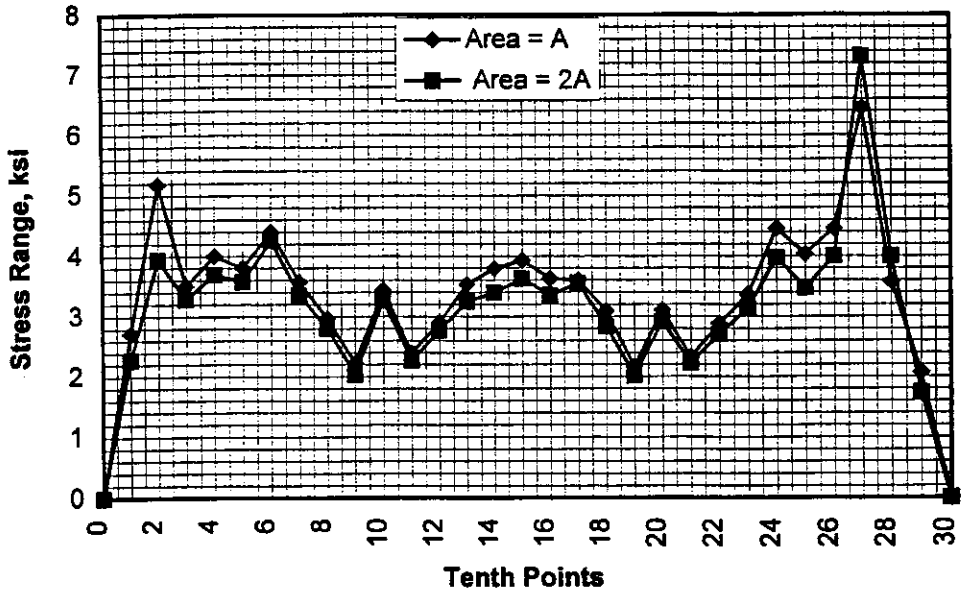

Figure 2.43-b Stress range diagram at bottom flange of girder G2 due to a Single HS20 Truck Load (a = 60°, X Type cross frames)

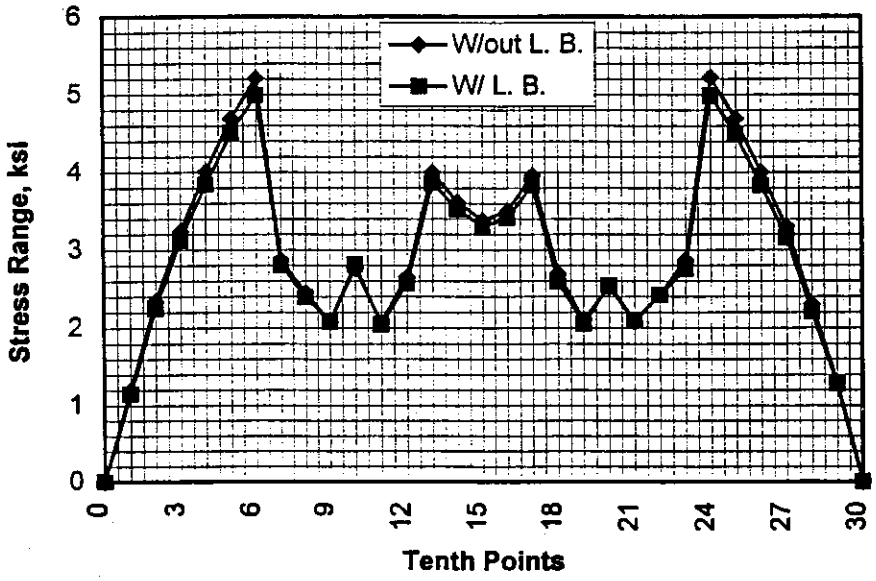

Figure 2.44-a Stress range diagram at top flange of girder G2 due to a Single HS20 Truck Load (Right bridge)

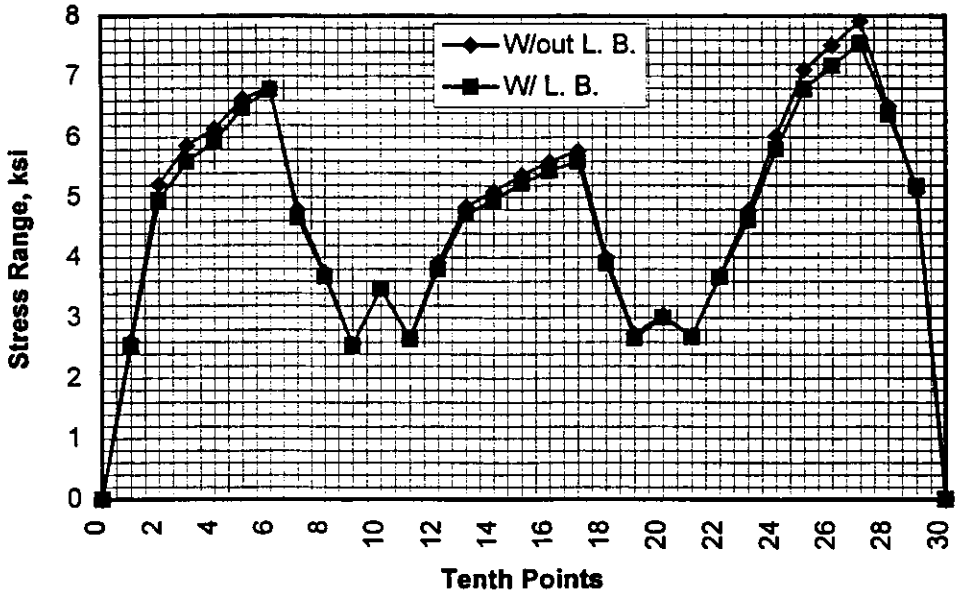

Figure 2.44-b Stress range diagram at bottom flange of girder G2 due to a Single HS20 Truck Load (Right bridge)

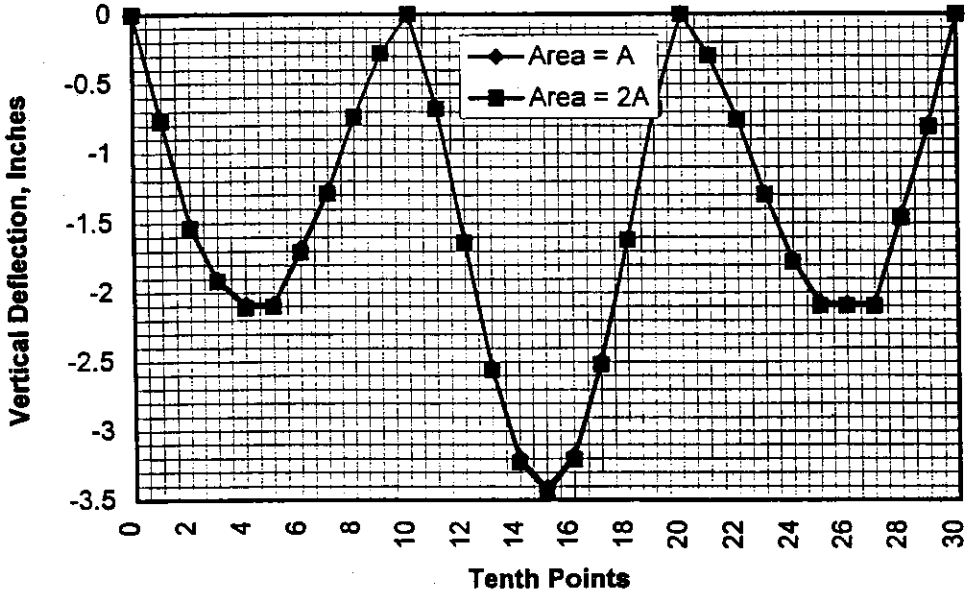

Figure 2.45-a Deflection diagram at girder G1 due to Multi-HS20 Truck Load (Right bridge, X Type cross frame)

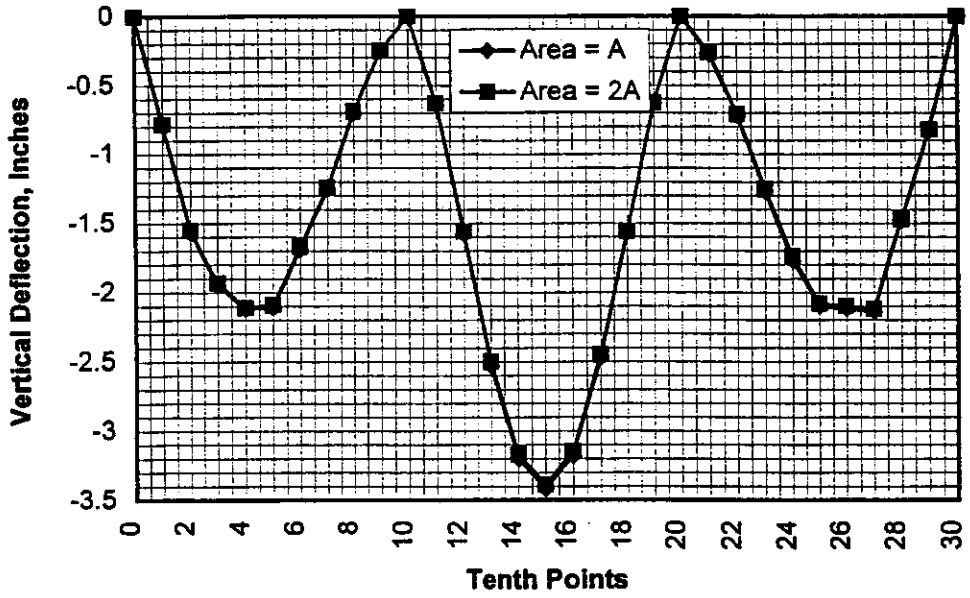

Figure 2.45-b Deflection diagram of girder G2 due to Multi-HS20 Truck Load (Right bridge, X Type cross frame)

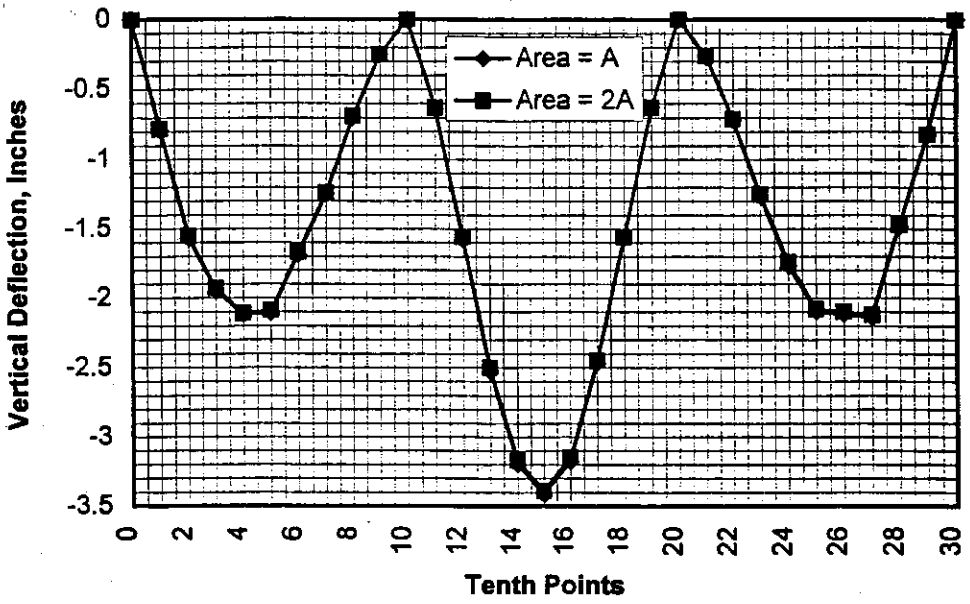

Figure 2.46-a Deflection diagram at girder G3 due to Multi-HS20 Truck Load (Right bridge, X Type cross frame)

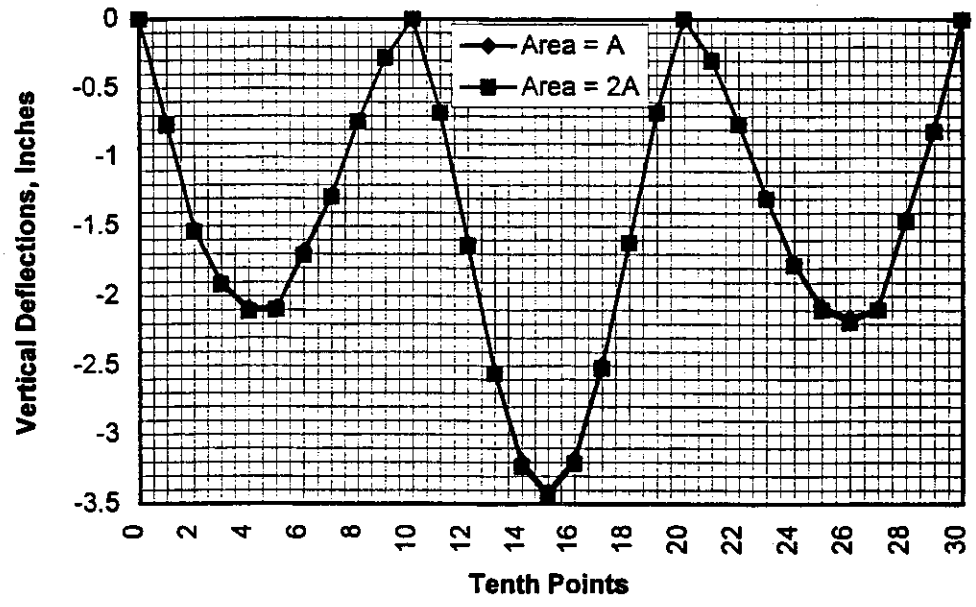

Figure 2.46-b Deflection diagram of girder G4 due to Multi-HS20 Truck Load (Right bridge, X Type cross frame)

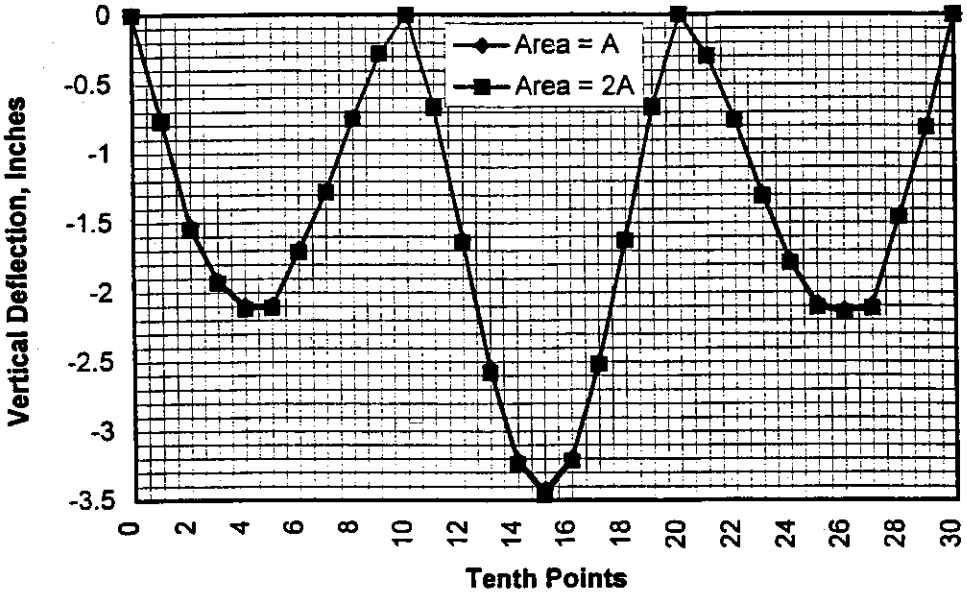

Figure 2.47-a Deflection diagram of girder G1 due to Multi-HS20 Truck Load
(Right bridge, K Type cross frame)

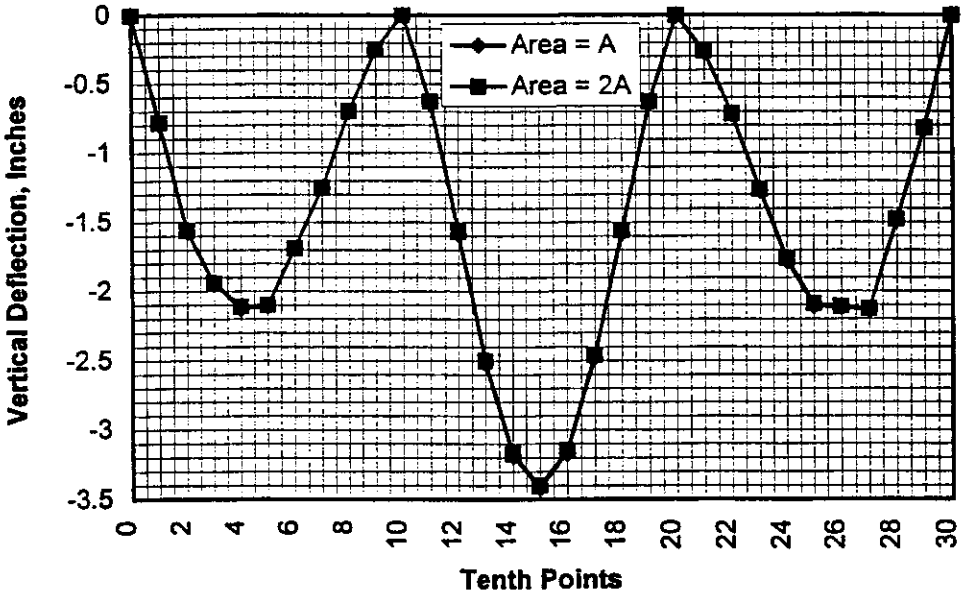

Figure 2.47-b Deflection diagram of girder G2 due to Multi-HS20 Truck Load
(Right bridge, K Type cross frame)

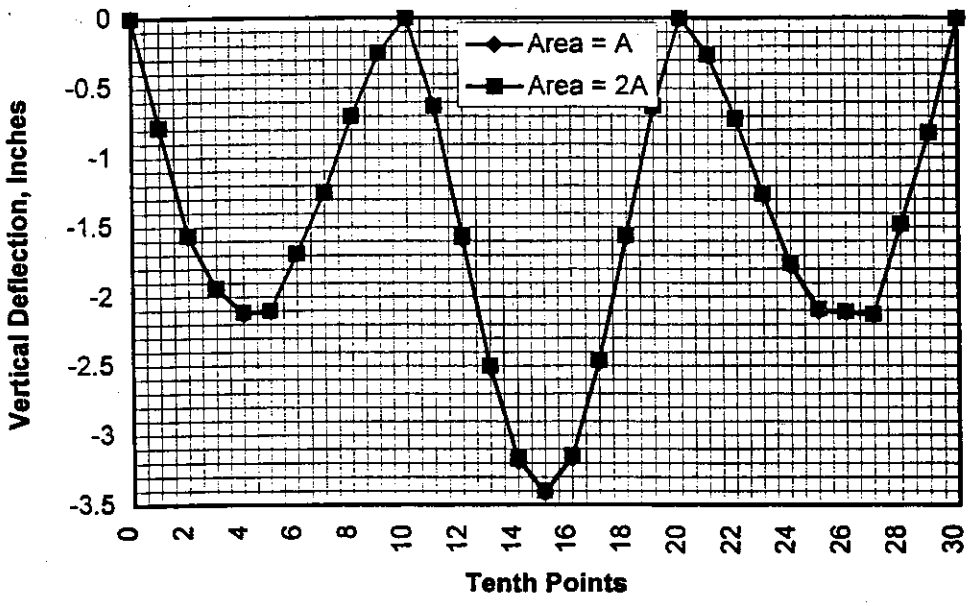

Figure 2.48-a Deflection diagram of girder G3 due to Multi-HS20 Truck Load
(Right bridge, K Type cross frame)

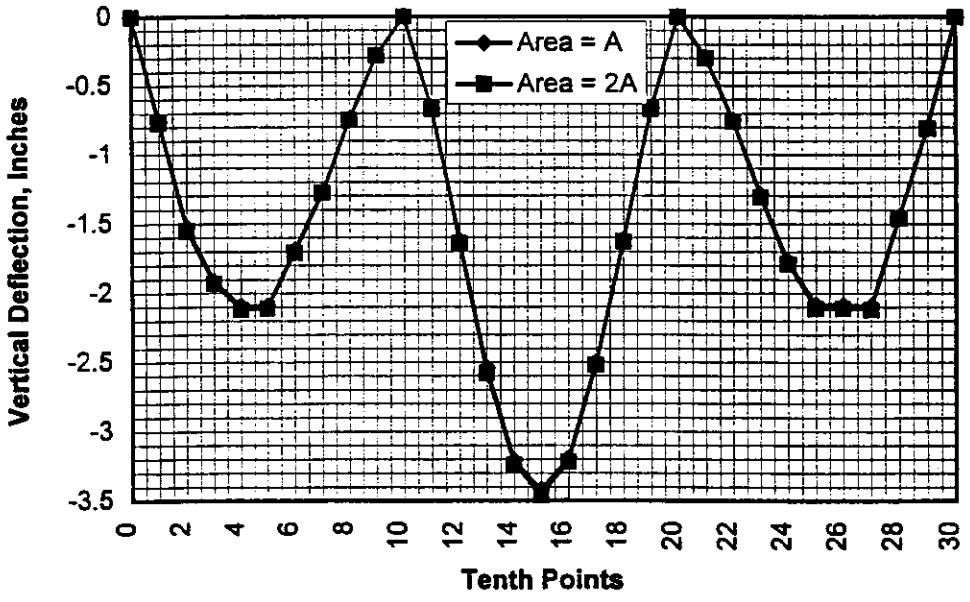

Figure 2.48-b Deflection diagram of girder G4 due to Multi-HS20 Truck Load
(Right bridge, K Type cross frame)

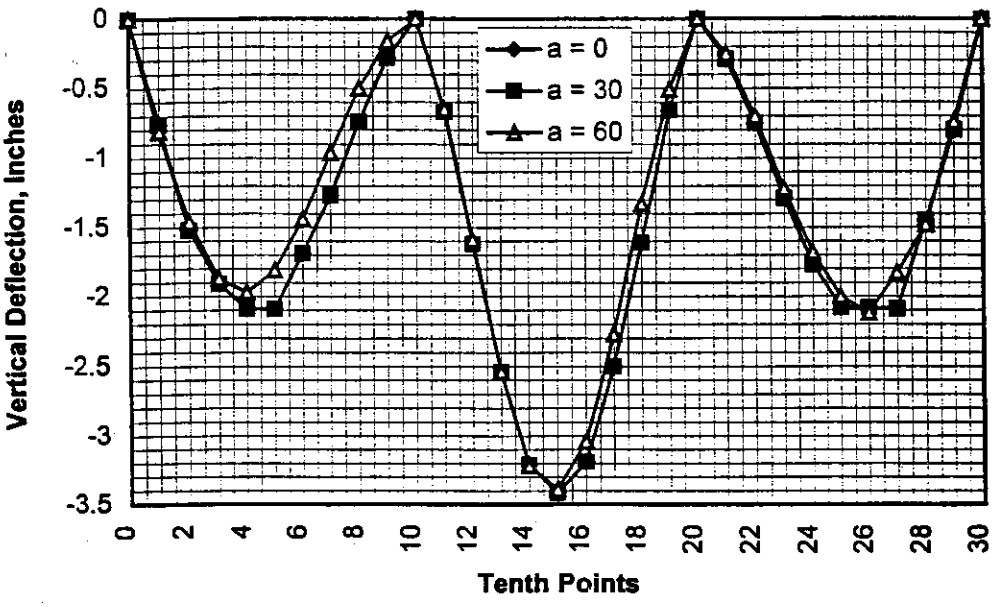

Figure 2.49-a Deflection diagram of girder G1 due to Multi-HS20 Truck Load
(Right bridge, K Type cross frame)

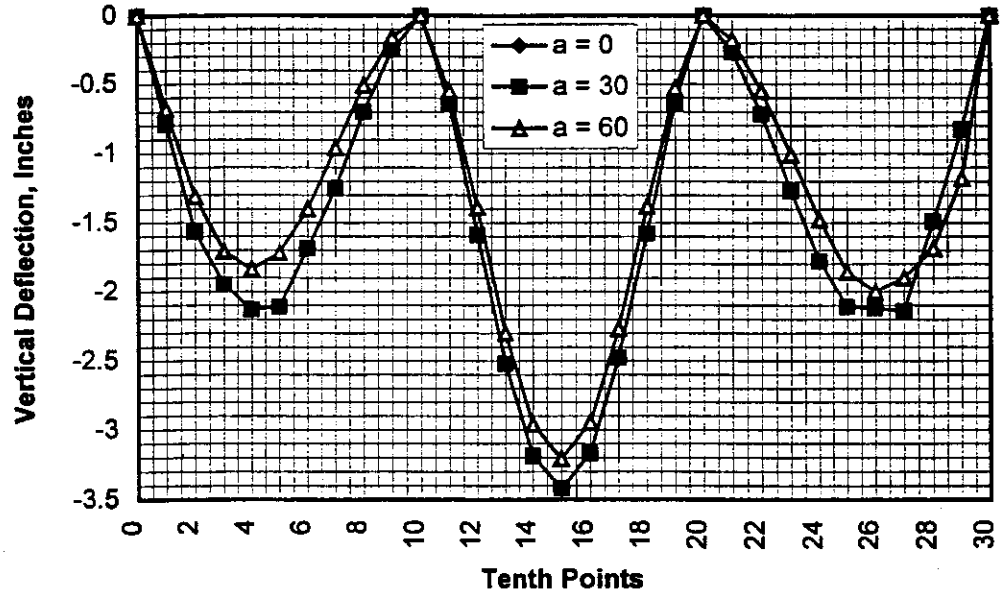

Figure 2.49-b Deflection diagram of girder G2 due to Multi-HS20 Truck Load
(Right bridge, K Type cross frame)

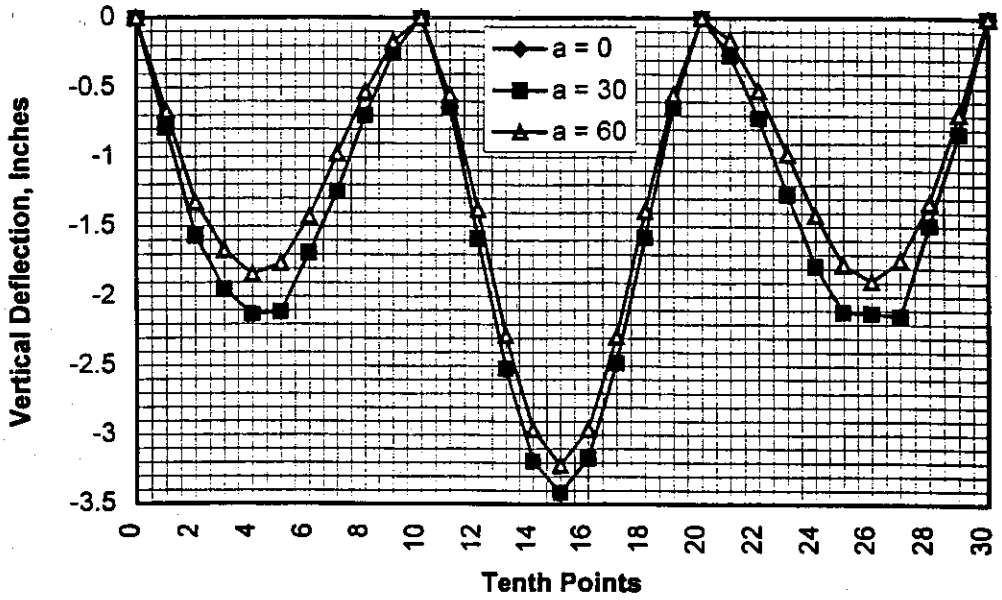

Figure 2.50-a Deflection diagram of girder G3 due to Multi-HS20 Truck Load
(Right bridge, K Type cross frame)

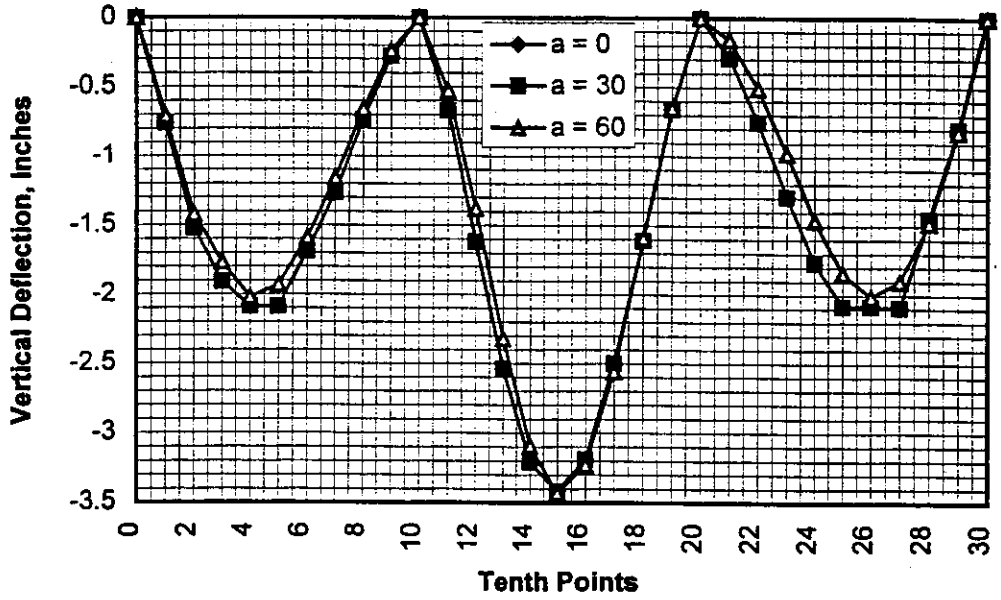

Figure 2.50-b Deflection diagram of girder G4 due to Multi-HS20 Truck Load
(Right bridge, K Type cross frame)

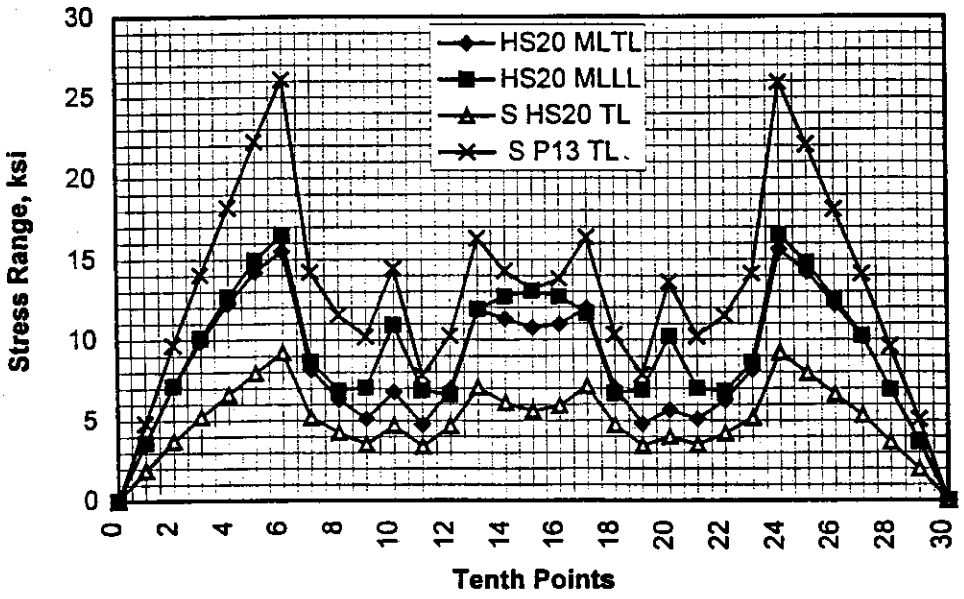

Figure 2.51-a Stress range diagram at top flange of girder G1 due to different live loads (Right bridge)

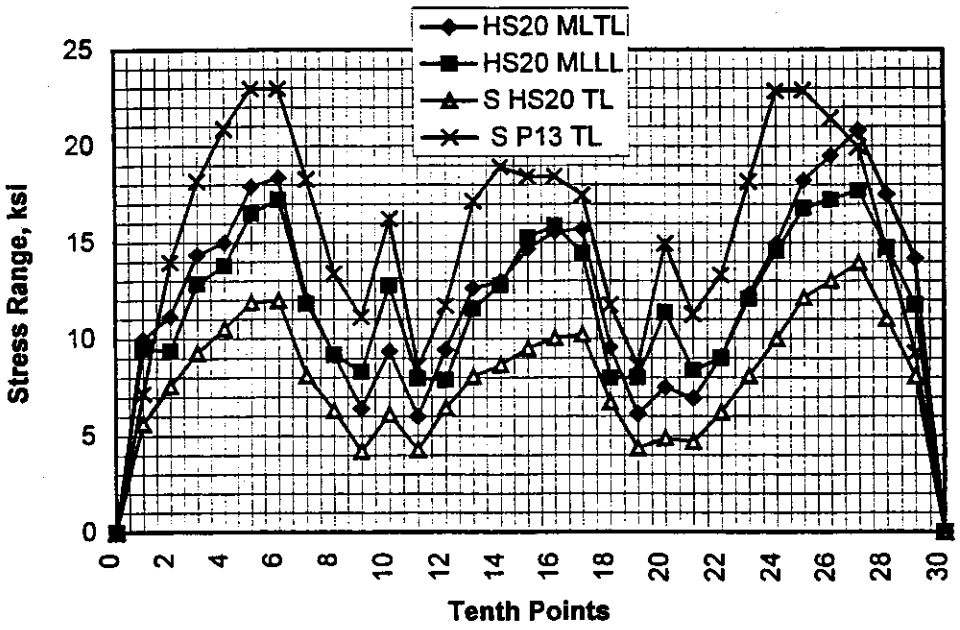

Figure 2.51-b Stress range diagram at bottom flange of girder G1 due to different live loads (Right bridge)

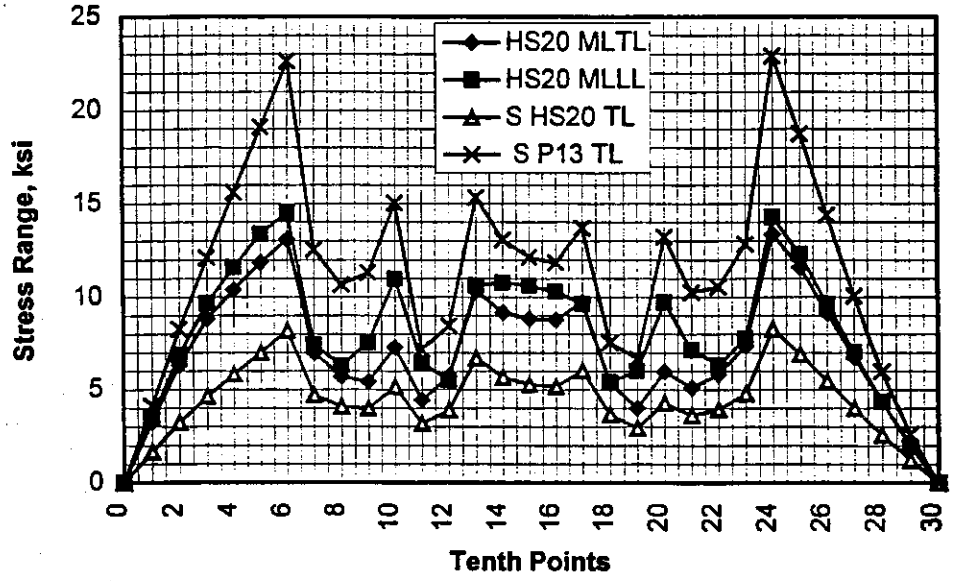

Figure 2.52-a Stress range diagram at top flange of girder G1 due to different live loads (a = 30°)

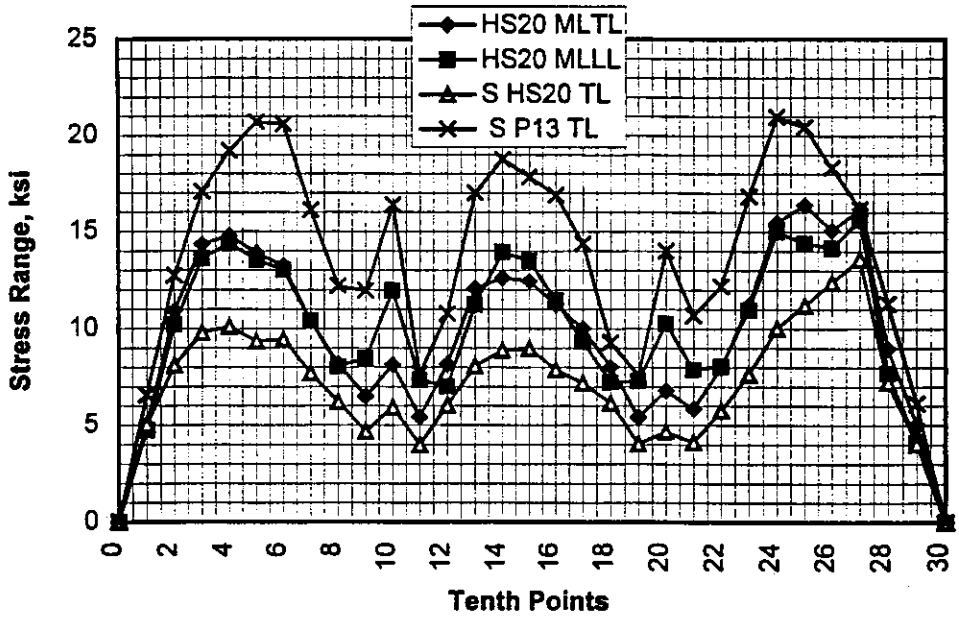

Figure 2.52-b Stress range diagram at bottom flange of girder G1 due to different live loads (a = 30°)

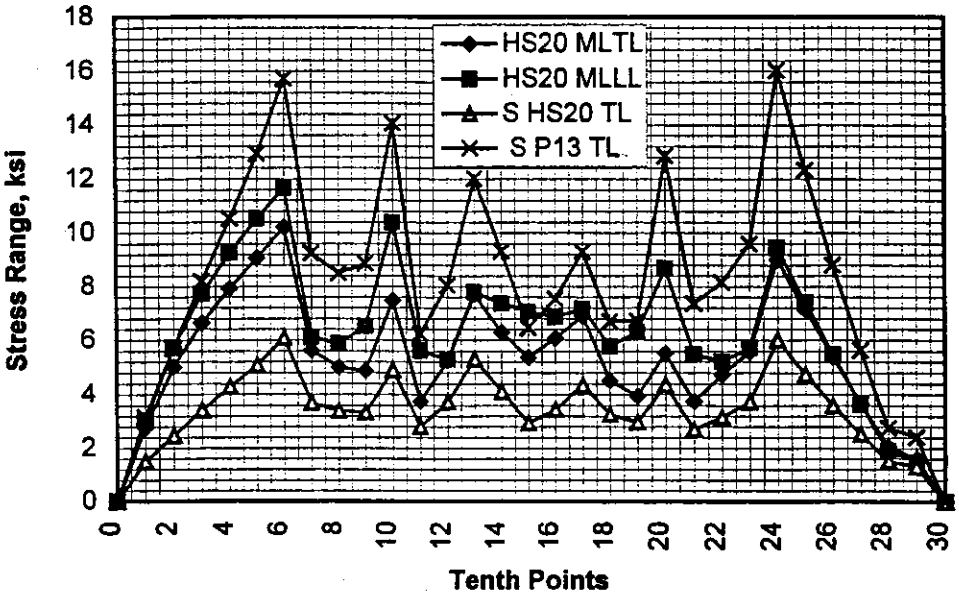

Figure 2.53-a Stress range diagram at top flange of girder G1 due to different live loads (a = 60°)

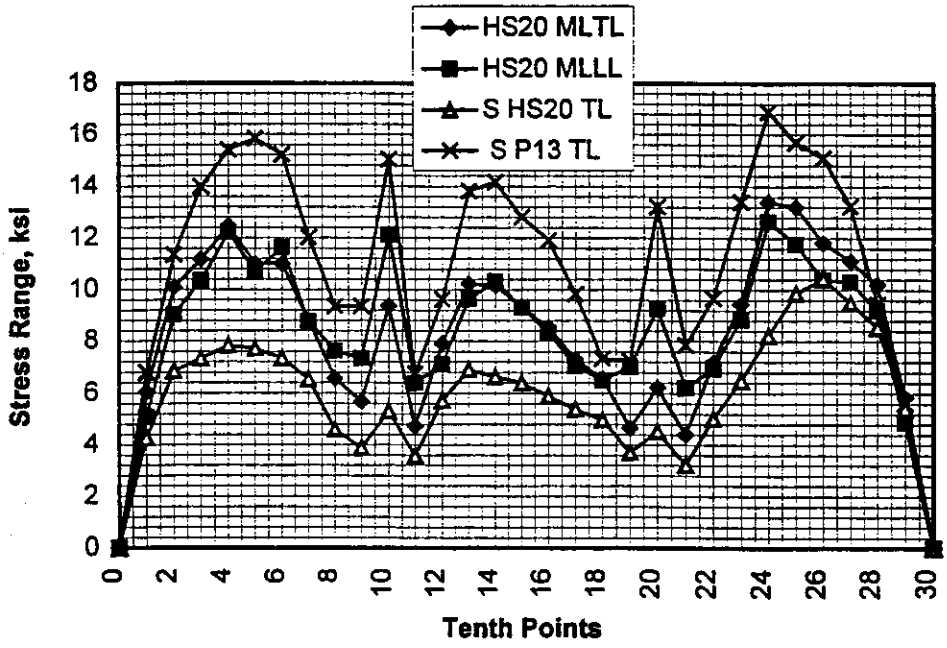

Figure 2.53-b Stress range diagram at bottom flange of girder G1 due to different live loads (a = 60°)

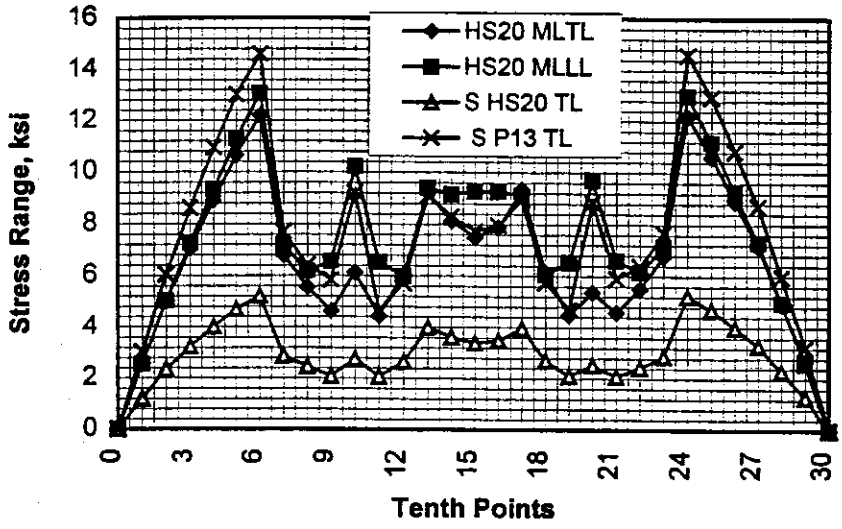

Figure 2.54-a Stress range diagram at top flange of girder G2 due to different live loads (Right bridge)

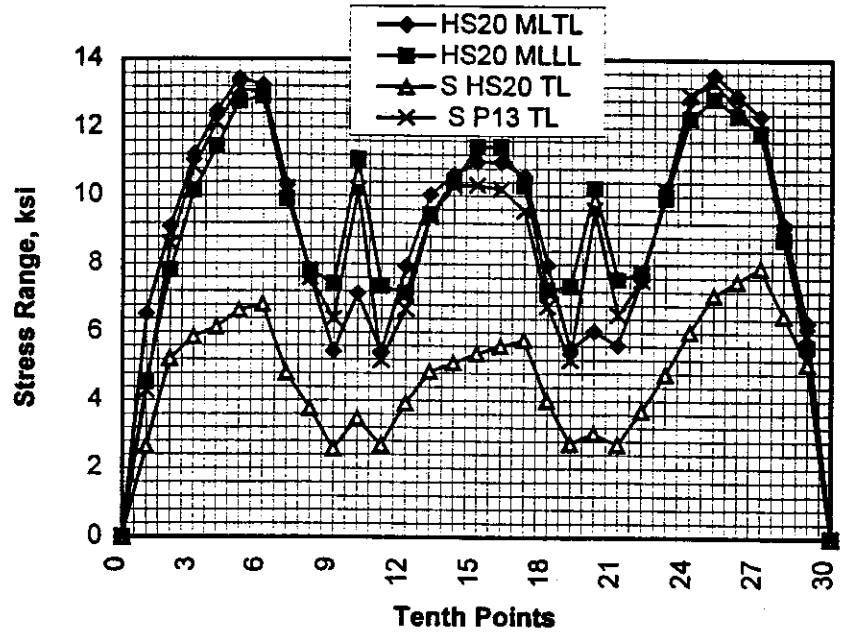

Figure 2.54-b Stress range diagram at bottom flange of girder G2 due to different live loads (Right bridge)

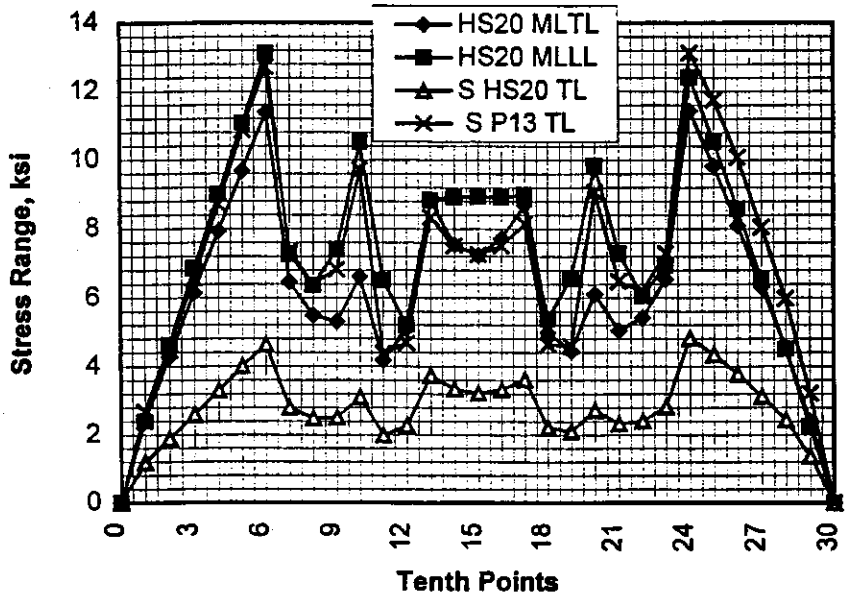

Figure 2.55-a Stress range diagram at top flange of girder G2 due to different live loads (a = 30°)

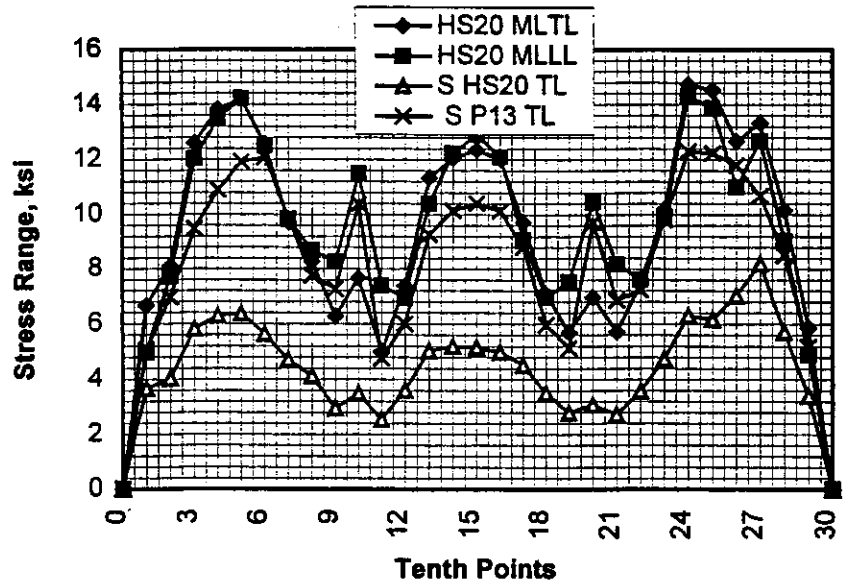

Figure 2.55-b Stress range diagram at bottom flange of girder G3 due to different live loads (a = 30°)

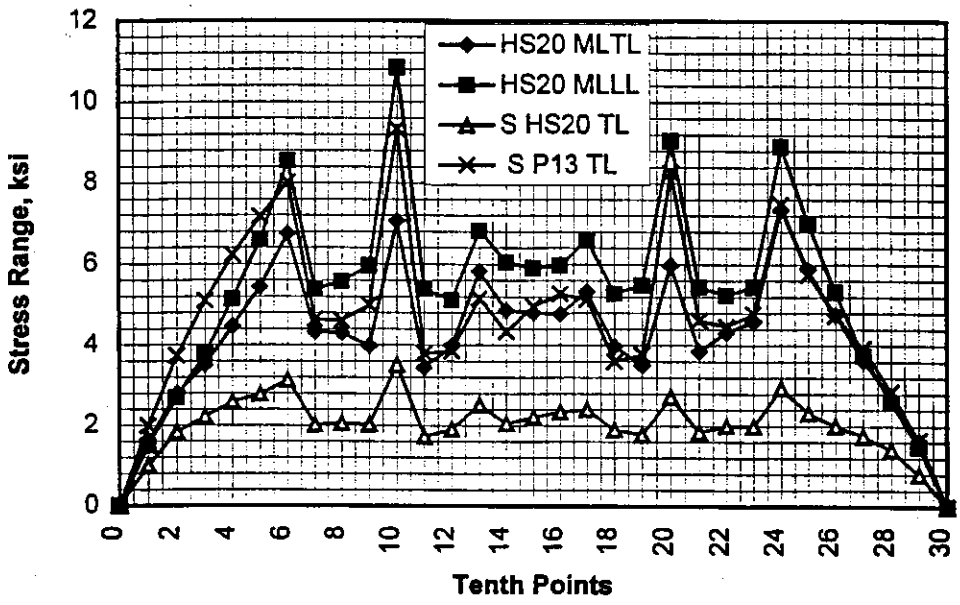

Figure 2.56-a Stress range diagram at top flange of girder G2 due to different live loads (a = 60°)

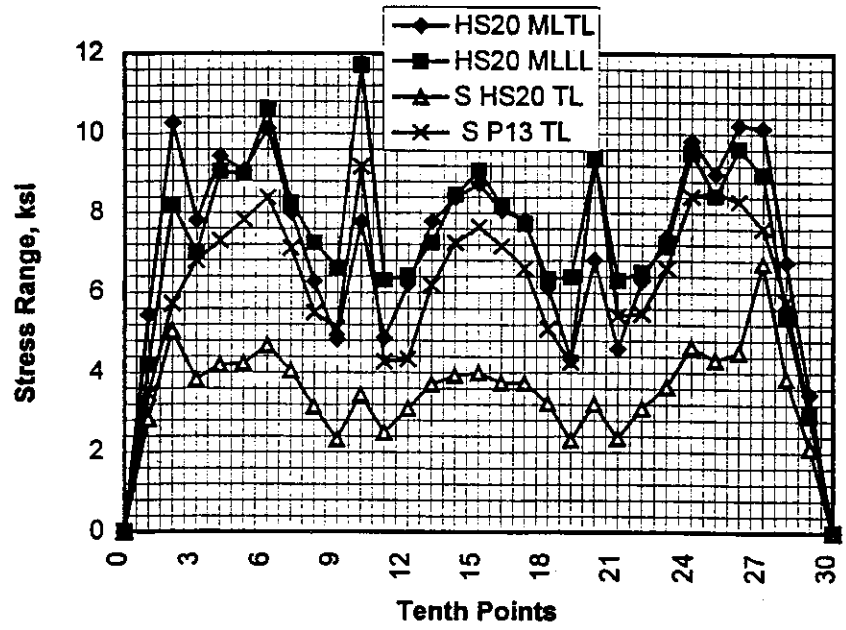

Figure 2.56-b Stress ranges diagram at bottom Flange of girder G2 due to different live loads(a = 60°)

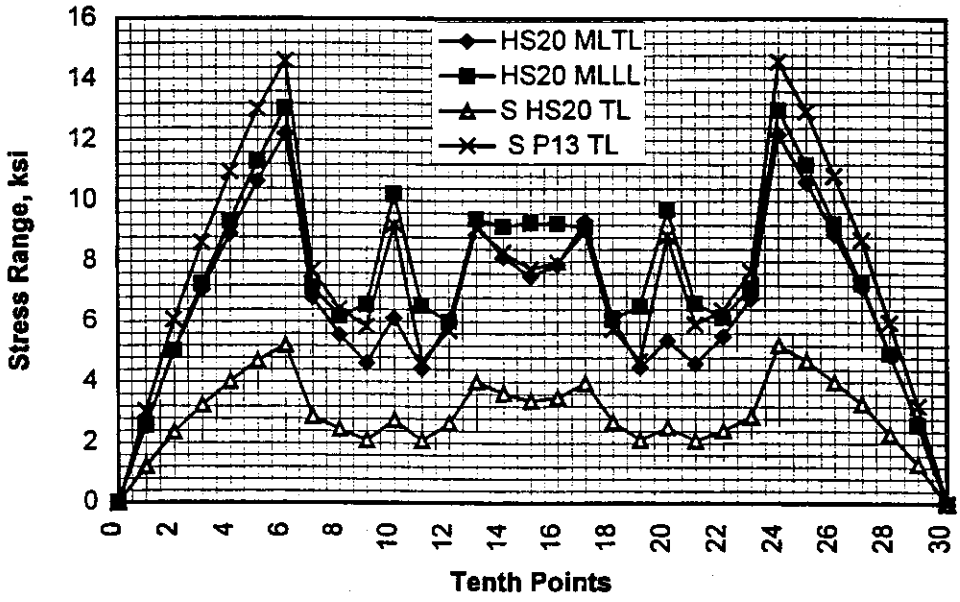

Figure 2.57-a Stress range diagram at top flange of girder G3 due to different live loads (Right bridge)

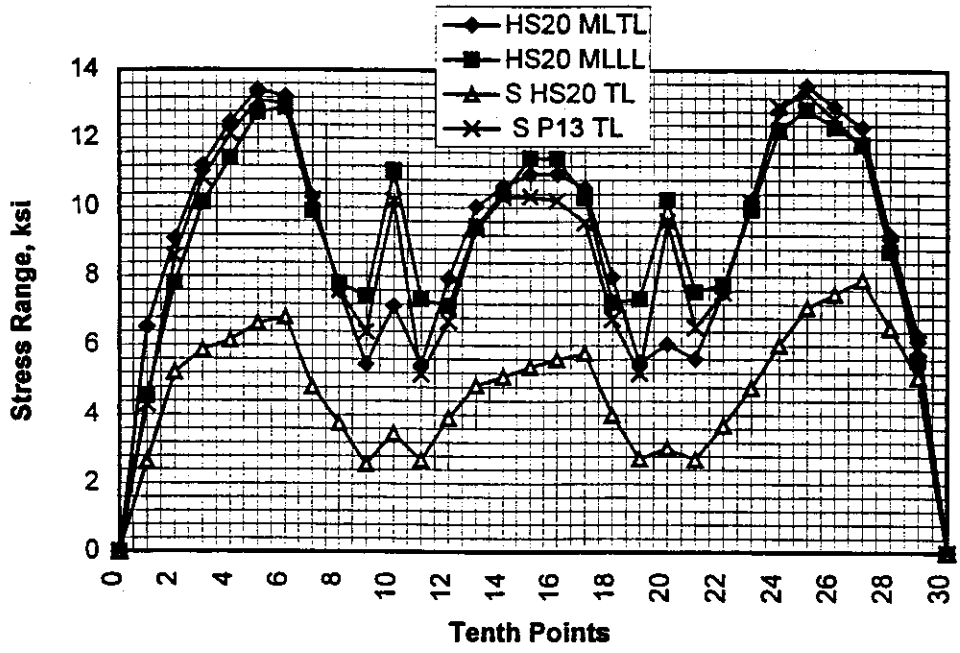

Figure 2.57-b Stress range diagram at bottom flange of girder G3 due to different live loads (Right bridge)

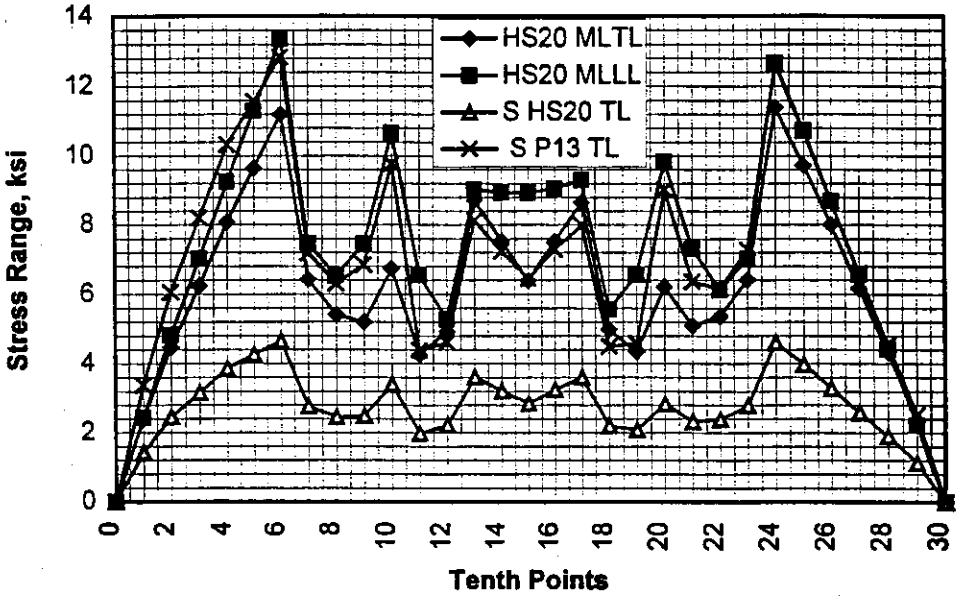

Figure 2.58-a Stress range diagram at top flange of girder G3 due to different live loads (a = 30°)

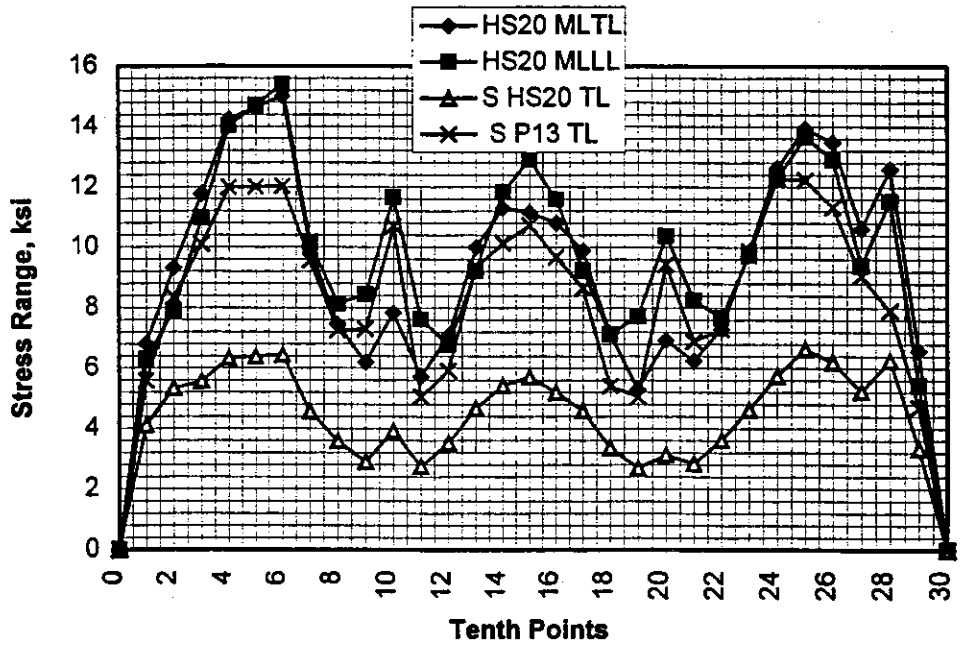

Figure 2.58-b Stress range diagram at bottom flange of girder G3 due to different live loads (a = 30°)

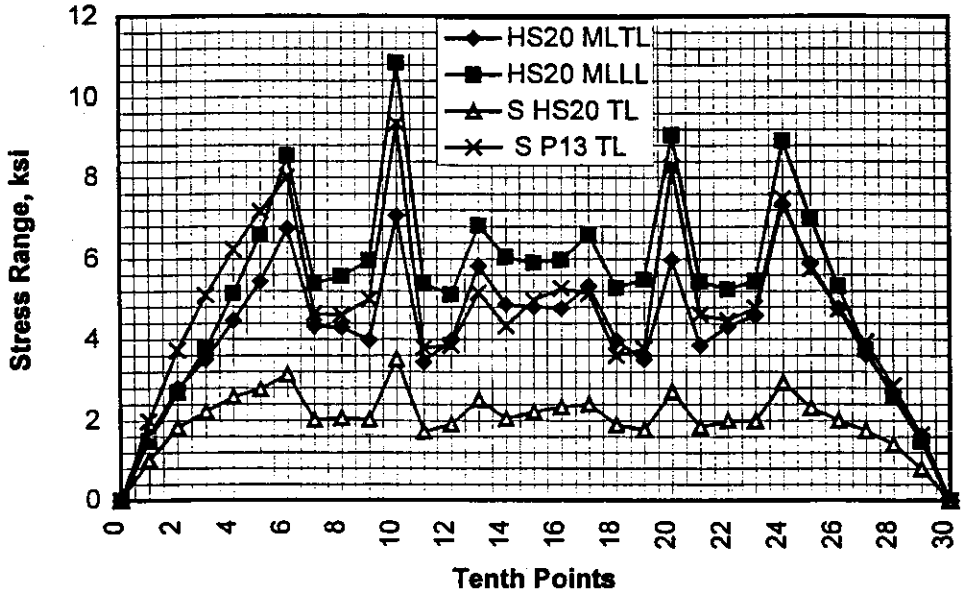

Figure 2.59-a Stress range diagram at top flange of girder G3 due to different live loads (a = 60°)

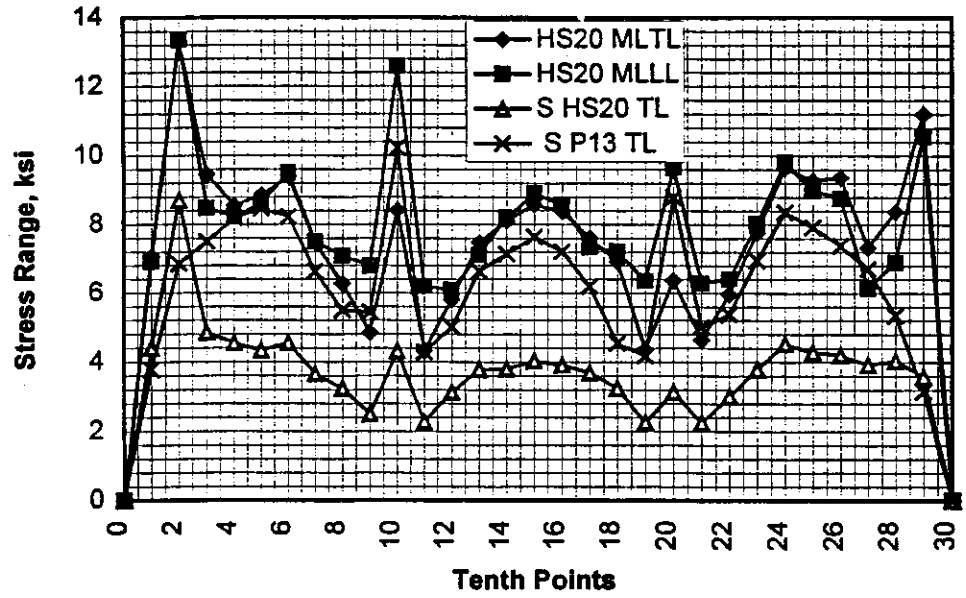

Figure 2.59-b Stress range diagram at bottom flange of girder G3 due to different live loads (a = 60°)

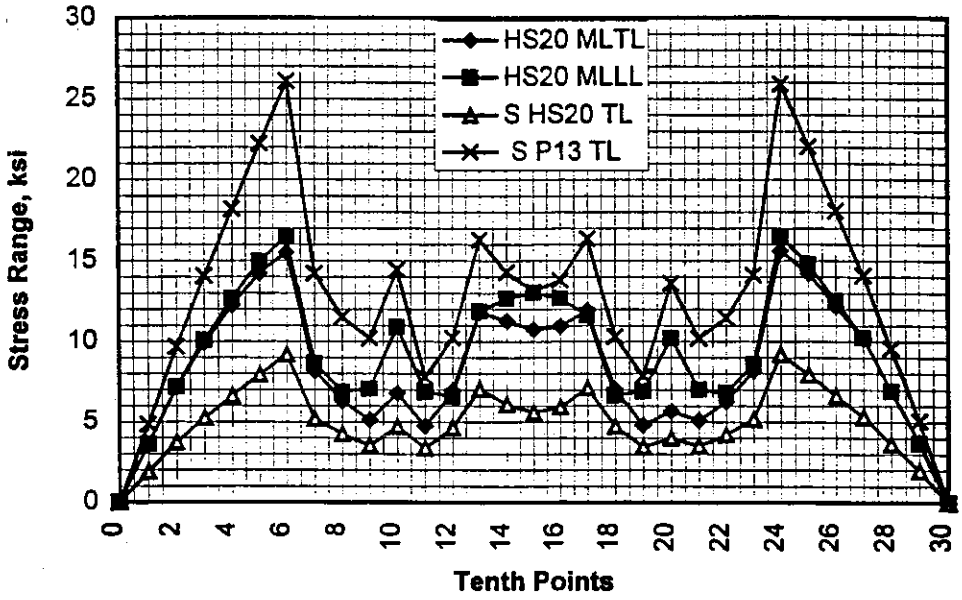

Figure 2.60-a Stress range diagram at top flange of girder G4 due to different live loads (Right bridge)

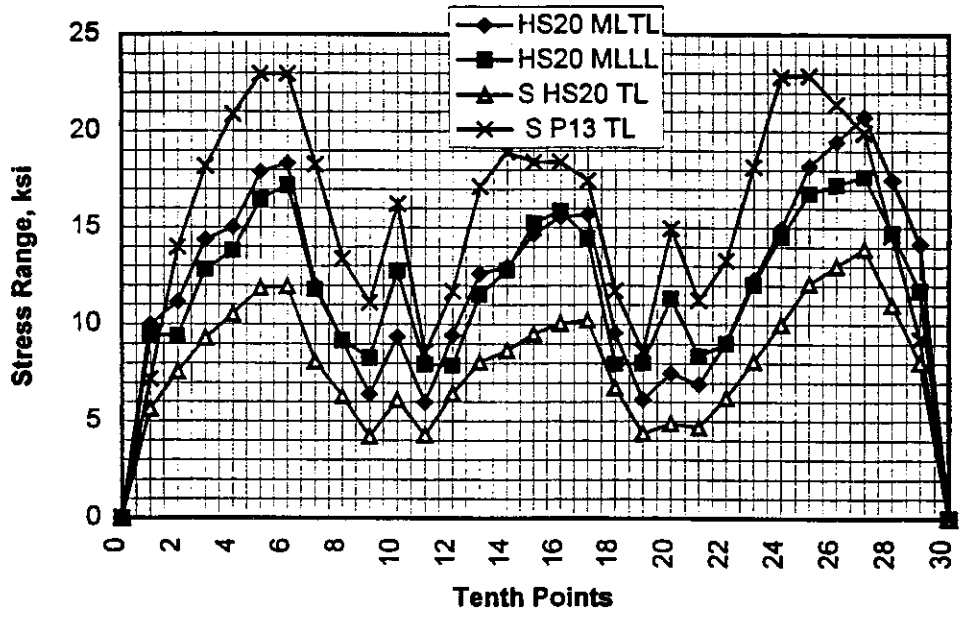

Figure 2.60-b Stress range diagram at bottom flange of girder G4 due to different live loads (Right bridge)

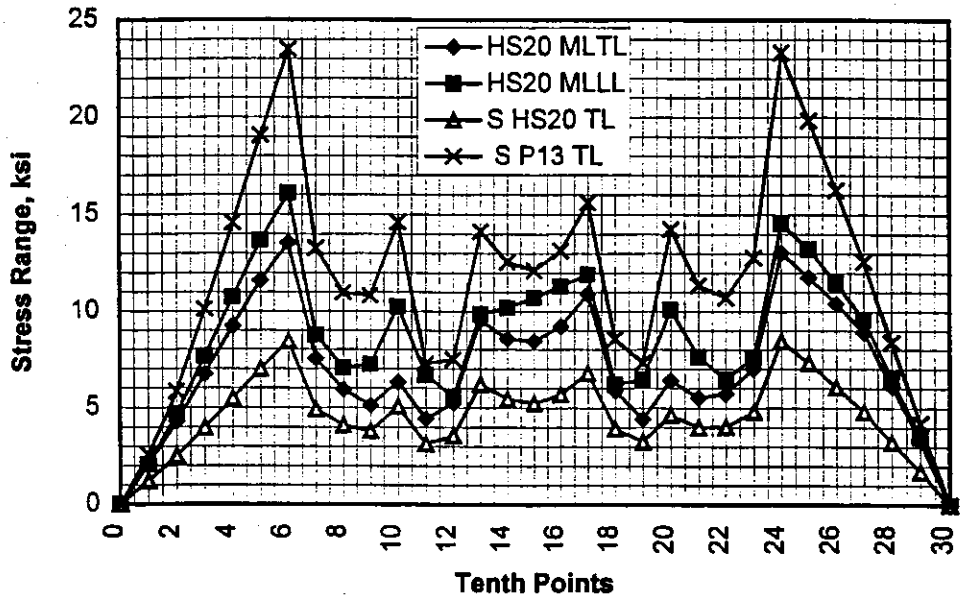

Figure 2.61-a Stress range diagram at top flange of girder G4 due to different live loads (a = 30°)

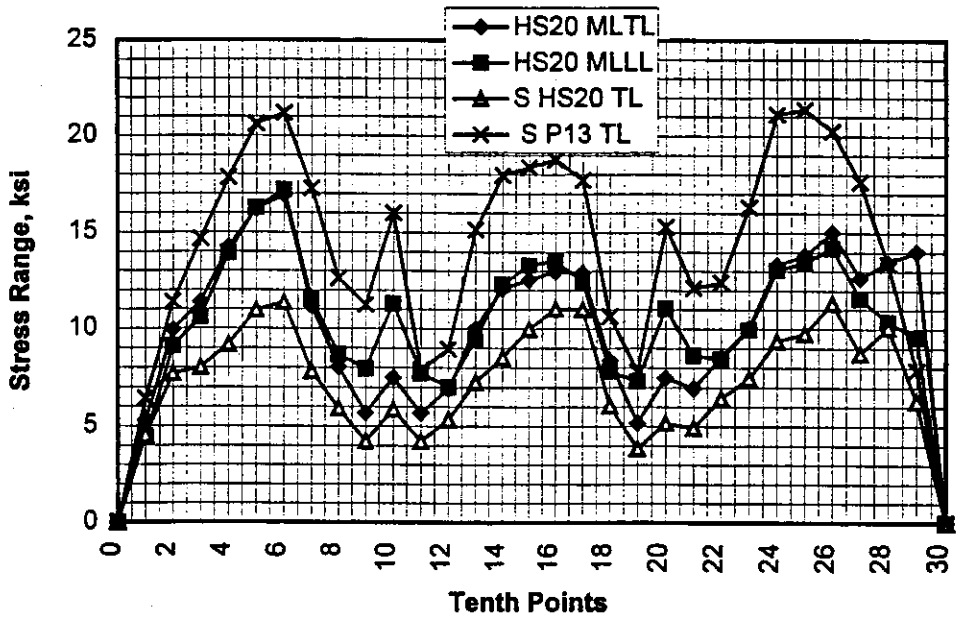

Figure 2.61-b Stress range diagram at bottom flange of girder G4 due to different live loads (a = 30°)

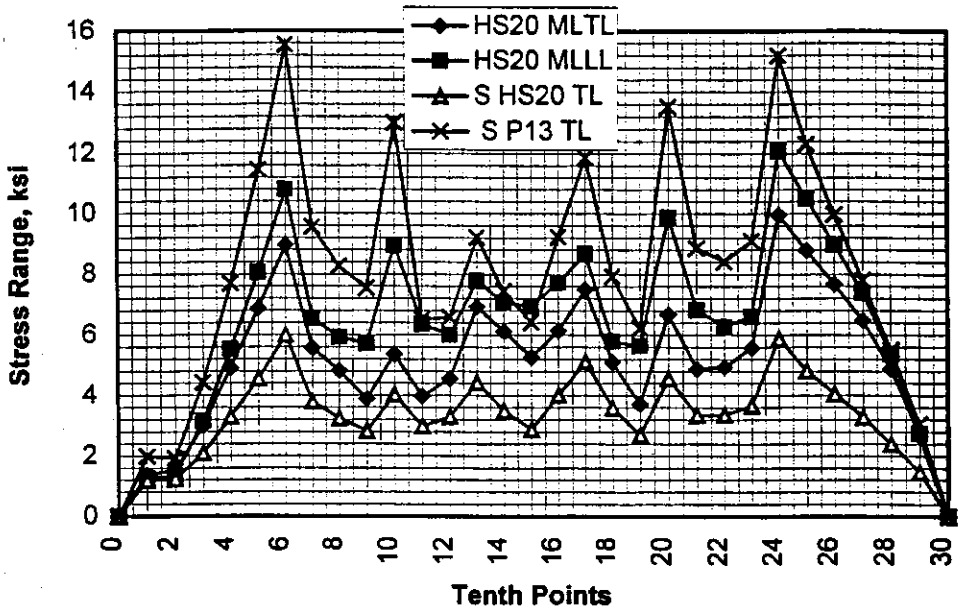

Figure 2.62-a Stress range diagram at top flange of girder G4 due to different live loads (a = 60°)

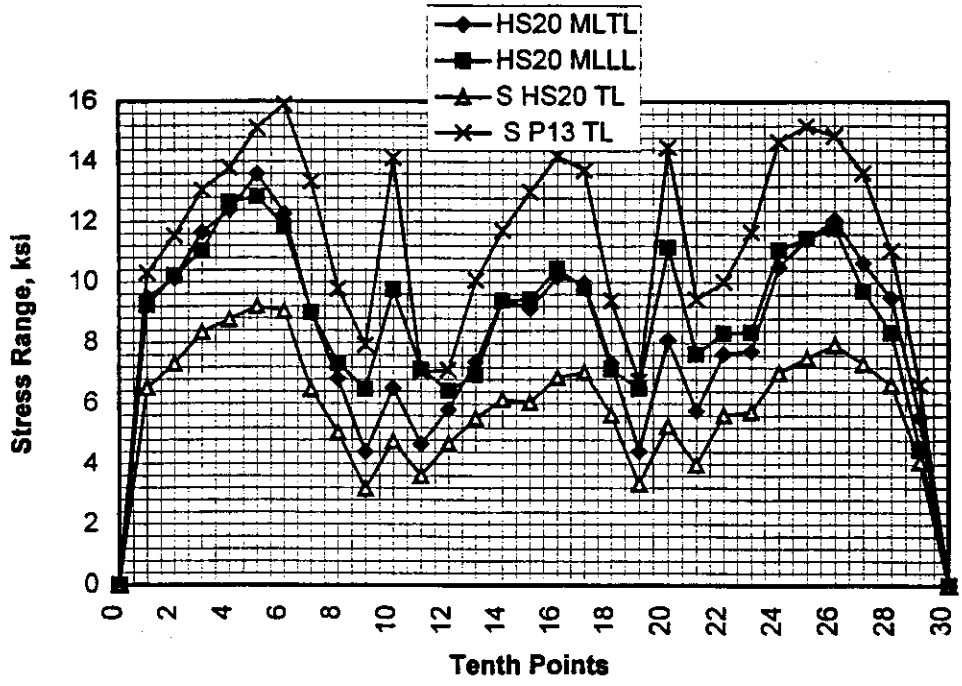

Figure 2.62-b Stress range diagram at bottom flange of girder G4 due to different live loads (a = 60°)

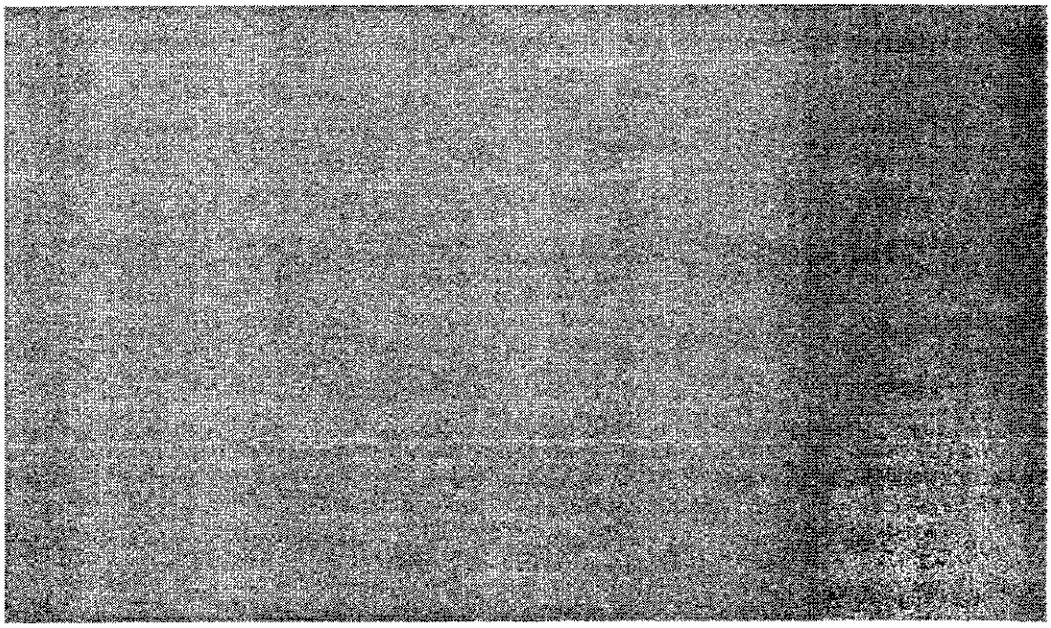

Figure A.1 Photographic view of the bridge

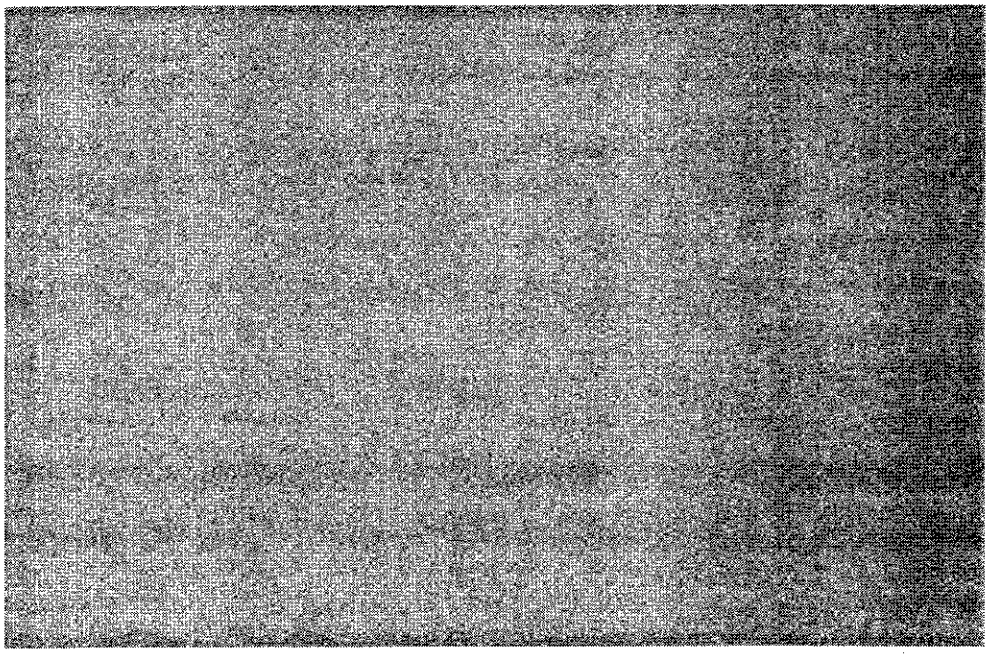

Figure A.2 Photographic view of the cross frame and its connection with the plate girder

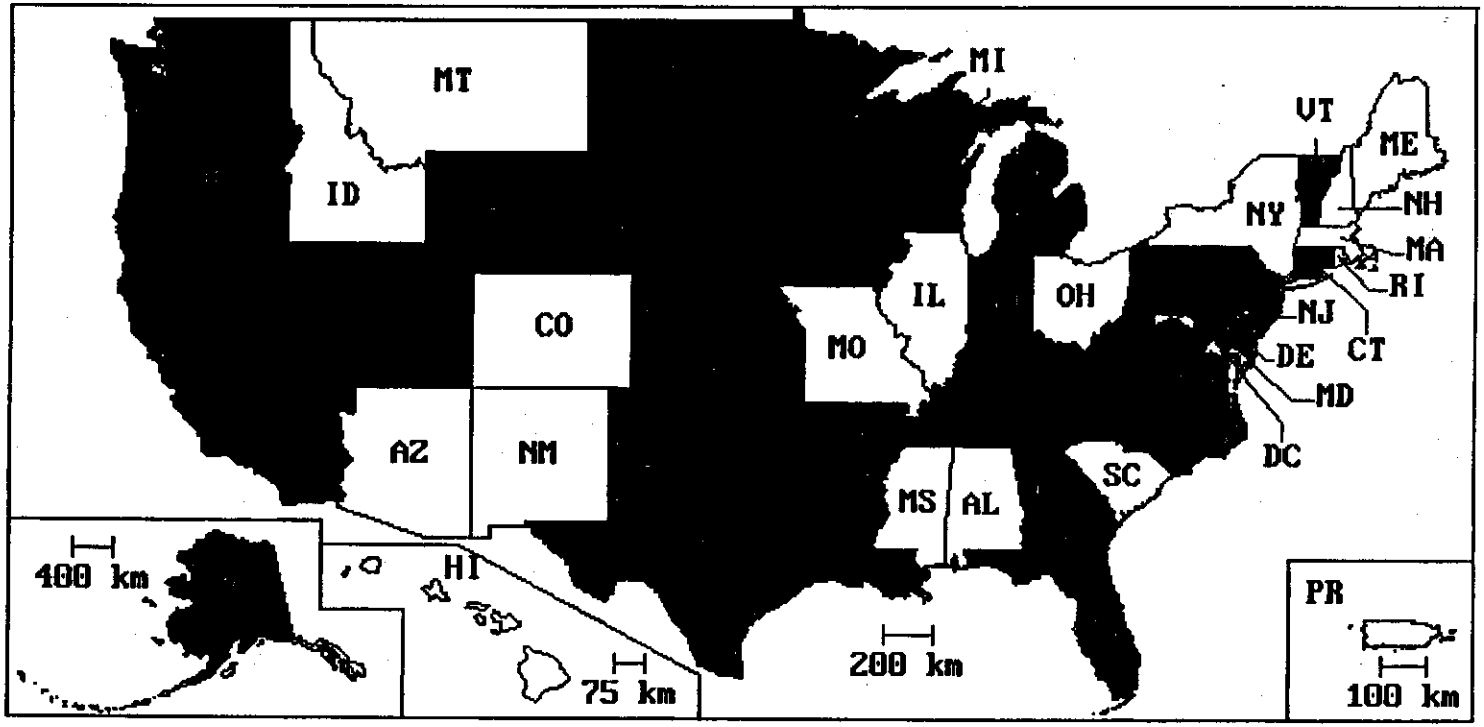

Figure 4.1 States from which information was obtained (Respondent states darkened).

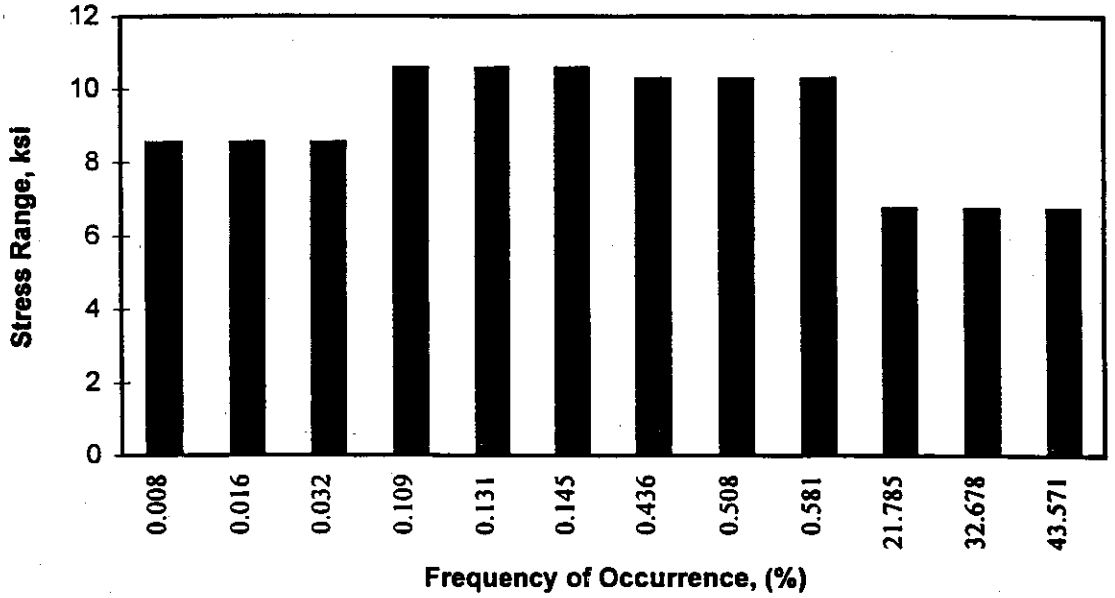

Figure 3.5 Stress histogram of original bridge (a=60, K Type cross frame)

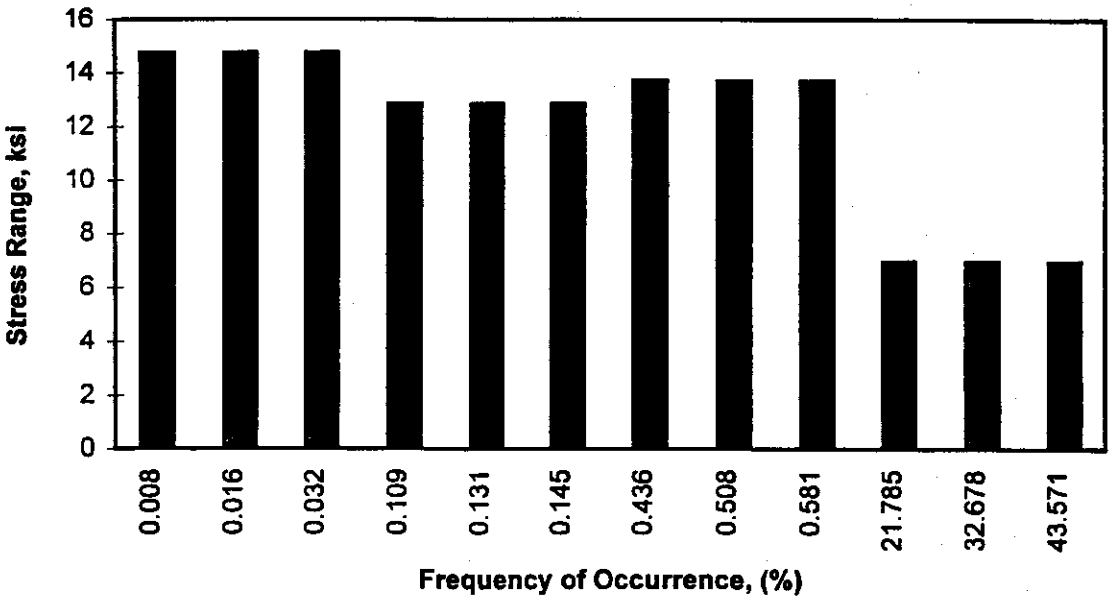

Figure 3.6 Stress histogram of original bridge (a=0, K Type cross frame, 2A)

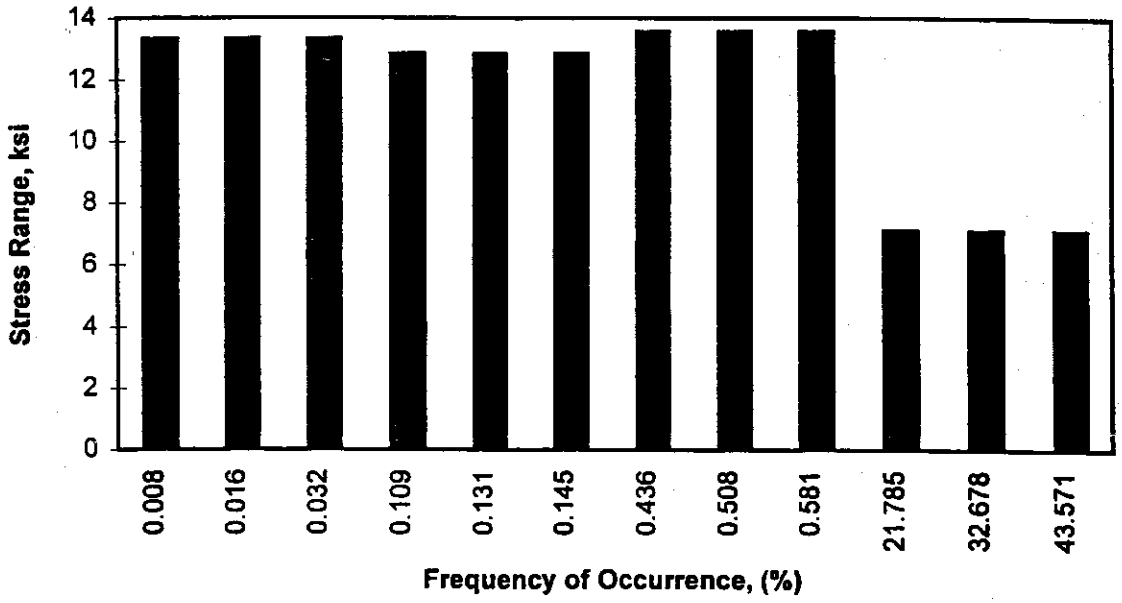

Figure 3.3 Stress histogram of original bridge (K Type cross frame)

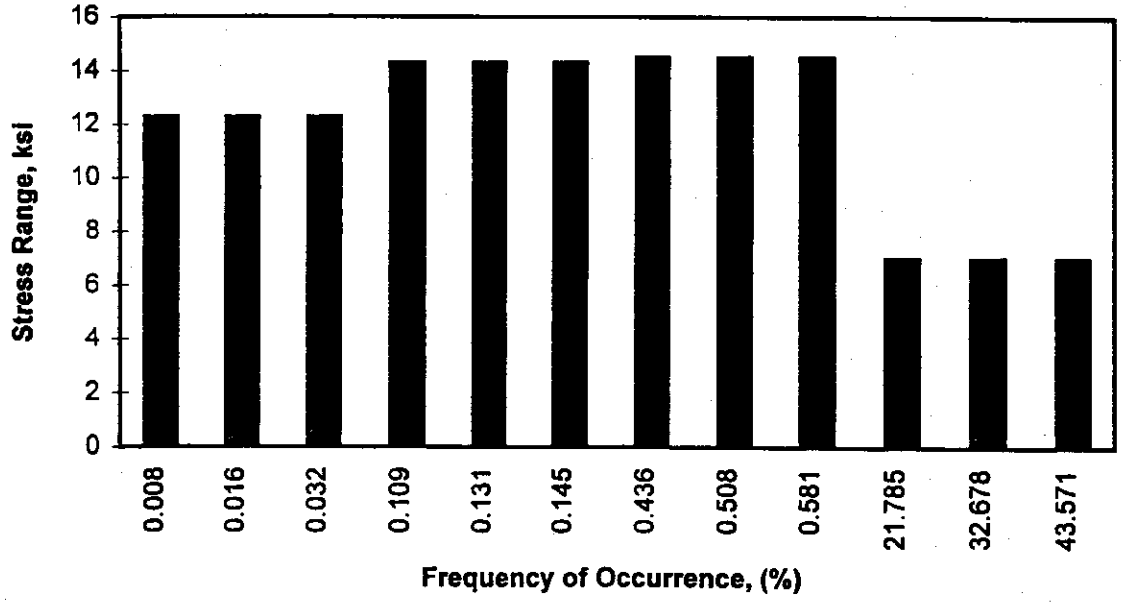

Figure 3.4 Stress histogram of original bridge (a=30, K Type cross frame)

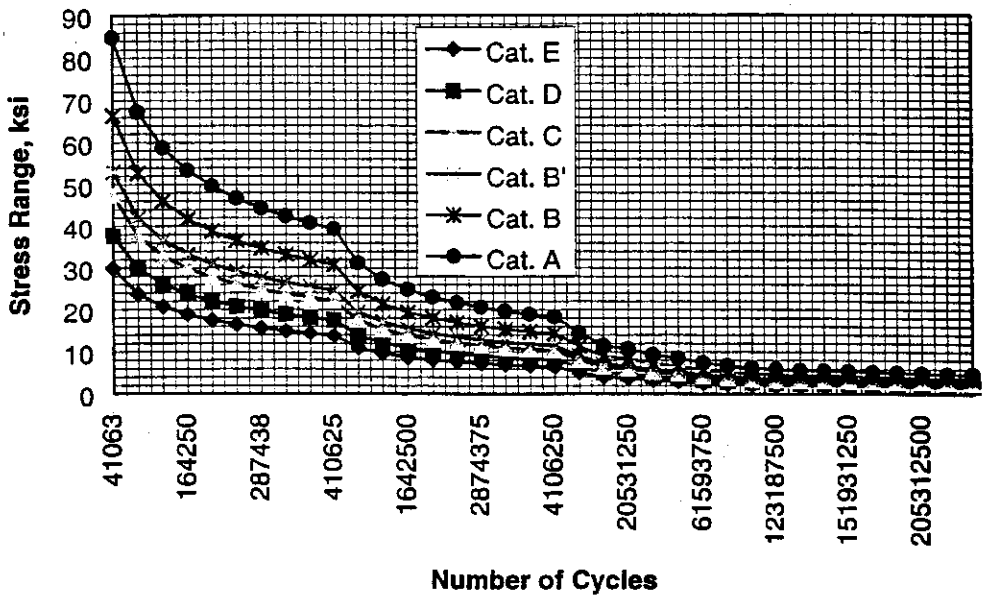

Figure 3.1 Variation of allowable stress range with number of cycles due to Single HS20 Truck Load

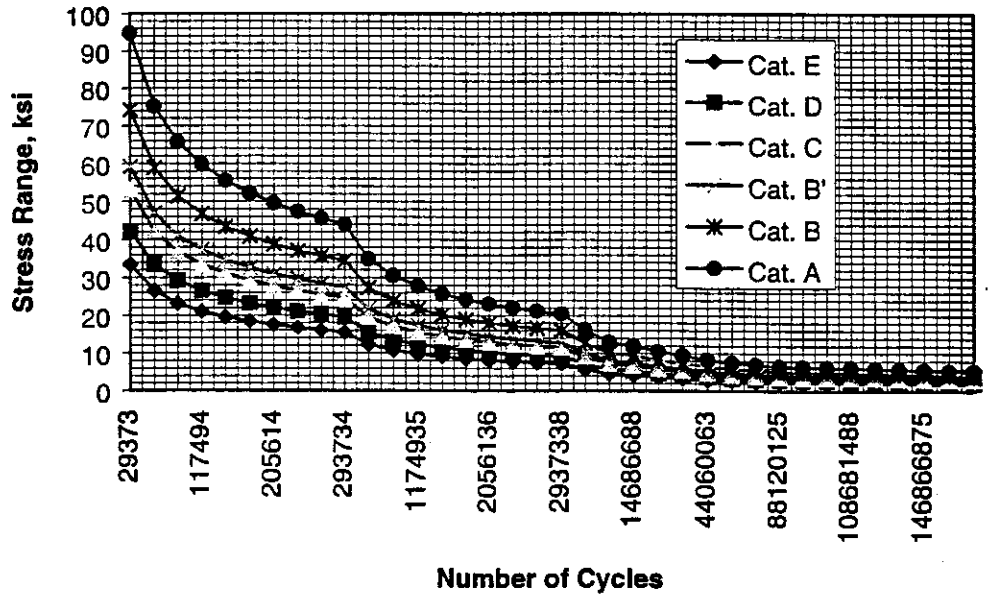

Figure 3.2 Variation of allowable stress range with number of cycles due to Single P13 Truck Load

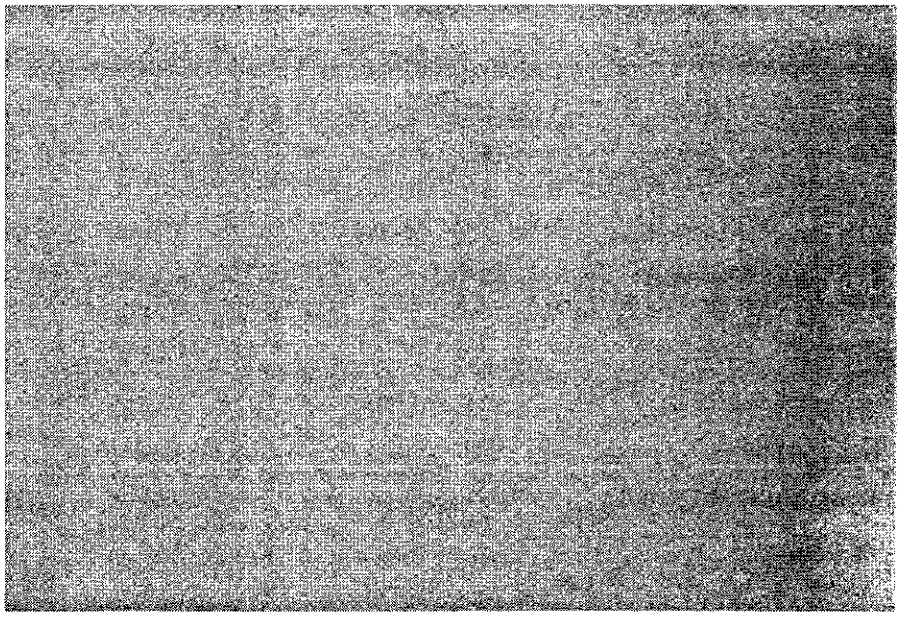

Figure A.3 Photographic view of the cross frame and lateral bracing with the plate girder

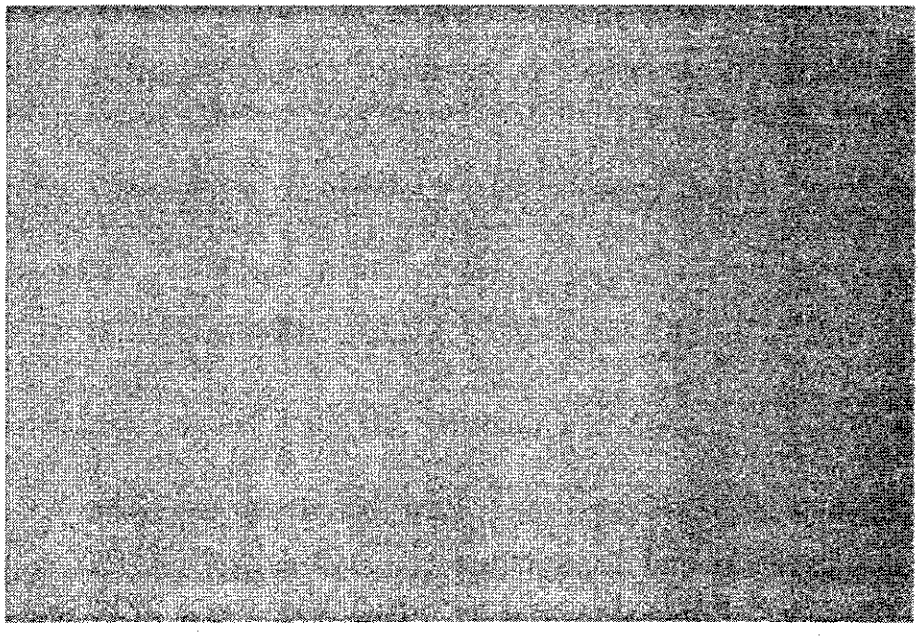

Figure A.4 Photographic view of the crack in the bottom flange and in the web of the plate girder

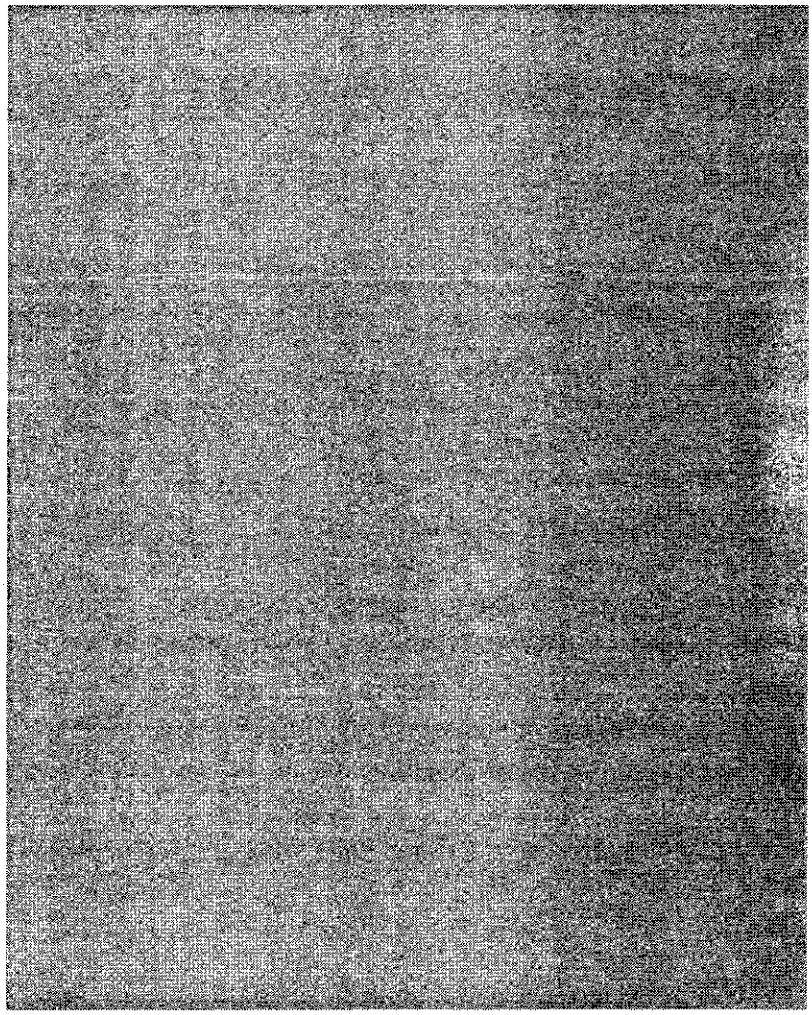

Figure A.5 Photographic view of crack in the bottom flange and in the web of the plate girder from the other side

Appendix 1

Questionnaire

A.1.1 Sample Letter of Questionnaire

June 15, 1996

State of _____

Department of Transportation

_____

Dear sir,

The Nevada State Highway System has experienced fatigue problems with some steel bridges. With the assistance of University of Nevada, Reno, NDOT has started a research project to identify appropriate parameters for fatigue evaluation and strategies for fatigue crack repair. To assist with this project, we would like to know your current fatigue evaluation procedures and repair methods. Please find enclosed a questionnaire that will help us collect and compile different fatigue repair methods currently used by the 50 state DOTs. We really appreciate answering these questions and sending them back to the address above by July 15, 1996.

Thank you very much for your time and effort.

Sincerely

Ahmad M. Itani, Ph. D., P. E.
Assistant Professor of Civil Engineering

Floyd I. Marcucci, P.E.
NDOT Chief Bridge Engineer

A.1.2 Questionnaire

State: _____

Name:_____ Title:_____

Please attach separate sheets if necessary to fully answer any of the questions.

1. Please categorize any fatigue problems that you have experienced in steel bridges in the last 15 years.

2. What are the evaluation procedures that you use to resolve in-plane load induced and out of plane distortion induced fatigue problems?

3. Please explain how do you account for the following in fatigue analysis.
   - Structural Analysis Level (2D or 3D)
   - Type and configuration of truck that you use in fatigue evaluation. Do you include the permit truck in your fatigue evaluation?
   - The number of truck passages. Do you use AASHTO or do you utilize weight station data?

- Do you use AASHTO's Fatigue Guides Specifications for determining allowable fatigue stress ranges?

4. What are the repair methods you follow for fatigue cracks?

5. Do you relate the repair method to the applied stress range?

6. Do you exclude welding from fatigue?

7. Do you evaluate the remaining life for relatively small fatigue cracks? What effect would it make on your choice of repair methods?

8. What is your state's opinions about welding on tension flange and termination of welding in tension zone?

Appendix 2

Fracture Assessment and Recommendations for Repair of Humbolt River Overpass

A.2.1 Introduction

A steel plate girder bridge along interstate 80 in Elko, Nevada, has experienced a brittle fracture that almost caused a complete failure of one steel plate girder of the five girder bridge. The bridge is the east bound Humboldt River Overpass, Nevada DOT Structure No. G-913E. According to the structure plans, the bridge was designed to the AASHO "Standard Specifications for Highway Bridges, 1961," and "Interim's Specifications through 1963." The legal live load that was used during the design process was the standard HS 20 Load or the Alternate Load.

The bridge has a total length of 800 ft, a skew of 36 degrees, and consists of six spans. The bridge is continuous over piers 1, 2, 4 and 5 and is simply supported over pier 3. A photographic view of the bridge is given in Figure A.1. The bridge contains five identical composite steel plate girders spaced at 7'-6" and carries two lanes of traffic. Each plate girder is comprised of a top flange plate that varied between 14"x3/4" over the middle span 1 to 16"x1$\frac{11"}{16}$ over pier 1, a bottom flange plate that also varied between 20"x1$\frac{1"}{6}$ over middle of span 1 to 20"x1" over pier 1, and a tapered web plate that varied in both thickness and depth between the middle spans and over the piers. The web plate over the middle of span 1 has a depth equal to 5 ft and 7/16" thickness, while over pier 1 has a depth equal to 8 ft and 1" thickness. The flange and the web plates are made of A36

steel through out the whole bridge. Transverse stiffeners were used on both faces of the intermediate girders and on the interior face of the facia girders. The stiffeners are spaced at a distance equal to 5 ft along the middle of the girder and at a distance equal to 2 ft over the support. These stiffeners are fillet welded to the web plate and to the compression flange and are "tight fit" to the tension flange. The bearing stiffeners that are located over piers are welded to the compression flange and are "tight fit" to the tension flange.

A longitudinal stiffener is placed over the intermediate piers where the web depth is 8 ft. The stiffener is located at 20 inches above the bottom flange and is extended to 13 ft on each side of the support. The horizontal stiffener is welded to the web by a fillet weld size equal to 3/8". The top flange of the steel girder is compositely connected to the deck by means of shear connectors in the regions of the positive bending moment only. The shear connectors are welded to the top flange by full penetration butt weld.

Cross frames were used throughout the bridge to stabilize the top flange plates during erection and construction, to prevent lateral torsional buckling of the compression flange near the support locations, and also to satisfy the 1963 AASHO requirements that the cross frame spacing should not exceed 25 ft. The interior cross frame (intermediate diaphragm as called on the structure plans) is comprised of three rolled sections: Two diagonals that have an X-pattern and a horizontal strut connected just above the bottom flange. The cross frame members are welded to the intermediate transverse stiffener which is welded to the web and to the compression flange only. Therefore, no rigid attachment exists between the end of the transverse stiffeners and the tension flange. This prevented the connection of resisting out-of-plane distortion caused by differential

deflection between the various girders due to live loads. Figure A.2 shows a photographic view of the cross frame and its connection with the plate girder.

Lateral bracing are located between the interior girders with a V-pattern. The bracing is comprised of one rolled section ST 5 WF 10.5 connected to the web of the plate girder by means of a gusset plate of thickness 3/8", width equal to 6" and a length that exceeds 10" in most cases. The lateral bracing are welded to the gusset plate which is welded to the web by fillet weld of size 5/16". Figure A.3 shows photographic view of the cross frame and lateral bracing with the plate girder. It should be recognized that the original plans do not accurately reflect the lateral bracing as installed.

A.2.2 Description and Evaluation of the Fracture

In September 1995, contractor personnel observed a single crack in the middle of girder 2 at the bottom flange that extended through the web of the plate girder between piers 4 and 5 and notified NDOT resident engineer. After this discovery, NDOT engineers closed one traffic lane above the fractured girder and requested the contractor to shore the girder at the location of the fracture. To prevent any crack propagation, a hole was drilled at the tip of the crack in an attempt to arrest the crack. These temporary measures were taken to allow some time to evaluate the crack, determine its cause, and to develop a retrofit strategy to repair the girder and open the bridge to full traffic.

The following is a description of the bridge condition based on observation made during a September 19, 1995 inspection with NDOT engineers. The crack is located in girder 2, according to NDOT structure plans, between piers 4 and 5 at the intersection of lateral bracing, cross frame No. 5 and the web of the girder. The crack penetrated the

bottom flange and extended vertically throughout almost the full height of the web. In fact, the fracture was arrested just 3 inches below the top flange. The compression flange remained intact with the deck of the bridge due to the composite action between the top flange and the bridge deck. Figures A.4 and A.5 show a photographic view of the crack in the bottom flange and in the web of the plate girder, respectively.

In general, the most likely location resulting from fatigue cracking are the following: (i) at details with the lowest fatigue strength, (ii) in zones of highest tension stress range, (iii) at details exhibiting displacement induced fatigue, and (iv) at section loss due to corrosions or flaws. By examining the location of the fracture that occurred in the second girder, it can be concluded that three out of the above four conditions were present at that location.

The cause of the brittle failure could be associated to in-plane and out-of-plane distortion induced fatigue. The out-of-plane distortion induced fatigue is normally associated with forces caused by secondary members in steel bridges that are not designed for strength such as cross frames, diaphragms, and lateral bracing. Even though these members are not designed for strength, however they do participate in distributing the live load force to the main girders. Therefore, these secondary members must have a rigid attachment to the main girder to ensure an uninterrupted load path and to prevent out-of-plane distortion induced fatigue. The cross frame at which the fracture occurred is not rigidly attached to the bottom flange of the girder, as discussed earlier, which might have caused the initiation of fatigue cracking. However, it seems that the fatigue cracking propagated in a very fast manner due to in-plane fatigue which also helped the initiation of the crack. The end of the gusset plate connection between the lateral bracing

to the web is the main cause of the crack initiation/propagation and thus the brittle fracture. According to the current AASHTO "Standard Specifications for Highway Bridges" this detail may be described as "Fillet Welded Attachment for Longitudinally Loaded Members". This term is normally used to describe base metals adjacent to details attached by fillet welds, with a length of more than 4 inches, in the direction of tension or reversal stresses. This detail is called Category E detail which has a low fatigue strength stress and in many cases cause the initiation/propagation of the fatigue cracking.

According to the current AASHTO Specifications, for Case I Freeways where the Average Daily Truck Traffic (ADTT) ≥ 2500, bridges with redundant load path should be checked for the following loading cycles

Type of Load	No. of Cycles	Stress Range for Category E ksi
Multi lanes HS20 Truck Load	2,000,000	8
Multi Lanes HS20 Lane Load	500,000	13
Single HS20 Truck Footnote c in table 10.3.2A	Over 2,000,000	4.5

However, Case II Freeways where the Average Daily Truck Traffic (ADTT) < 2500 is chosen, bridges with redundant load path should be checked for the following loading cycles

Type of Loads	No. of Cycles	Stress Range for Category E ksi

Multi Lanes HS20 Truck Load	500,000	13
Multi Lanes HS20 Lane Load	100,000	22

For any new design or for fatigue evaluation of existing bridges, Case I Freeways should be chosen because it consists a check for single HS20 Truck for over 2 million cycles. The allowable stress ranges for the various detail categories for over 2 million cycles are the Constant Amplitude Fatigue Threshold (CAFT) which is the fatigue endurance limit. This means that the applied stress ranges for new bridges should always be below the CAFT to insure that the micro crack would not propagate in case of fatigue cracking. If the applied stresses, in case of existing bridges, were more than the CAFT, this would mean that fatigue cracking/propagation is likely to occur at this location and special precaution should be taken to prevent that.

The number of the stress cycles that are in the current AASHTO Specifications are very low when compared to the actual number of cycles in real bridges. Moreover, the allowable stress ranges for the specified low number of cycles are relatively high when they are compared to the actual allowable stresses obtained from testing of steel beams with welded stiffeners and attachments. Therefore, using the current AASHTO in evaluating steel bridges would give unrealistic number of stress cycles and would make it very hard to interpret the results. In an effort to change this, the AASHTO T-14 Committee (Steel Bridges) adopted major modifications in the fatigue design and evaluation of steel bridges in its biannual meeting in February 16 and 17, 1995 in

Berkeley, CA. The basic concept behind these modifications is to use a realistic number of stress cycles and low values for allowable fatigue stresses.

Assuming the bridge was open to traffic in 1965 and assuming the average daily traffic ADT is equal to 15,000. The ADTT can be determined from the ADT by multiplying the fraction of trucks in the traffic. Fraction of trucks in traffic is 20% for rural interstate highway [2, Table C3.6.1.4.2-1]. The single-lane ADTT is given by [2, equation 3.6.1.4.2-1]

$ADTT_{SL} = p \times ADTT$

where:

ADTT = (0.20) (15,000) = 3000

p = 0.85 for two-lanes [2,Table 3.6.1.4.2-1].

Therefore $ADTT_{SL}$ = (0.85) (3000) = 2550. The number of the cycles on this bridge is equal to:

$$N = (365)\ (30)\ n\ (ADTT_{SL})$$

where 365 is the number of days per one year, 30 is the assumed age of the bridge, and n is the number of stress range cycles per truck passage. The stress history at a particular detail caused by the passage of a single truck with three axles is strongly dependent upon several factors such as span length and member type and location. Generally, stress traces are composed of one primary or more primary cycles with superimposed smaller vibratory cycles. It has been found that for continuos bridges that have spans greater than 60 ft, complex primary cycles of 1.5 may occur during the passage of the legal load. Substituting a value of 1.5 for n in the above equation would give

$$N = 365 \times 30 \times 1.5 \times 3400 = 418837500 \text{ cycles}$$

Therefore, the bridge has seen during its life up to this date about 41.9 million cycles. The nominal fatigue strength of a specific detail is given by

$$(\Delta F)_n = \left(\frac{A}{N}\right)^{1/3}$$

where A is a constant that depends on the category detail and N is the number of cycles. The value of A for category E detail is equal to 11×10^8 which makes the nominal fatigue strength equal to 2.97 ksi. However, the value for nominal fatigue resistance should be greater or equal to half times the CAFL. Half times CAFL for Category E is equal to 2.25 ksi. Therefore the nominal fatigue strength for this bridge is 2.7 ksi.

The maximum applied stress range obtained for the fifth span of this bridge from the consultant was 12.90 ksi. Since 2-D analysis for a right bridge gave approximately 75% higher values of applied stress ranges than the 3-D analysis fo 30° skewed bridge, the value of applied stress range should be reduced to 7.35 ksi. This value of applied stress range is almost 150% higher than the nominal fatigue strength of the bridge and 225% higher than the CAFL of Categoty E making this detail susceptible to fatigue fracture.

Therefore, based on the above discussion the in-plane fatigue has the significant effect of initiating the crack coupled with the presence of out-of-plane distortion induced fatigue which accelerated the minute fatigue cracking to brittle fracture.

A.2.3 Recommendations for Bridge Repair

The recommendation for girder repair could be divided into two main parts: (1) repair the fractured girder and (2) eliminate the cause of the fracture from the entire

bridge. The second part of the repair strategy is as important as the first part because if the cause of this fracture is not eliminated from the bridge, future fatigue cracking and fracture might occur at other locations.

Based on the condition of the bridge as observed during the September 19, 1995 inspection and further discussions with NDOT engineers, recommendations for the repair of the east bound Humboldt River Overpass are discussed in the following sections.

A.2.3.1 Immediate Repair of the Fractured Girder

The immediate fracture repair that is proposed by NDOT engineers is sound and acceptable. The moment and shear capacity of the fractured girder should be restored by using a bolted field splice with high strength bolts for the web and the bottom flange. Prior to installation of the splice, the tip of the crack should be positively arrested and the whole region should be ground smooth.

It is highly recommended that limit state design procedure should be used for the splice design. This means that the splice should be design to the ultimate moment and shear capacity of the girder to ensure that the capacity of the splice plate is at least equal to the capacity of the original girder. The splice should be checked for fatigue stresses by using current AASHTO Case I freeways that includes the Single HS20 Truck Load for Over 2 millions cycles. As with any bolted connection, its fatigue resistance is dependent on the proper installation of the bolts.

The procedure that may be followed in adding the splice retrofit is by jacking up the girder to its initial position and clamping the various splice plates to the girder.

All splice plate drilling should be performed dry without coolant or lubricant for the hole cutters.

A.2.3.2 Material Testing

As discussed with NDOT engineers, cores may be taken from web area at the location of the cracks since the shear force is low at this location. This is important to assess the characteristics of the steel given the date of the construction of this bridge which is prior the establishment of the AASHTO Fracture Control Plan. Also, hardness testing may be conducted by performing Rockwell hardness measurements on the steel to determine its corresponding tensile strength.

A.2.3.3 Fatigue Retrofit of the Entire Bridge

The fracture of one girder shows the potential cracking in other girders since the same environment exits at other locations. It is highly recommended to fatigue retrofit the two bridges by eliminating any potential fatigue problems such as out-of-plane distortion induced fatigue and in-plane fatigue. For out-of-plane distortion induced fatigue, rigid connections should be provided between the transverse stiffeners and the web at cross frame locations. The in-plane fatigue of the bridge could be reduced by eliminating the low strength fatigue details such as category E details. These are found at gusset plate connections of the lateral bracing to the web. These gusset plates should be removed from the entire bridge and ground their location to a smooth polish finish.

Also of concern is the end location of the longitudinal stiffeners of the web plate that are located over the pier supports. Structural analysis should be performed to

ensure that these ends do not lie in a tension or reversal stress zone. If they do lie in a tension or reversal stress zone, the longitudinal stiffener should be removed. The shear capacity of the web without the presence of longitudinal stiffener should be checked to ensure that the web continues to have an adequate capacity to resist gravity shear.

A.2.3.4 Future Inspection

The bridge should be kept on short time inspection schedule to monitor the behavior of the splice plate and any fatigue prone details. It is highly recommend that NDOT take a close look at its all steel bridge inventory and check whether these bridges have Category E details and develop a plan to eliminate them. The presence of Category E details coupled with the age of these steel bridges make them very susceptible to fatigue cracking and fracture. It is also recommended to instrument some steel bridges to obtain real stress range measurements based on actual traffic loading. These measurements will enable an accurate assessment of the remaining fatigue life of fatigue prone details in order to a develop a program to prioritize fatigue retrofit of steel bridges in the State of Nevada. For any future fatigue evaluation of steel bridges, 3-D structural analysis should be used to determine the applied stress ranges for a Single HS20 Truck Load and and Case I Freeways.

Kenny C. Guinn, Governor

Nevada Department of Transportation
Tom Stephens, P.E. Director
Prepared by Research Division
Alan Hilton, Research Manager
(775) 888-7803
ahilton@dot.state.nv.us
1263 South Stewart Street
Carson City, Nevada 89712